Client:

DG Rijkswaterstaat

Rijksinstituut voor Kust en Zee, RIKZ

Reliability of SWAN at the Petten Sea Defence

Project HR-ontwikkeling

Joint Venture

WL | Delft Hydraulics - Alkyon Hydraulic Consultancy & Research

June 2003

CLIENT: DG Rijkswaterstaat
Rijksinstituut voor Kust en Zee, RIKZ

TITLE: Reliability of SWAN at the Petten Sea Defence

ABSTRACT:

In this report the reliability of the wave prediction model SWAN and the reliability of the hydraulic boundary conditions at the Petten Sea Defence have been investigated by hindcasting four or five instants from five storms, i.e. three in January 1995, one in February 2002 and one in October 2002.

In 1999 the hydraulic boundary conditions have been determined with SWAN, version 30.62 and have been assimilated in the RAND2001 database. Alkyon & WL | Delft Hydraulics (2002) have proposed an advanced method for hindcasting measured storm events with the SWAN model. In this study a first application of this generic hindcasting method has been presented. The results will be compared with the results obtained with the more simplified, standard hindcasting method that has been used in 1999. The reliability of the hydraulic boundary conditions contained in RAND2001 has been investigated by comparing the SWAN results for the standard and advanced hindcasting method with measurements.

Since 1999 SWAN has developed significantly. The present standard version 40.11 contains improvements in physical formulations, handling of the boundary and pre- and postprocessing. After version 40.11 only research versions have been developed, each containing changes in one aspect. One of them is 40.16. Also with SWAN 40.16 computations have been carried out applying the standard and advanced hindcasting method. The SWAN results have been compared with measurements by means of scatter plots and statistical parameters. The reliability of SWAN has been investigated by comparing the scatter plots and statistical parameters for all SWAN versions. The comparison has been made based on a subdivision in locations, storm days and classes (current following and opposing wind direction, depth or not-depth limited situations and presence of low-frequency energy).

The major conclusions that have been drawn from this study are the following. The RAND2001 data set is not necessarily reliable, since the computational results at MP6 are questionable. Furthermore, the advanced hindcasting approach generally leads to improved results in comparison with the 'standard' approach. The inclusion of current effects and the use of a more recent bottom topography improves the results the most. Finally, the performance of SWAN 40.16 is similar to SWAN 30.62.

REFERENCES: Proposal no. MCI03614/H4197/JG, d.d. 30 October 2002
Contract no. RKZ-1244, d.d. 26 November 2002
Revised contract no. RKZ-1244A, d.d. 15 april 2003

VER.	ORIGINATOR		DATE	REMARKS	REVIEW		APPROVED BY	
1	J. Groeneweg et al.		February 7, 2003	draft phase1	A.R. van Dongeren		W.M.K. Tilmans	
2	J. Groeneweg et al.		April 28, 2003	draft	M.R.A. van Gent		W.M.K. Tilmans	
3	J. Groeneweg, G.Ph. van Vledder, D. Hurdle, N. Doorn, C. Kuiper		June 19, 2003	final	M.R.A. van Gent		W.M.K. Tilmans	

PROJECT IDENTIFICATION: H4197 / A1044

KEYWORDS: Spectral wave modelling, hindcasting, Petten Sea Defence, storm conditions

NUMBER OF PAGES 35

CONFIDENTIAL: ☐ YES, until (date) ☒ NO

STATUS: ☐ PRELIMINARY ☐ DRAFT ☒ FINAL

Contents

Appendices

List of Figures

In Appendix Figures:

List of Tables

In Text:

List of Symbols

Symbol	Units	Meaning
H_{m0}	m	significant wave height
$H_{1/3}$	m	average height of the 1/3 highest waves
m_0	m^2	variance of free surface elevation, i.e. total wave energy
m_n	m^2Hz^n	nth moment of frequency spectrum
$T_{m0,1}$	s	wave period based on zero-th (m_0) and first (m_1) moment
$T_{m0,2}$	s	wave period based on zero-th (m_0) and second (m_2) moment
$T_{m-1,0}$	s	wave period based on zero-th (m_0) and first negative (m_{-1}) moment
T_p	s	peak period
T_{pb}	s	block peak period
T_{pbeq}	s	equivalent block peak period
T_{pm}	s	characteristic peak period

The definition of the spectral period measures have been given in Appendix A. The spectral moments are determined by integrating over the finite frequency domain with $f_{low} = 0.03\text{Hz}$ and $f_{high} = 0.50\text{Hz}$.

1 Introduction

1.1 Background of the study

In this report results are described of the project ‘Betrouwbaarheid SWAN bij de Pettemer Zeewering’ (Dutch for ‘Reliability of SWAN at the Petten Sea Defence’, contract no. RKZ 1244), which is part of the project “HR-ontwikkeling”. The reliability of the wave conditions at the Petten Sea Defence in the dataset RAND2001 and the reliability of the wave prediction model SWAN have been investigated.

In 1999 wave conditions for large parts of the Dutch coast have been determined with SWAN, version 30.62 and have been assimilated in the RAND2001 database. The wave conditions near Petten are considered to be representative for those along the closed Dutch coast. In Alkyon & WL | Delft Hydraulics (2002) a generic method has been proposed for hindcasting measured storm events with the SWAN model. In this study a first application of this generic hindcasting method is presented. The results will be compared with the results obtained with the more simplified hindcasting method that has been used in 1999. In this study the two approaches will be referred to as ‘advanced’ and ‘standard’, respectively. For clarity, the aim of this study is to determine the reliability of the wave prediction at the Petten Sea Defence, not to apply the most appropriate hindcasting method. The two methods are only a tool and are applied to SWAN to fulfil the goal.

The SWAN model is being developed at Delft University of Technology. Detailed information about this model can be found e.g. in Booij et al. (1999). This paper contains information about the model at its state of approximately six years ago. Since then, SWAN has developed significantly. The present standard version 40.11 (status October 2000) contains improvements in physical formulations, and handling of the boundary and pre- and postprocessing (see SWAN User Manual, 2000). After version 40.11 only research versions have been developed, each containing changes in one aspect. In version 40.16 the functionality of calculating triads and quadruplets simultaneously has been incorporated. Anticipating to new releases, also with SWAN 40.16 computations have been carried out for both the standard and the advanced hindcasting method. For each SWAN version and each hindcasting method we compare the computational results with measurements and determine scatter plots and statistical parameters. The reliability of SWAN and the wave conditions in RAND2001 for the closed Dutch coast have been investigated by analysing the scatter plots and the statistical parameters and comparing them for the four different cases. In order to structure the analysis the large set of parameters and plots has been subdivided per location, per storm day and per physical situation.

WL | Delft Hydraulics and Alkyon Hydraulic Consultancy & Research carried out this study as a joint venture. WL | Delft Hydraulics acted as leading partner. J.J. Jacobse and A.T.M.M. Kieftenburg were involved for RIKZ. The study described in this report was performed by G.Ph. van Vledder and D.P. Hurdle of Alkyon and J. Groeneweg, N. Doorn and

C. Kuiper of WL | Delft Hydraulics. Quality Assurance was carried out by A.R. van Dongeren in the first phase of the study and M.R.A. van Gent in the final stage.

1.2 Objective

In this project a hindcast of four storm events divided over five days at the Petten Sea Defence has been carried out. First of all, these hindcasts aim at proving the reliability of the wave loads computed in 1999 and stored in the database RAND2001. Besides, the results of the study are used to validate the SWAN versions 30.62 and 40.16. The following questions will be answered:

- How reliable are the wave conditions in RAND2001, that have been determined with SWAN version 30.62 applying the standard hindcasting method?
- Does a better description of input by means of a more advanced hindcasting method lead to better results?
- Does the most recent version of SWAN provide more reliable results than SWAN version 30.62?

1.3 Approach of the study

An extensive hindcast study has been carried out in which use is made of measurements and computations, provided by RIKZ, of five storms in 1995 and 2002. The exact dates of the storms are the following:

- January 1, 1995
- January 2, 1995
- January 10, 1995
- February 23, 2002
- October 26/27, 2002

In this study each storm has been hindcasted in four different types of SWAN computations. These types are indicated as case 1 through case 4. Case 1 comprises the results of SWAN 30.62 with the standard hindcasting method. Case 2 comprises the results of SWAN 30.62 with the advanced approach. And the cases 3 and 4 comprise the results obtained with SWAN 40.16 using the ‘standard’ and ‘advanced’ approach, respectively. In more detail this boils down to:

Case 1: SWAN 30.62

The reliability of the database RAND2001 is investigated by computing the wave conditions with SWAN 30.62, applying the ‘standard’ hindcasting method. Using the standard hindcasting method the obtained wave conditions form the basis of the table of wave loads for the Dutch coast at Petten, as it has been incorporated in the RAND2001 database. Note that the conditions near Petten are considered to be representative for the stretched Dutch coast.

Case 2: SWAN 30.62+

Since 1999 new insight in hindcasting storms has developed. The new insight has lead to a generic, advanced hindcasting method, which has been applied here to test whether the SWAN 30.62 results lead to a better agreement with the measurements. Here we restricted ourselves to the inclusion of a tidal current, spatially varying water level field, more accurate description of the wind field and the use of actually measured spectra. Numerical settings in SWAN were left unaltered in case 2.

Case 3: SWAN 40.16

Since 1999 new model developments have been incorporated in SWAN versions. Presently, the newest (standard) SWAN version is 40.11. Here we use research version 40.16. In version 40.11 the triad and quadruplet source terms are computed in separation, depending on the Ursell number. In this way, computational time and memory requirements are reduced. However, the convergence behaviour is worse, compared to the situation in which the two source terms are determined simultaneously. The functionality of simultaneously determining the two nonlinear wave-interaction source terms has been implemented in version 40.16.

In this case the standard hindcasting method will be applied using SWAN version 40.16. The difference with case 1 is the applied version of SWAN.

Case 4: SWAN 40.16+

The quality of the latest SWAN version will be judged on the basis of the newest insights in hindcasting of storm events. Besides the use of SWAN version 40.16, the execution of case 4 is identical to case 2.

In all cases a comparison has been made with measurements, resulting in scatter plots and statistical parameters. As already mentioned, results in case 1 lead to conclusions about the reliability of the wave conditions in the database RAND2001. The emphasis of this study is on this case. Comparing cases 1 and 2 or case 3 and 4, insight in a possible added value of the advanced hindcasting method is obtained. Possible improvements of SWAN 40.16 compared to version 30.62 have been investigated by comparison of case 1 and 3, and case 2 and 4.

1.4 Restriction of the study

In the present study we consider four configurations that are formed with the two versions of SWAN (version 30.62 and 40.16) and the two hindcasting methods ('standard' and 'advanced'). In developing SWAN more than one issue has been changed, not necessarily improved, from version 30.62 to 40.16. On the other hand, the standard and advanced hindcasting method differ in several aspects. By considering only the four configurations above, it will be unlikely to ascribe the changes to one specific aspect that has been changed in SWAN or in the hindcasting method. The hindcast study performed here is a comparison of results, rather than a more detailed explanation of the observed differences.

Although the storm periods are moderate to highly instationary, the SWAN computations have been carried out in stationary mode. Furthermore, wave run-up is not considered in this study, although it was measured.

1.5 Outline

The report consists of three parts. In Chapter 2 preparatory activities, such as the choice of instants in the selected storm days, generation of bottom files, wind, flow and water level fields, SWAN input files, and computational grids. The SWAN computations for the four cases are described in Chapter 3. The analysis of the SWAN results is presented in Chapter 4. The conclusions and recommendations are given in Chapter 5.

2 Preparatory activities

2.1 Introduction

In previous hindcast studies (e.g. Jacobse 2000) SWAN has been applied in stationary mode at instants at which the wave motion as well as the wind field could be regarded as more or less stationary. Since these instants are not representative for the wave loads occurring in a storm, here instants have been chosen at which the wind and wave conditions are instationary. The instants represent several phases in tide and development of the storm. Both temporal and spatial variation of the tidal flow and water level have been considered, as well as the temporal variation of integral wave parameters and wind velocities that have been measured at several stations. Per storm day four typical instants have been chosen.

The RIKZ has provided us with both measured data (wind, wave conditions and water level) and computed data (current and water level) for the SWAN computations. These data files have been checked carefully and transformed in a suitable format for SWAN. The locations of the measurement stations mentioned in this report are given in Figure F-1.a, and more detailed near Petten in Figures F-1.b and F-1.c. The co-ordinates of these locations, as well as their used abbreviations are given in Table 2.1. Tidal current and water level data, which have been obtained by applying the flow model WAQUA, have been interpolated on the computational grids of SWAN. The wind fields have been generated from KNMI measurements at three stations in the vicinity of the Petten ray (YMS, TXH, 064 or MPN). Furthermore, for the computations of case 1 and case 3 wave spectra that were measured at the stations IJmuiden (YMW) and Eierlandse Gat (ELD) have been changed to JONSWAP wave spectra that are characterised by spectral wave parameters for significant wave height and wave period (based on characteristic peak period). Finally, the received bottom files are updated with more recent ray measurements.

name location	code	co-ordinate (x, y in RDM)	used in	instrument
Eierlandse Gat	ELD	106514, 587986	Jan 1995, Feb 2002	Wavec buoy
IJmuiden	YMW	65344, 507662	Jan1995, Feb/Oct ‘02	Wavec buoy
Meas. point 1	MP1	98981, 536444	Jan 1995	Dir. Waverider
	011	99003, 535832	Oct 2002	Dir. Waverider
Meas. point 2	MP2	103000, 533800	Jan 1995	Waverider
	021	102890, 533728	Feb/Oct 2002	Dir. Waverider
Meas. point 3	MP3	105230, 531990	Jan 1995	Staff gauge
	033	105234, 531985	Feb/Oct 2002	Radar level meter
Meas. point 5	MP5	105520, 531830	Jan 1995	Dir. Waverider
Meas. point 6	MP6	105650, 531746	Jan 1995	Capacity wire
	062	105661, 531752	Feb/Oct 2002	Pressure sensor
	063	105661, 531752	Feb/Oct 2002	Radar level meter
Meas. point 16	161	105377, 531886	Feb 2002	Pressure sensor
	162	105377, 531886	Oct 2002	Pressure Sensor
Meas. point 17	171	105522, 531817	Feb/Oct 2002	Pressure sensor
	175	105522, 531817	Oct 2002	Pressure sensor
Meas. point 18	181	105617, 531771	Oct 2002	Pressure sensor

Table 2.1 Locations of wave instruments

2.2 Choice of instants of selected storm days

In the beginning of January 1995 a north-western storm occurred over the North Sea. The depression causing this storm was first observed on December 29^{th}, 1994. At January 1^{st}, 2^{nd} and at January 10^{th} 1995 the depression caused storm fields at the North Sea. Similarly at 22 and 23 February 2002 and at the end of October 2002 a depression above Great Britain caused a severe western storm. During the October storm the wind turned from west to south and back to west again.

During these storms wave, wave run-up, wind and water level measurements have been carried out near and at the Petten Sea Defence and other locations. The present section gives a brief description of the measurements and computations that have been used for hindcasting purposes in the present study. Furthermore, using these measurements and computation instants have been selected at which SWAN computations have been carried out. In the presented figures the vertical black lines denote the instants that have been selected for the actual hindcast.

2.2.1 Wind measurements

During the January 1995 storm, wind measurements have been taken at the following locations near Petten (see Figure F-1.a): Meetpost Noordwijk (MPN), IJmuiden (YMS) and Texel (station Texelhors, TXH). For the two storms in 2002 the wind data at the locations Texelhors (TXH), IJmuiden (YMS) and at MP6 near Petten (064) have been considered. Note that the wind speed at MP6 are 10 minutes averaged at the measuring height. These values have not been corrected to U_{10}, in contrast to the other two KNMI stations (TXH and YMS). The height at which the wind is measured is 9.8m, which is close to 10m. The location of the wind measuring equipment is questionable, since the effects from the dike at the wind field are significant. However, the period of maximum wind speed is the same for all locations.

The wind measurements for the five storms are shown in the first (wind speed) and second (wind direction, nautical convention) panel of Figures F-2, respectively. As can be seen in Figure F-2.a and F-2.b, the 1-2 January storm had its first windpeak at 19:00 hour (January 1) and a second at 7:00-9:00 hour (January 2^{nd}). At January 10^{th}, 1995 the storm was most severe at approximately 4:00 hour (see F-2.c). At approximately 6:00 hour the storm is maximal at 23 February 2002. The October storm has two distinct peaks at both 26 (7:00 hour) and 27 October (approximately 15:00 hour).

2.2.2 Water level measurements

The January 1995 storm caused dangerously high water levels at a number of locations along the Dutch coast. Near the Petten Sea Defence (location Petten South, PEZ or PTZ, see Figure 1) the highest water level was measured during the first high water of January 2^{nd} at 4:10 hour (see Figure F-3b). The water level stayed 3 centimetres below the level at which a warning for springtide is sent out (i.e. NAP +2.32 m). The water level at this location is taken as representative for the whole computational area. In panel 4 of the Figures F-3.a-e the time signals of the measured water level have been given at locations Meetpost Noordwijk (MPN), Petten South (PEZ or PTZ) and IJmuiden (YMB). The black line shows the water level as computed with the WAQUA model (originally in GMT, but translated to MET) at a location near Petten (denoted with PNT) with co-ordinates x = 105255.539 m, y = 531726.813 m (see also Section 2.2.4).

2.2.3 Wave measurements

Wave data have been obtained out at 10 locations. The measured spectra at the two offshore locations (Eierlandse Gat (ELD) and IJmuiden (YMW), see Figure F-1.a) have been imposed at the offshore boundary in the SWAN computations. The 8 other measuring locations (MP1 in deeper water and MP2, MP3, MP5, MP6, MP16, MP17 and MP18 in shallow water, see Figure F-1.b) have been used for validation of the SWAN model.

As can be seen in Table 2.1 not every instrument was operational during each storm. Compared to the storms of January 1995 (locations of measuring equipment plotted in Figure F-1.c) wave data have been obtained from more wave instruments. MP5 has been replaced by MP16 (016) and MP17 (017). At MP6 a pressure sensor (062) and a radar level meter (063) were placed in 2002. For the storm in October 2002 also measurements from a pressure sensor at location MP18 (018) have been taken into account. At MP3 a radar level meter was used in October 2002, whereas in February a staff gauge provided the wave signals. In February 2002 MP1 was not active. The wave spectra measured at the offshore locations YMW and ELD are scarce (see Figure F-3.d, panel 1). During the October 2002 storm the directional wave rider at ELD disappeared and only at YMW wave spectra have been obtained for every 20 minutes. Furthermore, MP1 malfunctioned after 13.00hr and MP2 and MP16 after 17.30hr, which is just after the peak of the storm (see Figure F-3.e, panel 1).

The first three panels of Figures F-3.a-e give an overview of the measured spectral wave parameters at the available locations for each storm day. The first panel shows the spectral wave height H_{m0}, the second panel the spectral period $T_{m-1,0}$ and the third panel the spectral period $T_{m0,1}$. For the definitions of these spectral parameters, see Appendix A. The radar observations at MP6 (063) are not reliable. Unrealistic small values for H_{m0} and large values for the wave periods $T_{m-1,0}$ and $T_{m0,1}$ have been measured (see Figure F-3e and Roskam and Hoekema, 2003, p.4). Within this study the radar observations at MP6 (063) will not be considered further. Furthermore, at January 1 and 10, 1995 the data at MP2 are questionable (see Figure F-3.a and F-3.c).

Figures F-4.a-e show time signals of the ratio of the wave height $H_{1/3}$ and the total water depth at all locations. Waves with a wave height to water depth ratio of less than a critical value are not limited by the water depth, whereas waves with a higher value of the ratio of wave height and water depth are limited by the water depth. In Section 2.2.5 a choice has been made for this critical value. Depth limitation generally occurs at the shallowest measuring locations MP3, MP6, MP16 and MP18. Notice the high values of the ratio of wave height and water depth at MP6. The gaps in the plots at YMW and ELD are due to absence of data.

In Figures F-5.a-e the measured one-dimensional wave spectra have been plotted at each location for all instants per storm day. These spectra will be used to determine if a significant amount of low-frequency energy is present.

2.2.4 Flow computations

Results of the model WAQUA have been used for the simulation of the flow. WAQUA is a two-dimensional water movement and water quality simulation system. It can be used for hydrodynamic and water quality simulation of well-mixed estuaries, coastal seas and rivers. The WAQUA storm surge model calculates the sea level and the depth-averaged current on the Northwest European Continental Shelf (CSM) on a grid with cells of approximately 8km x 8km, using wind and pressure forecasts from the Dutch Royal Meteorological Institute (KNMI). For the present purpose the ‘Kuststrook-fijn’ model along the Dutch coast has been used. The resolution of this model varies from 100m to 300m.

The fourth and fifth panels of Figures F-2 show the results of the model. The measured flow conditions at a point near Petten (x = 105255.539 m, y = 531726.813 m) are considered to be representative for the entire Petten ray (MP1-MP18). We have used the information to indicate whether the indicative flow direction is parallel, opposite or perpendicular to the wind direction. The fourth panel shows the flow velocity and the fifth panel the direction of the flow (nautical convention). The ebb and flood tide can be clearly distinguished. For the first January storm (i.e. January 1st and 2nd) the ebb and flood current is almost completely opposite (flood) or parallel (ebb) to the wind direction. For the second January storm (i.e. January 10th) and the February 2002 storm the current is more or less perpendicular to the wind direction. At 27 October 2002 the turning wind causes the wave propagation direction to turn from parallel to perpendicular with respect to the current.

2.2.5 Selection of instants to be hindcasted

One of the aims of the present study is to see how the model SWAN performs under different conditions. To do so, five different situations have been defined:

1. a situation where the current direction is opposite to the wind direction;
2. a situation where the current direction is parallel to the wind direction;
3. a situation where the wave height is limited by the water depth;
4. a situation where the wave height is not limited by the water depth;
5. a situation where the spectrum contains a significant amount of low frequency energy.

For all storms four instants have been chosen in which all situations are represented. For the October 2002 storm an extra instants has been selected (see Table 2.2). The instants that have been chosen for simulation with SWAN have been selected such that all relevant measured data is available and that the data looks reliable. Wind, flow and wave motion is not necessarily stationary at the selected instants. Whereas in previous hindcast studies with the SWAN model only stationary situations have been considered, especially instationary sea-state conditions are taken into account in the present study.

In the third column of Table 2.2 an estimate of the wind direction (from Figure F-2.a-e, panel 2, averaged over wind direction at 3 stations) has been compared with the computed flow direction of the wind direction (Figure F-2.a-e, panel 5). If the relative direction is in between -45 degrees and 45 degrees the wind direction (and thus the ‘wind-driven’ wave propagation direction) and current direction are classified as being in the same direction (following), in between 135 and 225 degrees as opposite, and as perpendicular otherwise.

The criterion which determines whether the wave field at a certain location is depth-limited is $H_{1/3}/h>0.3$ (Figure F-4.a-e). When the value for the wave height over depth ration is close to the critical value of 0.3 (in between 0.25 and 0.35), the wave field at the particular location is classified neither as depth-limited nor as not depth-limited. In Table 2.2 also the locations have been indicated at which the wave energy spectra contain low-frequency energy. The locations are all in the coastal area, where non-linear interactions generate both low- and high-frequency wave energy. In general, low-frequency energy can be observed at MP18 and MP6 (see Figure F-5.a-e).

2.3 Transformation of measured to parametric spectra

At the offshore locations ELD and YMW wave measurements have been obtained with directional waveriders. The processed wave data from these buoys are available at 20 minute intervals (in the form of so-named GD data files). These files contain per measurement block the energy density, mean wave direction and directional spreading as a function of frequency. For application in this study these data have been converted into wave boundary conditions for the SWAN model.

As noted in section 1.4 four cases are distinguished. For each case the wave boundary conditions were specified in a different way. For the cases 1 and 3, the measured wave spectra were converted to parametric JONSWAP spectra assuming a peak enhancement factor $\gamma = 3.3$, the directional spreading factor m (appearing in the $D(\theta)=A.\cos^m(\theta)$ model) was set to 4 (corresponding to a directional spreading of 24.9°) and the mean wave direction was taken equal to the wind direction at the Petten location. The peak period was estimated by computing the block peak period, which provided a robust estimate of the peak period. For case 3, the same parametric spectra have been used as for case 1. The only difference with case 1 is the SWAN format used to specify the parametric wave boundary conditions.

For the cases 2 and 4, the measured wave spectra were converted to input spectra for SWAN. Since the measured spectra are rather grassy due to the inherent statistical variability, they have been smoothed before they were converted to a JONSWAP spectrum to obtain more robust estimates of the spectral shape. Figure F-6 shows an example of the smoothing and fitting procedure to obtain robust estimates of the measured wave boundary spectra at offshore station ELD. The upper panel of Figure F-6 shows the measured spectrum and its smoothed version. As can be seen the measured spectrum shows a lot of variability with frequency. The smoothed spectrum after 5 smoothing operations is shown as the dashed line. The method of smoothing is described in Alkyon (1999c). The effect of smoothing the measured spectrum is that all secondary peaks vanish and that a more evenly spectral distribution is obtained. The lower panel of Figure F-6 shows the smoothed spectrum, the position of the block peak frequency, and 2 fitted JONSWAP spectra. The block peak frequency has been computed with the procedure described in the Appendix A. The first JONSWAP spectrum (dashed line) assumes a peak enhancement factor of 3.3, as used in SWAN.

	instants	wind vs current	depth-limited	not depth-limited	low-freq. energy
	1:00	135°	MP6	MP1, MP5	MP5, MP6

1 January 1995	2:00	135°	MP6	MP1, MP2, MP5	MP6
	6:40	-45°	MP3, MP6	MP1, MP5	MP5, MP6
	10:00	-45°	MP2, MP3, MP6	MP1, MP5	MP5, MP6
2 January 1995	4:20	135°	MP2, MP3, MP6	MP1, MP5	MP3, MP6
	14:40	135°	MP6	MP1, MP5	MP3, MP5, MP6
	16:40	180°	MP6	MP1, MP5	MP3, MP5, MP6
	21:20	0°	MP6	MP1, MP5	MP5, MP6
10 January 1995	9:20	110°	MP2, MP3, MP6	MP1	MP2, MP3, MP5, MP6
	11:20	110°	MP3, MP6	MP1	MP3, MP5, MP6
	16:20	-90°	MP6	MP1, MP5	MP3, MP5, MP6
	20:20	-90°	MP6	MP1, MP2, MP3, MP5	MP5, MP6
23 February 2002	7:20	-90°	MP2, MP3, MP16, MP6	MP17	MP6
	10:20	90°	MP2, MP3, MP16, MP6	MP17	MP6
	13:20	90°	MP3, MP16, MP6	MP17	MP6
	19:20	-90°	MP2, MP3, MP16, MP6	MP17	MP6
26 October 2002	7:00	90°	MP16, MP6	MP1, MP17	MP18, MP6
27 October 2002	6:00	0°	MP6	MP1, MP2, MP3, MP17	
	11:00	45°	MP16, MP6	MP1, MP17	
	14:20	60°	MP2, MP3, MP16, MP6	MP17	MP18, MP6
	17:00	90°	MP2, MP3, MP16, MP6	MP17	MP18, MP6

Table 2.2 Conditions at selected instants in 5 storms

The second JONSWAP spectrum (dash-dot line) is based on a fitting technique to obtain all JONSWAP parameters simultaneously. It follows directly that estimating the peak enhancement factor results in a better fit to the smoothed measured spectrum. In all cases considered the resulting peak enhancement factor was lower than 3.3. This indicates that the actual spectral shapes are less peaked than assumed in the standard hindcasting method, where the energy levels are under-predicted at either side of the spectral peak. For consistency reasons, all spectra correspond to the same significant wave height and peak frequency. It is noted that the parameters of the fitted JONSWAP spectra are not used in this study for consistency reasons with previous studies.

For the cases 2 only a constant spectral shape can be specified for each boundary using the option BOUNDSPEC STAT SIDE UPPER/LOWER X/Y. For the north-western boundary the average of the two measured (both smoothed) spectra at ELD and YMW has been used. For the north-eastern boundary the measured (and smoothed) spectrum at ELD has been used, and for the south-western boundary the measured (and smoothed) spectrum at YMW has been used. For case 4 the variation of the spectral shape along the boundaries can be specified, using the BOUNDSPEC VAR FILE option.

For the actual computations, the wave boundary conditions were imposed 20 minutes earlier than the instant used for the verification of the wave model results in the Petten ray (MP1-MP6). This duration roughly corresponds to the time needed for wave propagation in the area of interest. In the case one of the measured spectra at ELD or YMW was not present at the selected moments of time, the available spectrum was used. At 1 January 1995, 6:20 hour, 2 January 1995, 16:20 hour, and at 23 February 2002, 10:00 hour and 13:00 hour spectra are unavailable at YMW. At ELD wave data are not available at 26 and 27 October 2002.

2.4 Update of digital bottom file with ray measurements

The present RAND2001 database is filled with results of SWAN wave model computations using a digital bottom topography based on measurements from the years 1996 and 1997. As the offshore bottom near Petten is subject to morphological changes, the standard digital bottom topography was supplemented with ray measurements obtained in the period September-November 1994, which is just before the January 1995 storms, and with ray measurements obtained in the months February 2002 and November 2002, which is close to the periods of the 2002 storms.

For use in the hindcast of the 1995 storms, the update of the digital bottom topography was performed in a few steps. In the first step all individual locations in the rays were plotted to define an envelop polygon. In the second step a regular grid equal to the computational grids was defined, followed by a triangle-based line interpolation to infer the depth on the grid points. For this step the program MATLAB was used, applying the standard command GRIDDATA. The result of these steps are shown in Figure F-7. The envelop is indicated with the thick red line. The wave measurement locations are indicated with the blue/yellow circles, and the approximate location of the coastline is plotted with a thick black line.

As can be seen in Figure F-7 the envelop polygon does not surround the locations of the measurement stations MP5 and MP6 (dots closest to the shoreline in Figure F-7), despite the fact that bottom information is available in the Petten ray (i.e. the ray connecting the measuring stations MP1-MP6 in Figure F-7). To be able to interpolate the depth information in the ray to a regular grid, part of the data in the Petten ray was copied to additional rays, obtained by shifting the near-shore part of the Petten ray along the coast. The result of this third step is shown in Figure F-8. The modified envelope polygon is indicated with the thick red line.

In the fourth step the updated bottom topography within the envelope polygon has been included in the various digital bottom topographies for the various computational grids used in this study. This was achieved by performing the interpolation to each computational grid followed by a point to point replacement of the depth values within this polygon. The resulting changes in the bottom topography for computational grid E24 are shown in Figure

F-9. The difference is of the order 1 meter. Apparently, the bed is in motion continuously and has changed significantly over a period of 2 years that contains at least three storm events.

For the use in the 2002 storms, the update procedure was slightly adapted. For February 2002 and November 2002 bottom measurements are only available in 9 rays in the Petten ray. Use of this information would lead to an update of the bottom in a small strip along the Petten ray with a width of 500 m. Inspection of the results of the interpolation procedure showed that large variations in bottom depths occur along the envelop of the these nine rays, especially near the Pettemer polder, a shallow bank about 3 km offshore. Such strong variations are undesirable since they may lead to strong refraction effects, which affect the predicted wave conditions in an unknown way.

To improve the quality of the bottom updates, two additional steps were performed. In the first step additional ray data were obtained from the 2002 Jarkus measurements. This provided an update of the 1996 bottom topography in a region along the coast, see Alkyon (2001) for a description of this method. In the second step, the area from which information of the 9 rays was used, was narrowed to a region with a length of about 1500 m from the coast. The offshore boundary of this area was obtained by considering the area were only small bottom variations occur. As a result, only near-shore changes were accounted for, and the Pettemer Polder was left unchanged.

The results of the above procedure are illustrated in the Figures F-10 and F-11. Figure F-11 shows the updated bottom topography for computational grid E24 for the situation of November 2002, whereas Figure F-11 shows the difference in bottom topography with respect to the 1996 situation. In both figures, the position of the 9 rays, the Jarkus 2002 rays, the envelope polygon, and the output locations are shown.

2.5 Generation of wind fields

Three types of wind fields have been created. The first type is based on a parameterisation of storm wind fields. In the second method local wind measurements have been used to estimate the wind field near Petten as well as possible. In the third method, local wind measurements were supplemented with the digital wind fields used in the WAQUA flow computations. The first type of wind fields was used in the computations for the cases 1 and 3. The second type of wind fields was used in the computations for the 1995 storms for the cases 2 and 4, whereas the third type of wind fields was used in the computations of the 2002 storms for the cases 2 and 4.

The first method has also been used in the SWAN studies for the Wadden Sea and the Dutch coast (Alkyon, 1999a,b). In this method the pattern of the spatial variation of the wind speed is the same for a certain wind speed corresponding to a certain storm severity level. Each severity level corresponds to a certain return period (see Alkyon 1999b for details) The wind direction is uniform for the whole wind field. The contour lines with a certain wind speed are based on tables of wind speeds for each storm severity as obtained in the wind stations Vlissingen, Hoek van Holland, IJmuiden, Texel, Terschelling, Lauwersoog and Delfzijl.

For each condition, the wind speed near Petten was linked to a certain storm severity, and the values of the wind speed on each contour line were determined on the basis of the tables mentioned above. Next, the wind speed was interpolated to a spatial grid with a step size in *x*- and *y*-direction of 2500 m. Numerical characteristics of this grid (WND) are given in Table 2.3. Values of the wind speed between two iso-lines were obtained by interpolating in the distance from a hypothetical origin (located at *x*=400,000 m, *y*=500,000 m), in the direction formed by the vector between that point and the output point being considered. This point was chosen so that rays from this point pass over the iso-lines of the wind strength approximately normal to their direction in the area of interest. The wind direction is taken equal to the wind direction near Petten. The wind characteristics at Petten were obtained by interpolation between the wind measurements at Texelhors (TXH) and Noordwijk (MPN). An example of a wind field constructed in this way is shown in Figure F-12.

In the second method, wind measurements were used from three locations around the Petten location, viz. TXH, MPN and K13. The first two locations were used to estimate the gradient in wind characteristics along the coast. The third location was used in addition to estimate the gradient in wind characteristics perpendicular to the coast. The co-ordinates of K13 are (10240,583356), which is just outside the domain in Figure F-1.a. These three locations define a hypothetical box in which the spatial variation of the wind field was estimated. Beyond the boundaries of this box, the wind speed and direction were kept constant. An example of a wind field obtained with this method is shown in Figure F-13. In contrast to Figure F-12, the variation in wind direction can be seen in this figure. The corner points of this hypothetical box are visible in Figure F-13. Wind speeds and directions outside this box were obtained by keeping them constant along each side of the box. For the 1995 storms no information was available from pressure maps which might give additional information on the structure of the wind. On the other hand, nearby wind measurements were used to put more emphasis on the wind field in the coastal zone near Petten.

In the third method, local wind measurements around the Petten location, viz. Texelhors (TXH) and IJmuiden Semafoor (YMS) were used in combination with digital wind fields used in the WAQUA flow computations. Wind measurements at the Petten location were deemed unusable because of strong land-sea effects. In the first steps, the digital wind fields on the WAQUA grid were converted to a 2500 m wind grid. In the second step, the computed wind speeds at the locations TXH and YMS were compared with the measured wind speeds at these locations to obtain an overall scaling factor of the digital wind field. The computed wind directions were left unchanged. In this way the spatial variation of the wind field was unchanged. Figure F-14 shows an example of a wind field obtained with this method. It can clearly be seen that this wind field shows much more structure than the other types of wind field. Especially, land-sea effects are visible in this figure.

2.6 Generation of flow and water level fields

Results of current and water level simulation were obtained from RWS/RIKZ who used the WAQUA-based Kuststrook model. The Kuststrook model uses a curvi-linear grid with a varying spatial resolution. For use in the SWAN model, the results of the Kuststrook model were converted to the regular rectangular computational grids, accounting for the local resolutions of the flow model and the rectangular SWAN grid. In areas were the flow model has a finer resolution than the rectangular SWAN grid, an averaging technique was used. In the other areas bi-linear interpolation was used to obtain the current velocity components and water level values in the points of the computational grid.

Special attention was needed to account for exception values, in-active and dry-falling grid points of the flow model. Exception values were identified by large dummy values for the location *x*-and *y*, the *u*- and *v*-flow components and the water level *z*. The conversion to the rectangular grid can only be made for those grid points that lie within four valid (non-exception) points of the flow model.

In-active grid points from the WAQUA computation were identified with zero-values for the current components and in some areas also with a zero water level. Dry-falling points were identified with zero values for the current components, but with non-zero values for the water level. In such points the computed water level is equal to the local land height. To avoid unrealistic water levels in the SWAN model, the water level in dry points was set to zero.

In the coastal area near the Petten ray, the resolution of the flow model is much coarser (about 200 m) than the resolution of the finest computational grid E24 (20 m x 20 m). As a result no current and water level information could be obtained from the flow model for a small strip of water points between the last line of flow model points with non-zero values and a hypothetical line of land points of the computational E24 grid. An example of the application of the necessary extension of flow information is shown in Figure F-15. The left panel shows the spatial variation of the water level field as obtained from the flow model. The right panel shows the spatial variation of the water level field after it has been extended to the coast. The crosses in Figure F-15 (and F-16) indicate the output locations of the flow model. The black line is the approximate position of the coast line.

To obtain realistic values for the current velocities and water levels, the following modifications were made to the converted (from WAQUA grid to SWAN grid) current and water level fields. The water level fields were extended to the coast using the same water level as the first non-zero value in a direction perpendicular to the coast. As can be seen, the extended water level field extends over the land points as well, up to the right boundary of the detailed computational grids. This is not a problem since in the actual SWAN computations the computational depth is taken as the sum of the water depth and water level.

The current velocities were extended to the coast using a local Chézy approximation, conform the SWAN 1D methodology. In this approximation it is assumed that the gradient of the water level along the coast is constant along a line perpendicular to the coast and that at each point along this line the current is aligned with the coast. For the situations in this study, the assumption seems to be valid. The current speed can then be described with the equation:

$$U = C\sqrt{hi} \tag{2.1}$$

in which C is the Chézy coefficient, h the local water depth and i the gradient of the water level field. In this study the value of the Chézy coefficient was taken equal to 50. The value of the gradient i was estimated from the first non-zero current velocity U_0 obtained by searching in the direction perpendicular from the coast and the water depth at this location h_0 as:

$$i = \left(\frac{U_0}{C}\right)^2 \frac{1}{h_0} \tag{2.2}$$

Next, the current velocities for all grid points towards the coast were computed according to:

$$U_j = \begin{cases} C\sqrt{h_j i} & \text{for} \quad h_j > 0 \\ 0 & \text{for} \quad h_j \leq 0 \end{cases} \tag{2.3}$$

with j the index of each grid point. The water depth h_j was obtained on the basis of the modified bottom topography, and the extended water level for each conditions. In practise, the extension of the current and water level fields to the coast was performed on a row by row basis in the rectangular files for the current and water level fields. This was allowed since one of the major axis of the detailed computational grids was aligned with the coast line near Petten.

An example of the application of this extension is shown in Figure F-16. The left panel shows the spatial variation of the current speed and current direction (indicated with arrows) as obtained from the flow model. The right panel shows the spatial variation of the current speed and direction after it has been extended to the coast using the Chézy approximation. As can be seen in Figure F-16 the current velocities decrease with decreasing water depth. For the land points the currents are zero, resulting in the white strip along the coast.

2.7 Adaption of SWAN input and output files for version 40.16

The SWAN input and output files used or created by SWAN 30.62 could not directly be used by SWAN 40.16. The following differences needed to be accounted for:

- The commands to define the output parameter $T_{m-1,0}$ differ. In SWAN 30.62 the command SET POWER 0 is used and the output parameter TM01 is used to store the value of $T_{m-1,0}$. This implies that the parameter $T_{m0,1}$ was not output by SWAN 30.62. In SWAN 40.16 the command “QUANTITY POWER 0” is used to define this output parameter and the output parameter PER is used to store its value.
- The format for specifying the wave boundary conditions differs between SWAN 30.62 and SWAN 40.16.
- In SWAN 40.16 the command CGRID needs to be specified for each nested grid.
- The position in the input file of the specification of the wave boundary conditions for nested grids differs between SWAN 30.62 and SWAN 40.16. In SWAN 30.62 it is defined before the bottom topography has been defined. In SWAN 40.16 it needs to be specified after the computational grid and bottom topography have been defined.

- SWAN 40.16 has the BOUN SHAPE command to specify the variation of the parametric spectra to be imposed at the boundary.
- The output spectra of SWAN 30.62 needed to be converted to the format of SWAN 40.01 and higher.
- The source code for SWAN 30.62 and 40.16 was modified with respect to the format of the output block files to obtain rectangular output matrices.
- SWAN 40.16 has an additional command to specify some threshold values for some limiters and the Ursell number, to allow the simultaneous computation of triad and quadruplets:

  TRIAD URSELL=0.01
  LIM URSELL=10 qb=1 iter=100

2.8 Generation computational grid and output points

In the present study two sets of computational grids have been used. In the first set, more or less the same computational grids (N02, K12, and D33) have been used as in the SWAN study for computing the wave conditions along the Dutch coast (Alkyon, 1999b). In this set the outer grid N02 has a resolution of 500 m, the intermediate K-grid a resolution of 100 m and the detailed D grid a resolution of 20 m (see Figure F-17). In contrast to the previous SWAN study the intermediate K2 has been replaced by the smaller K12 grid to save computational time. Still, this grid is large enough to provide the same boundary conditions for the detailed grids near the Petten ray. In the second set, the detailed D33 20 m grid has been replaced by the detailed 20 m grid E24 (see Figure F-18), which is better centred around the Petten ray.

In the preparation phase of this study, some tests were carried out to obtain the proper resolution of the detailed computational grid. To that end some SWAN computations were carried out with grids with spatial resolutions of 100 m, 50 m and 20 m. Output was generated along the Petten ray for a number of integral wave parameters. The results of such a test computation are shown in Figure F-19. For each integral wave parameter a line-plot was made with the variation of these parameters along the ray based on the three grids. The grids K12, E14 and E24 correspond to grids with resolutions of 100 m, 50 m and 20 m respectively. The results in Figure F-19 indicate that noticeable differences occur between results based on the K12 and E14 grids, but that differences between results based on the E14 and E24 grids are rather small. It was therefore decided that a spatial resolution of 20 m is sufficiently accurate for the present study.

For the purposes of this study output points have been defined at the location were the boundary conditions are specified (ELD and YMW) and at the measurement locations in the Petten ray. Numerical characteristics of the computational grids are included in Table 2.3. The names and locations of the output points are included in Table 2.1.

No tests were carried out with different spectral resolution because the resolution used in previous SWAN studies was deemed satisfactory. Moreover, using other resolutions would probably lead to a time-consuming re-calibration of the SWAN model. Therefore, in this study 31 discrete frequencies in the range 0.03 Hz – 0.8 Hz, and 36 directions distributed over the full circle were used.

Grid	X_0 (m)	Y_0 (m)	X_{len} (m)	Y_{len} (m)	α (°)	M_x	M_y	Δx (m)	Δy (m)
N02	81500	450000	155000	40000	66	310	80	500	500
K12	105521	511382	40000	22000	70	400	220	100	100
D33	105500	525000	9000	4000	82	450	200	20	20
E24	105500	529000	7000	4500	74	350	225	20	20
WND	-40000	360000	340000	310000	0	136	124	2500	2500

Table 2.3 Name and numerical characteristics of computational grids and grid of wind field

3 SWAN computations

3.1 Four cases

In order to determine the quality of SWAN and to judge the reliability of the hindcasting method that has been used in 1999, four cases have been considered in this study. They are formed by two versions of SWAN (30.62 and 40.16) and two approaches to carry out hindcasts of storm events (standard and advanced).

In Chapter 2 a number of issues have been described that have been incorporated in the advanced method for hindcasting storm events. Summarising, the following changes in the standard hindcasting method have resulted in the advanced approach:

- Supplementary bed level measurements along rays have been incorporated in the less recent bottom file.
- Tidal currents have been included.
- The constant water level field has been replaced by a spatially varying water level field.
- The wind field is based on wind measurements at three local stations.

In Table 3.1 the input for the 4 cases has been summarised.

	Case 1	Case 2	Case 3	Case 4
SWAN version	30.62	30.62	40.16	40.16
Water level	Uniform, based on measurements near Petten	Non-uniform, based on WAQUA computations. Extended to coastline for D and E grids	See case 1	See case 2
Current	None	Non-uniform, based on WAQUA computations. **January 1995**: Extended to coastline based on 1995 bed **February 2002**: Extended to coastline based on February 2002 bed **October 2002**: Extended to coastline based on February 2002 bed Extensions only for D and E grids	See case 1	See case 2

Wind	**Wind speed** non-uniform, based on 'kust-project' parametric wind fields, scaled with measurements at TXH and MPN. **Wind direction** uniform and based on measurements at TXH and MPN	1995: Based on measurements at TXH, MPN and YMW 2002: Based on HIRLAM/WAQUA and scaled with measurements at TXH and YMS	See case 1	See case 2
Wave boundary conditions	Parametric JONSWAP, based on measured H_s and T_p at ELD and YMW. Tanh-variation along boundaries. Wave direction equal to wind direction	Based on measured spectra at ELD and YMW, no variation along boundaries	See case 1	Based on measured spectra at ELD and YMW, variation along boundaries
Bathymetry	'Kust-project' bed from 1996	**January 1995**: bed 1996 extended with ray measurements from November 1994 **February 2002**: bed 1996 extended with ray measurements from March 2002. **October 2002**: bed 1996 extended with ray measurements from November 2002. Extensions only for K, D and E grids.	See case 1	See case 2

Table 3.1 Input for SWAN computation for four cases

All SWAN computations (both versions) have been carried with the following basic settings:

- The standard WAM3 settings (option KOMEN) for wave growth, white-capping and non-linear quadruplet wave-wave interactions.
- Surf breaking with α=1 and γ=0.73.
- Bottom friction with default JONSWAP parameterisation.
- Triad wave-wave interactions activated.

As far as relevant for the present study, the following items are included in SWAN 40.16, whereas they are not present in version 30.62:

- Triads and quadruplets are determined simultaneously. In previous versions either one of the source terms was active, depending on the value for the Ursell number. Here default the following criteria have been used.
- TRIAD URSELL=0.01
- LIM URSELL=10 qb=1 iter=100
- It is possible to impose stationary boundary conditions defined by wave spectra that vary along the boundary. The model interpolates linearly between the boundary conditions at given points. The command BOUNDSPEC controls this.

3.2 Output

For the purposes of this study table and spectral output is generated in the set of output points specified in Table 2.2. The spectral output consists of 1d and 2d wave spectra that are input in the SWAN testbank post-processing software to assess the performance of SWAN. Since the testbank software uses SWAN spectra in the SWAN 40.01 and higher format, the spectra obtained with SWAN 30.62 were converted to this new data format. The table output was generated to be able to check the computation of certain spectral parameters.

In addition to the table and spectral output, also block files were created to show the spatial variation of integral wave parameters, wind fields and currents fields. In this way they provide background and control information on the hindcasted storms. Figures F-20 and F-21 show examples for the storm of January 1, 1995, 0.100 hour for grid K12 for case 2 (SWAN 30.62 advanced method). Figure F-20 shows the spatial variation of the significant wave height, in which the arrows indicate the mean wave direction. Figure F-21 show the spatial variation of the mean wave period $T_{m-1,0}$. The Figures F-22 and F-23 show similar results for grid E24.

Figures showing the spatial variation of all integral wave parameters, current fields and wind fields for all computational grids, simulation times and cases will be made available separately to this report on CD-ROM.

4 Analysis of results

4.1 Introduction

The results of the study are presented in various plots. Scatter plots have been generated for a qualitative statistical comparison. These scatter plots contain comparisons of the significant wave height H_{m0}, the mean wave periods $T_{m0,1}$, $T_{m0,2}$ and $T_{m-1,0}$, the peak period T_p, the block peak period T_{pb}, the equivalent block peak period T_{pbeq} and the characteristic peak period T_{pm} (see Appendix A for their definitions). The spectral moments that are required to determine the significant wave height and the mean wave periods are determined by integrating over the finite frequency domain with $f_{low} = 0.03\text{Hz}$ and $f_{high} = 0.50\text{Hz}$. This range was applied to both the measured and computed wave spectra.

Quantitative statistical measures indicating the agreement between computed and observed values are also generated. Indicatively, for one case (MP1 at all instants) the output of the statistical post-processing is shown in Table 4.1. The statistical parameters are: mean of observations (MEAN), bias (BIAS), mean absolute error (MAE), root-mean-square error (RMSE), scatter index (SCI) and standard deviation (STD). Their definition can be found in Appendix B.

Computed statistical parameters for case : s06loc01
Number of stations at which computed data is available : 15

	Hm0 [m]				Tm01 [s]				Tm02 [s]				Tm-10 [s]			
SWAN	30.62	30.62+	40.16	40.16+	30.62	30.62+	40.16	40.16+	30.62	30.62+	40.16	40.16+	30.62	30.62+	40.16	40.16+
mean	3.735	3.735	3.735	3.735	7.221	7.221	7.221	7.221	6.096	6.096	6.096	6.096	8.538	8.538	8.538	8.538
bias	-0.062	-0.050	-0.087	-0.127	-0.101	-0.345	0.002	-0.290	-0.065	-0.206	-0.028	-0.164	-0.090	-0.232	0.041	-0.178
mae	0.599	0.424	0.617	0.424	0.804	0.403	0.780	0.354	0.634	0.452	0.623	0.390	0.893	0.307	0.838	0.314
rmse	0.787	0.559	0.826	0.545	1.096	0.600	1.064	0.514	0.803	0.552	0.779	0.472	1.216	0.539	1.150	0.471
sci	0.211	0.150	0.221	0.146	0.152	0.083	0.147	0.071	0.132	0.091	0.128	0.077	0.142	0.063	0.135	0.055
std	0.813	0.577	0.850	0.549	1.130	0.507	1.102	0.439	0.829	0.530	0.806	0.459	1.255	0.503	1.190	0.451

Table 4.1 Output statistical postprocessing

The scores are given for:

1. Each individual instant.
2. Each storm (i.e., averaged over four simulations within one storm).
3. Each physical process (i.e., ebb current, flood current, wave height limited by the depth, wave height not limited by the depth and spectra with a significant amount of energy in the lower frequencies).
4. Each location (i.e., MP1, MP2, MP3, MP5, MP6, MP16 and MP17).
5. All cases (i.e. at all locations and at all instants).

Note that location MP18 is not used in the analysis. Although measurements and computations are available at this location, it was deemed to be difficult to incorporate location MP18, which has not been considered in the 1995 storms, in the runscripts that have been developed for the analysis of the wave measurements and computations.

The scores mentioned above are presented in tables. The four columns per wave parameter correspond to the four cases mentioned in Section 3.1: SWAN 30.62, SWAN 30.62+, SWAN 40.16 and SWAN 40.16+. The case descriptions in the table correspond to the instants and locations described in Table 4.2. Case names corresponding to individual instants start with an ‘F’: The following two characters, either ‘1a’, ‘1b’, ‘2a’, ‘2b’ or ‘3a’, indicate a specific storm day (1a: 1 January 1995; 1b: 2 January 1995; 2a: 10 January 1995; 2b: 23 February 2002; 3a: 26/27 October 2002). The last two digits in the case names denote the number of the instant in that storm day. These cases are not mentioned in Table 4.2, since they have not been used in the analysis. The statistical information for each instant is stored on CD-ROM. On the other hand, all instants of one storm day have been combined to one case. Casenames starting with an ‘S’ correspond to separation in classes, either in storm days (‘str’), locations (‘loc’) or physical processes (‘opp’, ’par’, ‘dep’, ‘nde’ and ‘dbl’).

Casename	Simulation date and time	Locations
S01opp01	1995/01/01 01:00, 02:00	MP1, MP2, MP3, MP5, MP6
(opposing cur)	1995/01/02 04:20, 16:40	MP1, MP2, MP3, MP5, MP6
S02par01	1995/01/01 06:40	MP1, MP2, MP3, MP5, MP6
(following	1995/01/01 10:00	MP1, MP3, MP5, MP6
current)	1995/01/02 21:20	MP1, MP2, MP3, MP5, MP6
	2002/10/27 06:00	MP1, MP2, MP3, MP17, MP6
	2002/10/27 11:00	MP1, MP2, MP3, MP16, MP17
S03dep01	1995/01/01 01:00, 02:00	MP6
(depth limited)	1995/01/01 06:40	MP3, MP6
	1995/01/01 10:00	MP2, MP3, MP6
	1995/01/02 04:20	MP2, MP3, MP6
	1995/01/02 14:40, 16:40, 21:20	MP6
	1995/01/10 09:20	MP2, MP3, MP6
	1995/01/10 11:20	MP3, MP6
	1995/01/10 16:20, 20:20	MP6
	2002/02/23 07:20, 10:20, 19:20	MP2, MP3, MP16, MP6
	2002/02/23 13:20	MP3, MP16, MP6
	2002/10/26 07:00	MP16, MP6
	2002/10/27 06:00	MP6
	2002/10/27 11:00	MP16, MP6
	2002/10/27 14:20	MP2, MP3, MP16, MP6
	2002/10/27 17:00	MP2, MP3, MP16, MP6

S04nde01 (not depth limited)	1995/01/01 01:00, 06:40, 10:00 1995/01/01 02:00 1995/01/02 04:20, 14:40, 16:40, 21:20 1995/01/10 09:20, 11:20 1995/01/10 16:20 1995/01/10 20:20 2002/02/23 07:20, 10:20, 13:20, 19:20 2002/10/26 07:00 2002/10/27 06:00 2002/10/27 11:00 2002/10/27 14:20, 17:00	MP1, MP5 MP1, MP2, MP5 MP1, MP5 MP1 MP1, MP5 MP1, MP2, MP3, MP5 MP17 MP1, MP17 MP1, MP2, MP3, MP17 MP1, MP17 MP17
S05dbl01 (low freq. energy)	1995/01/01 01:00, 06:40, 10:00 1995/01/01 02:00 1995/01/02 04:20 1995/01/02 14:40, 16:40 1995/01/02 21:20 1995/01/10 09:20 1995/01/10 11:20, 16:20 1995/01/10 20:20 2002/02/23 07:20, 10:20, 13:20, 19:20 2002/10/26 07:00 2002/10/27 14:20, 17:00	MP5, MP6 MP6 MP3, MP6 MP3, MP5, MP6 MP5, MP6 MP2, MP3, MP5, MP6 MP3, MP5, MP6 MP5, MP6 MP6 MP6 MP6
S06loc01 (MP1)	All 12 instants in 1995 2002/10/26 07:00 2002/10/27 06:00, 11:00	MP1 011 011
S07loc01 (MP2)	11 instants in 1995 (excl. 1995/01/01 10:00) All 9 instants in 2002	MP2 021
S08loc01 (MP3)	All 12 instants in 1995 2002/02/23 07:20, 10:20, 13:20, 19:20 2002/10/26 07:00 2002/10/27 06:00,11:00, 14:20, 17:00	MP3 031 033 033
S09loc01 (MP16)	2002/02/23 07:20, 10:20, 13:20, 19:20 2002/10/26 07:00 2002/10/27 11:00, 14:20, 17:00	161 162 162
S10loc01 (MP17)	2002/02/23 10:20, 13:20, 19:20 2002/10/26 07:00 2002/10/27 06:00, 11:00, 14:20, 17:00	171 175 175

S11loc01 (MP5)	All 12 instants in 1995	MP5
S12loc01 (MP6)	All 12 instants in 1995 2002/02/23 07:20, 10:20, 13:20, 19:20 2002/10/26 07:00 2002/10/27 06:00, 14:20, 17:00	MP6 062 062 062
S13str01	1995/01/01 01:00, 02:00, 06:40 1995/01/01 10:00	MP1, MP2, MP3, MP5, MP6 MP1, MP3, MP5, MP6
S14str01	1995/01/02 04:20, 14:40, 16:40, 21:20	MP1, MP2, MP3, MP5, MP6
S15str01	1995/01/10 09:20, 11:20, 16:20, 20:20	MP1, MP2, MP3, MP5, MP6
S16str01	2002/02/23 07:20 2002/02/23 10:20, 13:20, 19:20	MP2, MP3, MP16, MP6 MP2, MP3, MP16, MP17, MP6
S17str01	2002/10/26 07:00 2002/10/27 06:00 2002/10/27 11:00 2002/10/27 14:20, 17:00	MP1, MP2, MP3, MP16, MP17, MP MP1, MP2, MP3, MP17, MP6 MP1, MP2, MP3, MP16, MP17 MP2, MP3, MP16, MP17, MP6

Table 4.2 All cases considered in analysis

E.g., for case S14str01 the measured and computed wave conditions are compared at four instants of the storm of January 2, 1995 at five locations, resulting in 20 comparisons. For case S05dbl01 we end up with 30 comparisons.

Case S10loc01 denotes measuring point 17 (MP17, 171, 175). Note that in the analysis pressure sensor 175 has been used for the storm of October 2002 (see Table 4.2), although measurements from pressure sensor 171 have been obtained during that storm period as well (see Table 2.1). However, these measurements have been discarded. In Figure F-24 scatter plots (for more detail on plots see Section 4.2) have been given of measured and computed values for significant wave height and mean wave periods at 171, obtained in both February and October 2002. Whereas for February 2002 the measured values are predicted accurately by the SWAN model, the measured values for the significant wave height are all approximately 50% lower than the computed values during the October 2002 storm (in circle in Figure F-24). In the next section one can observe that the measurements and computations at MP5, which is at almost the same location as MP17, agree very well, implying that the measurements rather than the SWAN results at pressure sensor 171 are at least questionable during the storm of October 2002. For that reason they have not been used in the analysis and have been replaced by the measured values obtained with pressure sensor 175.

4.2 Scatter plots and statistical information

As mentioned in the previous section, the results of the SWAN versions 30.62 and 40.16 for the standard and advanced hindcasting method have been analysed by means of statistical information and scatter plots. The most valuable information is obtained by analysing the results per measurement location, per physical situation (ebb/flood current, depth limitation or presence of low frequency energy) and per storm day. According to Table 4.2 this corresponds to the cases: S01opp01, S02par01, S03dep01, S04nde01, S05dbl01 (distinction per physical process) and S06loc01, S07loc01, S08loc01, S09loc01, S10loc01, S11loc01, S12loc01 (distinction per location) and S13str01, S14str01, S15str01, S16str01, S17str01 (distinction per storm day).

In the Appendix 'Figures' scatter plots have been presented for each of the 17 cases mentioned above. For each case a figure is presented consisting of four subplots, in which the computations for the four cases (SWAN 30.62, 30.62+, 40.16 and 40.16+, indicated with different markers) are plotted against measured values for the significant wave height H_{m0} and the spectral mean wave periods $T_{m0,1}$, $T_{m0,2}$ and $T_{m-1,0}$. For each case the performance of the SWAN versions and hindcasting methods can be compared in a glance. Figures in which the cases have been considered separately are available on CD-ROM. A similar set of figures has been generated for the wave periods based on the peak period: T_p, T_{pb}, T_{pbeq}, T_{pm}. These figures have been stored on CD-ROM as well. Only for those cases that are explicitly mentioned in the analysis of T_{pm} the figures are given.

The statistical parameters are given in Appendix C for all cases mentioned in Table 4.2. The format is equal to the format in Table 4.1. Per spectral wave parameter H_{m0}, $T_{m0,1}$, $T_{m0,2}$ and $T_{m-1,0}$ and characteristic peak period T_{pm} the statistical parameters are given for the four cases 30.62, 30.62+, 40.16 and 40.16+, making the comparison convenient. For the peak period measures T_p, T_{pb} and T_{pm} not only scatter plots have been generated for the 17 cases mentioned above, but also statistical parameters have been generated. This information has not been included in the Appendices 'Figures' and C, but have been stored on CD-ROM. The discrete peak period measures are very sensitive for fluctuations in the (measured) spectra. Therefore, the emphasis is on the spectral mean wave period measures in the following analysis.

The scatter plots and statistical parameters provide useful information about the performance of SWAN and the reliability of the hindcasting methods. The performance of the four cases will be discussed for each spectral wave parameter H_{m0}, $T_{m0,1}$, $T_{m0,2}$ and $T_{m-1,0}$.

Reliability of RAND2001: Case 1

In Table 4.3a the bias between computed and measured significant wave height (defined in (B.1) in Appendix B), relative to the average measured significant wave height (defined in (B.3) in Appendix B), is given for all locations. In Table 4.3b-d the same statistical values are given for the three mean wave periods. The information is obtained from the tables in Appendix C, for the cases Sxxloc01, with xx=06, 07, …, 12. The standard deviation (defined in (B.2) in Appendix B), relative to the average measured significant wave height, is given as well. When the standard deviation is smaller than the bias there is a structural mismatch between measurements and computations. Note that the measured data also have error bands. Since these are unknown, a difference in relative bias of 10% has been accepted in the analysis below.

As mentioned in Section 1.3 the reliability of the wave conditions in the RAND2001 dataset is investigated by considering Case 1. The bias of the significant wave height is negative at all locations (except MP17), indicating an under-prediction by the model. The bias is less than 10% for all locations except at MP17 and MP6 (and approximately 10% at MP16). Except at MP17, MP3 and MP6, the relative bias between the measured and computed wave periods is less than 10%. Similar results can also be found in WL | Delft Hydraulics (2000). In that study SWAN results have been compared with laboratory measurements of waves propagating over the shallow foreshore (scale 1:40) in front of the Petten Sea Defence. In shallower regions $T_{m-1,0}$ and T_{pm} are predicted less accurate.

In Figure F-25 the measured and computed wave spectra have been plotted at four instances for three different locations, i.e. MP3 (Figure F-25a), MP5 and MP17 (Figure F-25b) and MP6 (Figure F-25c). Especially at MP6 the total amount of wave energy is under-predicted. A second peak is predicted by SWAN, but the amount of energy at the higher frequencies is underestimated, resulting in an under-prediction of $T_{m0,1}$ and $T_{m0,2}$. The strong under-prediction of low-frequency wave energy leads to an under-prediction of $T_{m-1,0}$.

H_{m0}	relative bias				relative standard deviation			
	30.62	30.62+	40.16	40.16+	30.62	30.62+	40.16	40.16+
MP1	-1.7%	-1.3%	-2.3%	-3.4%	21.8%	15.4%	22.8%	14.7%
MP2	-4.3%	-4.6%	-4.5%	-5.9%	15.7%	12.3%	16.4%	13.3%
MP3	-8.2%	-8.5%	-5.5%	-7.8%	16.1%	9.8%	17.9%	9.6%
MP16	-10.1%	-9.6%	-8.6%	-2.1%	4.9%	6.3%	5.1%	7.1%
MP17	22.6%	22.3%	20.3%	27.5%	18.2%	10.3%	20.1%	13.0%
MP5	-3.1%	-0.6%	-6.7%	-1.1%	13.3%	6.4%	13.1%	7.8%
MP6	-30.0%	-6.9%	-25.7%	0.8%	9.2%	10.2%	9.0%	11.2%
Total	-7.4%	-4.4%	-6.7%	-3.1%	18.8%	13.9%	19.0%	14.6%

Table 4.3a Relative bias and standard deviation of significant wave height H_{m0} at all locations

$T_{m0,1}$	relative bias				relative standard deviation			
	30.62	30.62+	40.16	40.16+	30.62	30.62+	40.16	40.16+
MP1	-1.4%	-4.8%	0.0%	-4.0%	15.6%	7.0%	15.3%	6.1%
MP2	-9.2%	-7.4%	-14.2%	-7.4%	12.8%	7.0%	13.5%	7.3%
MP3	6.2%	8.5%	2.4%	10.1%	12.3%	7.7%	10.9%	8.1%
MP16	-5.1%	8.3%	2.8%	13.6%	5.1%	5.0%	5.4%	6.1%
MP17	-21.0%	-7.2%	-19.2%	-1.8%	6.1%	8.2%	9.5%	10.7%
MP5	-7.4%	3.7%	3.5%	9.9%	8.7%	6.0%	20.3%	8.0%
MP6	-7.1%	19.5%	10.8%	25.2%	11.4%	12.6%	14.4%	13.8%
Total	-5.2%	3.0%	-1.6%	5.9%	13.6%	12.5%	16.5%	14.1%

Table 4.3b Relative bias and standard deviation of spectral wave period $T_{m0,1}$ at all locations

$T_{m0,2}$	relative bias				relative standard deviation			
	30.62	30.62+	40.16	40.16+	30.62	30.62+	40.16	40.16+
MP1	-1.1%	-3.4%	-0.5%	-2.7%	13.6%	8.7%	13.2%	7.5%
MP2	-9.8%	-7.3%	-25.2%	-8.5%	13.6%	8.1%	17.0%	8.0%
MP3	13.1%	15.2%	-0.8%	15.9%	14.9%	9.4%	13.1%	8.6%
MP16	-4.1%	10.3%	5.0%	16.9%	6.8%	7.3%	7.4%	8.7%
MP17	-27.3%	-12.9%	-32.1%	-7.1%	6.6%	9.4%	12.1%	12.7%
MP5	-4.9%	4.8%	-1.7%	10.9%	10.0%	7.6%	28.7%	7.8%
MP6	-0.4%	29.6%	22.8%	37.6%	14.9%	16.7%	19.1%	19.3%
Total	-3.1%	5.7%	-4.4%	8.7%	16.6%	16.5%	24.2%	18.5%

Table 4.3c Relative bias and standard deviation of spectral wave period $T_{m0,2}$ at all locations

$T_{m-1,0}$	relative bias				relative standard deviation			
	30.62	30.62+	40.16	40.16+	30.62	30.62+	40.16	40.16+
MP1	-1.1%	-2.7%	0.5%	-2.1%	14.7%	5.9%	13.9%	5.3%
MP2	-8.1%	-5.5%	-6.7%	-4.9%	11.6%	6.5%	11.9%	6.6%
MP3	-0.9%	2.9%	0.1%	4.3%	8.8%	5.3%	8.5%	6.0%
MP16	-6.6%	5.6%	-2.0%	7.4%	4.1%	4.8%	4.1%	6.2%
MP17	-15.7%	-2.1%	-11.6%	0.2%	5.5%	7.9%	6.5%	9.0%
MP5	-9.0%	2.4%	1.5%	5.5%	8.2%	5.6%	12.0%	6.8%
MP6	-16.1%	2.5%	-7.9%	2.8%	8.8%	8.5%	9.2%	9.2%
Total	-8.1%	-0.3%	-3.9%	0.9%	11.8%	8.3%	11.3%	8.8%

Table 4.3d Relative bias and standard deviation of spectral wave period $T_{m-1,0}$ at all locations

T_{pm}	relative bias				relative standard deviation			
	30.62	30.62+	40.16	40.16+	30.62	30.62+	40.16	40.16+
MP1	3.9%	-0.7%	4.4%	-1.0%	11.5%	6.7%	11.2%	6.6%
MP2	-0.1%	-4.9%	0.3%	-5.0%	13.2%	11.1%	12.6%	10.9%
MP3	0.4%	-4.3%	3.0%	-3.0%	8.3%	6.8%	7.6%	7.0%
MP16	-0.4%	-1.8%	-0.4%	-2.2%	6.8%	7.0%	6.8%	9.1%
MP17	-1.2%	-0.5%	4.4%	2.3%	13.9%	9.7%	11.5%	10.8%
MP5	5.8%	-3.4%	5.9%	-3.7%	8.4%	9.1%	8.1%	10.7%
MP6	-18.4%	-18.0%	-18.7%	-22.2%	19.6%	17.7%	19.2%	18.3%
Total	-4.0%	-7.5%	-3.1%	-8.2%	18.6%	17.0%	18.5%	18.1%

Table 4.3e Relative bias and standard deviation of spectral wave period T_{pm} at all locations

Figure S10loc01a.a shows that H_{m0} is still strongly over-predicted at MP17, confirming the bias of 22.6% and a significantly smaller standard deviation of 18.2%. According to Figure F-25b the spectral shape is rather well predicted, but the amount of energy at all frequencies higher than $f_p/2$ is over-predicted. The results at 175 are better than at 171 for 26/27 October 2002 (compare Figures F-24 and S10loc01a.a), but the difference between measurements and computations is still significant. Also at 175 the measurements are questionable.

Also at MP6, and less profound at MP16, a structural under-prediction of the significant wave height is obtained, as well as for the wave period $T_{m-1,0}$. This has been observed by

Jacobse (2000) as well. Note that low-frequency energy is not taken into account in the modelling of SWAN. Furthermore, the wave period T_{pm} is structurally under-predicted by almost 20% (see also Figure S12loc01b.a).

An under-prediction of the high-frequency part of the spectrum would match with the observation of over-prediction of the spectral wave periods $T_{m0,1}$ and $T_{m0,2}$ by SWAN at MP3. However, the spectra in Figure F-25a (especially at 2 January 1995) only partly confirm the conclusion that at MP3 too less high-frequency energy is predicted by SWAN. Notice that an over-prediction at only MP3 was also observed by Jacobse (2000).

When the separate storm days are considered, one can observe from Tables 4.4a-d, which are generated from the tables in Appendix C for Sxxstr01 (xx=13, 14, …, 17), that the significant wave height and the spectral wave periods are predicted within an accuracy of 10% for almost all storm days. Conspicuous is the under-prediction of these four spectral wave parameters at January 2, 1995. A closer inspection of the data files shows that the largest deviations for the significant wave height are obtained at MP1 and MP2. This can also be observed by comparing Figures S06loc01a.a, S07loc01a.a and S14str01a.a. Since the agreement between measurements and computations obtained at January 1st is very good, and the computational results at these two locations are expected to be predicted rather accurately, the deviations might as well be caused by the measured data. Especially because the equipment has already suffered a storm the day before. On the other hand, the wave spectra at MP3, MP5 and MP6 for 2 January 1995 (16:40hr) all show a rather broad, almost double-peaked spectrum. This is not observed in the computational results. Only at this instant a measured spectrum is unavailable at YMW. At the boundary a spatially constant spectrum (i.e. spectrum at ELD) has been imposed at the boundary for this instant.

In contrast to all other storm days, the wave periods at January 10, 1995 are all over-predicted. However, the bias is less than the standard deviation. It is not clear what causes the over-predictions. An incorrect bottom profile might also contribute to these overpredictions.

H_{m0}	relative bias				relative standard deviation			
	30.62	30.62+	40.16	40.16+	30.62	30.62+	40.16	40.16+
1995/01/01	-3.0%	-2.4%	-3.2%	-2.2%	20,9%	16,6%	20,0%	16,1%
1995/01/02	-22.0%	-10.5%	-22.0%	-11.2%	18,2%	12,0%	20,4%	12,9%
1995/01/10	-0.1%	-5.5%	1.2%	-7.2%	15,6%	10,9%	16,2%	11,4%
2002/02/23	-6.6%	-7.1%	-5.0%	-4.3%	13,8%	11,3%	12,8%	12,1%
2002/10/27	-5.1%	2.1%	-4.3%	6.6%	17,7%	14,7%	17,0%	13,8%
Total	-7.4%	-4.4%	-6.7%	-3.1%	18.8%	13.9%	19.0%	14.6%

Table 4.4a Relative bias and standard deviation of significant wave height H_{m0} for all storm days

$T_{m0,1}$	relative bias				relative standard deviation			
	30.62	30.62+	40.16	40.16+	30.62	30.62+	40.16	40.16+
1995/01/01	-3.8%	2.0%	2.9%	5.5%	9.6%	8.0%	10.0%	11.3%
1995/01/02	-13.7%	0.8%	-11.9%	2.7%	14.0%	15.7%	18.2%	15.6%
1995/01/10	8.3%	5.8%	12.6%	8.3%	12.0%	13.1%	17.6%	14.6%
2002/02/23	-7.4%	5.6%	-1.7%	10.7%	8.6%	13.4%	10.3%	16.6%
2002/10/27	-8.0%	1.3%	-7.5%	3.5%	11.7%	10.4%	12.1%	11.1%
Total	-5.2%	3.0%	-1.6%	5.9%	13.6%	12.5%	16.5%	14.1%

Table 4.4b Relative bias and standard deviation of significant wave height $T_{m0,1}$ for all storm days

$T_{m0,2}$	relative bias				relative standard deviation			
	30.62	30.62+	40.16	40.16+	30.62	30.62+	40.16	40.16+
1995/01/01	0.0%	5.0%	2.9%	7.9%	11.8%	9.8%	15.3%	12.5%
1995/01/02	-12.4%	3.8%	-16.9%	4.8%	17.7%	19.1%	26.3%	18.0%
1995/01/10	11.7%	9.5%	9.2%	12.1%	12.0%	17.0%	28.7%	18.7%
2002/02/23	-5.7%	8.0%	-3.2%	14.4%	12.8%	18.3%	19.9%	23.4%
2002/10/27	-7.1%	3.3%	-10.5%	5.6%	16.5%	16.0%	20.4%	17.2%
Total	-3.1%	5.7%	-4.4%	8.7%	16.6%	16.5%	24.2%	18.5%

Table 4.4c Relative bias and standard deviation of significant wave height $T_{m0,2}$ for all storm days

$T_{m-1,0}$	relative bias				relative standard deviation			
	30.62	30.62+	40.16	40.16+	30.62	30.62+	40.16	40.16+
1995/01/01	-8,3%	-2,3%	-2,6%	-0,6%	11,8%	10,6%	10,9%	11,2%
1995/01/02	-15,7%	-1,9%	-10,9%	-1,3%	9,1%	9,1%	9,1%	8,8%
1995/01/10	2,5%	0,7%	7,6%	1,9%	12,1%	7,0%	11,8%	7,7%
2002/02/23	-9,0%	3,4%	-4,8%	5,4%	8,3%	7,6%	6,4%	8,7%
2002/10/27	-9,3%	-1,0%	-7,7%	-0,3%	8,7%	6,0%	7,1%	6,3%
Total	-8.1%	-0.3%	-3.9%	0.9%	11.8%	8.3%	11.3%	8.8%

Table 4.4d Relative bias and standard deviation of significant wave height $T_{m-1,0}$ for all storm days

T_{pm}	relative bias				relative standard deviation			
	30.62	30.62+	40.16	40.16+	30.62	30.62+	40.16	40.16+
1995/01/01	-8.0%	-11.4%	-6.5%	-11.1%	26.5%	28.4%	26.6%	28.7%
1995/01/02	-8.8%	-9.0%	-8.4%	-11.6%	18.3%	15.4%	18.0%	16.3%
1995/01/10	5.4%	-8.5%	5.1%	-9.1%	17.3%	15.0%	17.4%	15.9%
2002/02/23	-1.7%	-2.6%	-0.5%	-2.3%	15.1%	12.1%	15.3%	15.1%
2002/10/27	-6.9%	-5.7%	-4.7%	-5.9%	9.3%	8.9%	9.6%	10.5%
Total	-4.0%	-7.5%	-3.1%	-8.2%	18.6%	17.0%	18.5%	18.1%

Table 4.4e Relative bias and standard deviation of significant wave height T_{pm} for all storm days

In Tables 4.5a-d a distinction between physical processes has been made. The tables have been generated from the tables in Appendix C for S01opp01, S02par01, S03dep01, S04nde01, S05dbl01.

The measured spectral wave periods $T_{m0,1}$ and $T_{m0,2}$ are reasonably well predicted (within 10%). The significant wave height is under-predicted in the presence of an opposing or following current. We will return to this in the next subsection. Furthermore, the wave height is under-predicted at locations at which the waves are depth-limited. The effect of the bathymetry is significant in this situation. Accurate bed level data are crucial in the shallow areas. The largest differences between measurements and computations at depth-limited locations are observed at MP6, which happens to be the shallowest location. Also the spectral wave period $T_{m-1,0}$ is under-predicted by more than 10% at the depth-limited locations, denoting the relevance of modelling low-frequency energy.

H_{m0}	relative bias				relative standard deviation			
	30.62	30.62+	40.16	40.16+	30.62	30.62+	40.16	40.16+
opposing current	-11.8%	-4.8%	-12.2%	-5.6%	22.3%	12.3%	23.3%	12.3%
following current	-12.0%	-3.4%	-12.3%	-2.4%	20.9%	16.3%	21.6%	17.0%
depth-limitation	-13.9%	-9.6%	-10.8%	-5.7%	12.1%	10.9%	12.2%	12.7%
no depth-limitation	2.7%	3.5%	0.9%	3.0%	23.8%	16.0%	25.5%	16.9%
low-freq. energy	-16.5%	-6.2%	-15.0%	-3.1%	15.5%	9.3%	14.8%	10.8%

Table 4.5a Relative bias and standard deviation of significant wave height H_{m0} for all types of conditions

$T_{m0,1}$	relative bias				relative standard deviation			
	30.62	30.62+	40.16	40.16+	30.62	30.62+	40.16	40.16+
opposing current	-10.1%	1.9%	-8.3%	2.2%	15.4%	13.9%	19.6%	13.7%
following current	-7.4%	0.7%	-2.8%	5.1%	11.3%	10.5%	13.4%	12.5%
depth-limitation	-3.8%	9.5%	2.4%	13.0%	10.2%	12.7%	14.1%	14.7%
no depth-limitation	-6.5%	-2.1%	-3.3%	1.2%	16.1%	9.2%	17.7%	10.4%
low-freq. energy	-5.6%	12.4%	7.2%	17.5%	11.6%	12.8%	15.3%	14.1%

Table 4.5b Relative bias and standard deviation of significant wave height $T_{m0,1}$ for all types of conditions

$T_{m0,2}$	relative bias				relative standard deviation			
	30.62	30.62+	40.16	40.16+	30.62	30.62+	40.16	40.16+
opposing current	-7.8%	7.5%	-10.9%	7.0%	19.2%	16.0%	28.3%	15.3%
following current	-6.0%	0.5%	-5.8%	4.6%	15.7%	14.8%	19.8%	16.0%
depth-limitation	1.3%	15.6%	4.7%	19.6%	13.0%	16.1%	23.4%	19.5%
no depth-limitation	-7.7%	-2.8%	-10.1%	0.5%	17.5%	11.7%	22.3%	12.1%
low-freq. energy	0.2%	19.3%	11.3%	25.2%	14.8%	17.3%	23.6%	19.6%

Table 4.5c Relative bias and standard deviation of significant wave height $T_{m0,2}$ for all types of conditions

$T_{m-1,0}$	relative bias				relative standard deviation			
	30.62	30.62+	40.16	40.16+	30.62	30.62+	40.16	40.16+
opposing current	-12.7%	-1.9%	-8.7%	-2.3%	9.7%	8.7%	9.3%	8.2%
following current	-9.4%	-1.0%	-4.7%	1.3%	11.0%	9.7%	10.5%	10.0%
depth-limitation	-10.2%	1.1%	-5.7%	2.0%	10.1%	9.2%	8.6%	9.5%
no depth-limitation	-5.8%	-0.6%	-1.1%	1.0%	13.7%	6.6%	13.9%	7.3%
low-freq. energy	-12.2%	2.0%	-4.1%	3.3%	9.6%	7.6%	10.4%	8.4%

Table 4.5d Relative bias and standard deviation of significant wave height $T_{m-1,0}$ for all types of conditions

T_{pm0}	relative bias				relative standard deviation			
	30.62	30.62+	40.16	40.16+	30.62	30.62+	40.16	40.16+
opposing current	-4.8%	-7.1%	-4.9%	-10.1%	13.0%	11.7%	13.1%	13.1%
following current	-8.8%	-8.3%	-7.1%	-7.8%	24.9%	26.3%	25.1%	26.7%
depth-limitation	-10.5%	-12.4%	-9.6%	-14.0%	21.3%	20.2%	21.5%	21.3%
no depth-limitation	3.4%	-1.5%	4.9%	-1.4%	11.9%	8.5%	11.0%	9.2%
low-freq. energy	-7.8%	-11.9%	-7.9%	-14.4%	20.6%	16.8%	20.4%	18.7%

Table 4.5e Relative bias and standard deviation of significant wave height T_{pm} for all types of conditions

Improving the hindcast method

The question whether a better description of the input of the wave model SWAN by means of a more advanced hindcasting method leads to better results, is answered by comparing case 1 and 2, or case 3 and 4. In most situations the advanced hindcasting method has lead to better results for all spectral wave parameters. Clearly, there is a shift in the estimate for the wave period measures. In general, the wave period measures are no longer underestimated at all instants and at all locations. Not only the bias decreases, but also the standard deviation becomes smaller. In particular, the bias decreases at locations where the bias in the spectral parameters was large for the standard hindcast method (the mean wave periods $T_{m0,1}$ and $T_{m0,2}$ at MP6 excluded). The improvement of the prediction for $T_{m-1,0}$ is significant. The two wave period measures which lay more weight on the high frequencies of the spectrum, i.e. $T_{m0,1}$ and $T_{m0,2}$, improve at some locations. The bias sometimes increases, whereas the standard deviation decreases in general.

A number of interesting aspects are observed by considering Tables 4.3-4.5. First of all, from Table 4.5 the conclusion is drawn that inclusion of an existing current in the modelling, leads to better results for both wave height and wave period measures.

Secondly, according to Table 4.3a and 4.3d the prediction of the significant wave height and mean wave period $T_{m-1,0}$ at MP6 has significantly improved from case 1 (30.62) to case 2 (30.62+) and from case 3 (40.16) to case 4 (40.16+), but the mean wave period $T_{m0,1}$ and $T_{m0,2}$ are significantly and structurally overestimated. The amount of high-frequency wave energy is strongly under-predicted at MP6 (see Figure F-25c). The under-prediction of the wave period T_{pm} is comparable to the under-prediction obtained with the 'standard' hindcast method (see also Figure S12loc01b.a). At MP6 the update of the bottom profile in the advanced hindcast method seems to be successful. Since the still-water depth (without set-up) at MP6 is only 1.7m, depth-effects are dominant at this location and correct depth values are crucial for correct wave predictions. The wind input majorly acts on the high-frequency wave motion. It is questionable whether the newly generated wind fields are realistic in the coastal zone.

At the four instances at which the spectra are given in Figure 25, the spectra computed with version 40.16 are broader than those obtained with version 30.62. However, the spectra resulting from latter version have a stronger tendency to predict a secondary peak. Inspection of the source terms suggests that the positive lobe of the triads is cancelled by the negative lobe of the quadruplets in SWAN 40.16, where triads and quadruplets are calculated simultaneously. Furthermore, the computational depth determined by version 40.16 is often larger than the one obtained with version 30.62. Consequently, the dissipation due to breaking and bottom friction is smaller, which explains the higher amount of total wave energy, and the effect of three-wave interactions is less.

Improving SWAN

By comparing case 1 and 3, or case 2 and 4 possible improvements with the newer version 40.16 can be investigated. Generally the results obtained with version 30.62 and version 40.16 are more or less the same, either with the standard or the advanced hindcasting method. Only incidental differences are observed, especially when triads and quadruplets are both active, but these are not significant or structural enough, to conclude that neither one of the two model versions is better than the other.

4.3 Discussion

The standard hindcasting method that provided spectral wave parameters for the RAND2001 database using SWAN version 30.62 is reliable for most conditions and at most locations. The measurement data obtained at MP17 (171 and 175) seems to be unreliable for 26/27 October 2002. Furthermore, at MP6, and less profound at MP16, the significant wave height and the spectral wave period $T_{m-1,0}$ are strongly under-predicted. The difference between the actual bed levels during the storm events and the bed levels used in the computations might contribute to the disagreement between the measured and computed significant wave height and mean wave period $T_{m-1,0}$ at MP6 and MP16. The reliability of the wave conditions in the RAND2001 dataset at MP6 is questionable, especially because the hydraulic boundary conditions have to be determined in the vicinity of MP6.

Improving the computed wave conditions in RAND2001 has been investigated by considering a more recent SWAN version, i.e. version 40.16, and by considering a more advanced hindcasting method. The former did not lead to better results. The conclusion that SWAN 40.16 would be an improvement of SWAN 30.62 for the shallow foreshore at the Petten Sea Defence, cannot be drawn.

Applying the 'advanced' hindcast method, including more recent ray measurements of the bed level, strongly improved predictions for the spectral wave parameters H_{m0} and $T_{m-1,0}$ have been obtained. On the other hand, the wave period predictions for $T_{m0,1}$ and $T_{m0,2}$ become significantly worse. This is probably due to a poor estimate of the wind field near the coastline. Inclusion of the present flow field improves the prediction of all wave parameters.

Jacobse (2000) performed a hindcast study for the two storms in 1995 (1/2 January and 10 January) and chose instants at which the conditions could be considered more or less as stationary. The results in Jacobse can be compared with the results in case 1 in this study. Compared to the study of Jacobse (2000) the significant wave height is predicted with approximately the same accuracy, i.e. within 10% at all locations. At MP6 Jacobse (2000) obtained an under-prediction of 25%, which is of the same order (30%) as in this study. However, here the standard deviation is significantly higher.

Although there are some deviations, the bias in the mean wave periods $T_{m0,1}$ and $T_{m0,2}$ are of comparable magnitude. The standard deviation is significantly larger. This is also true for the wave period $T_{m-1,0}$, except for the shallower areas, where the mismatch in the presently performed hindcast study is larger. The strong temporal variations of the spectrum at the boundary at the instationary instants chosen in this study apparently cause a stronger scatter in the results.

5 Conclusions and recommendations

Measurements at the Petten Sea Defence have been used to investigate the reliability of the RAND2001 database, which consists of wave conditions for the Dutch coast, the Wadden Sea and Westerschelde. Petten is considered to be characteristic for the closed Dutch coast.

In this report results have been presented and analysed of SWAN computations (in stationary mode) for 21 moments on 5 storm days. Three of these storm days occurred in January 1995, one in February 2002 and one in October 2002. At the moments considered the wind and wave conditions are instationary. This is partly due to the fact that the observed boundary conditions in the stations ELD and YMW show a variation between succeeding time steps (20 minutes). Based on an analysis of the computational results and a comparison with measurements the following conclusions can be formulated:

- The results of the comparison of the computations (at MP6 and MP16) suggest that the computational results obtained with the method used for the RAND2001 database are unreliable. At MP16 the underestimation of the significant wave height and the spectral wave period $T_{m-1,0}$ is significant. Further offshore, the spectral wave parameters for the wave height and wave period are only underestimated slightly. These results imply that the data in RAND2001 are not necessarily reliable.
- The advanced hindcasting approach generally leads to improved results in comparison with the standard approach. The inclusion of current effects and the use of a more recent bottom topography improves the results significantly.
- Estimates for the spectral wave period $T_{m-1,0}$ have improved considerably by the more advanced hindcasting approach, whereas estimates for the spectral wave periods $T_{m0,1}$ and $T_{m0,2}$, have not been improved. The latter results can be attributed to a poor description of the wind field near Petten and to poor model behaviour for the high frequency range.
- In general the performance of SWAN 40.16 is similar to SWAN 30.62.
- Especially in shallow areas accurate knowledge of the bed location is important to obtain reliable information from a hindcast study.

Furthermore, the following recommendations are made:

- The differences in computational results between the various cases are the result of a number of modifications in modelling techniques that were included simultaneously. The contribution of each of these modifications to the final results can therefore not be identified. It is therefore recommended to perform sensitivity studies to the contribution of each of these effects.
- The predicted water levels and flow field at locations on the Petten ray should be compared with the observed water levels and flow fields at these locations. Available pressure gauges could be used to reconstruct the water level at the indicated locations. Especially in shallow areas accurate water level and flow field data should be available;
- In the case flow models are used for wave hindcast near Petten, they should be calibrated for proper results in the area of interest.

- The reliability of the measurements in general and postprocessing of these measurements in particular must be quantified in order to be able to draw correct conclusions in comparing measurements and numerical model results.
- The same wind fields should be used for the generation of the current fields and the wave fields for consistency purposes; although the quality of the local wind field is more important for the wave predictions at Petten than for the current modelling.
- Additional output points in the Petten ray should be defined and special test output (SWAN output option TEST) should be defined in this ray to investigate the relative contribution of individual source terms on the evolution of the wave field.
- In order to investigate directional effects, such as e.g. Bragg-scattering, measured directional information should be available from high-resolution directional wave measurements.
- Bottom information around the Petten ray should be obtained regularly for an area of at least 2 km in North and South direction, and not in a strip of only 500 m wide.

References

Alkyon (1999a): Wave computations in the Waddensea. Alkyon report A352, November 1999

Alkyon (1999b): Wave computations for the coast of the Netherlands. Alkyon report A480, November 1999

Alkyon (1999c): Operational peak period and test. Alkyon report A411, September 1999

Alkyon (2001): Maatgevende bodem. Onderzoek naar een maatgevende bodem, gebaseerd op 35 jaar jarkus-metingen. Alkyon rapport A843, November 2001

Alkyon & WL | Delft Hydraulics (2002): Generieke methode voor het hindcasten van gemeten stormen. Alkyon / WL | Delft Hydraulics report A1002/H4149 (in Dutch), September 2002

Battjes, J.A. and G.Ph. van Vledder (1984): Verification of Kimura's theory for wave group statistics. *Proc. 19th International Conference Coastal Engineering*, ASCE, Houston, 642-648

Booij, N., R.C. Ris and L.H. Holthuijsen (1999): A third-generation wave model for coastal regions. Part I: Model description and validation. *J. Geoph. Research*, 104 (C4), 7649-7666

Jacobse, J.J. (2000): Validatie van het SWAN-model voor de Pettemer zeewering (in Dutch). RIKZ werkdocument 2000.150x, December 2000

Ris, R.C., L.H. Holthuijsen and N. Booij (1999): A third-generation wave model for coastal regions. Part II: Verification. *J. Geoph. Research*, 104 (C4), 7667-7681

Roskam, B. and J. Hoekema (2003): Overzicht van de golfgegevens in de stormperiode 25-28 oktober 2002 (p02s3) t.b.v. de Petten-hindcast (in Dutch). Memo RIKZ, February 2003

SWAN User Manual (2000): SWAN Cycle III version 40.11 User Manual (not the short version). Delft University of Technology, Dep. of Civil Engineering, The Netherlands, October 19, 2000

WL | Delft Hydraulics (2000): Numerical model investigations on coastal structures with shallow foreshores, WL | Delft Hydraulics report H3351. May 2000

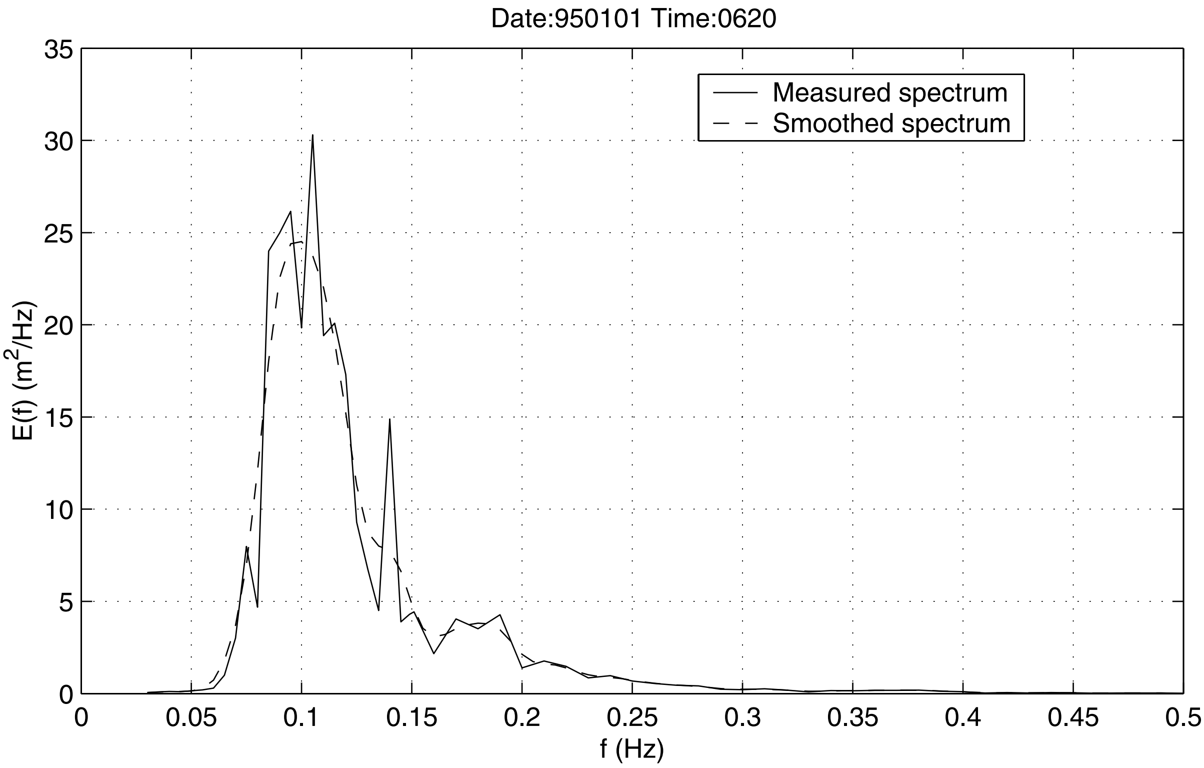

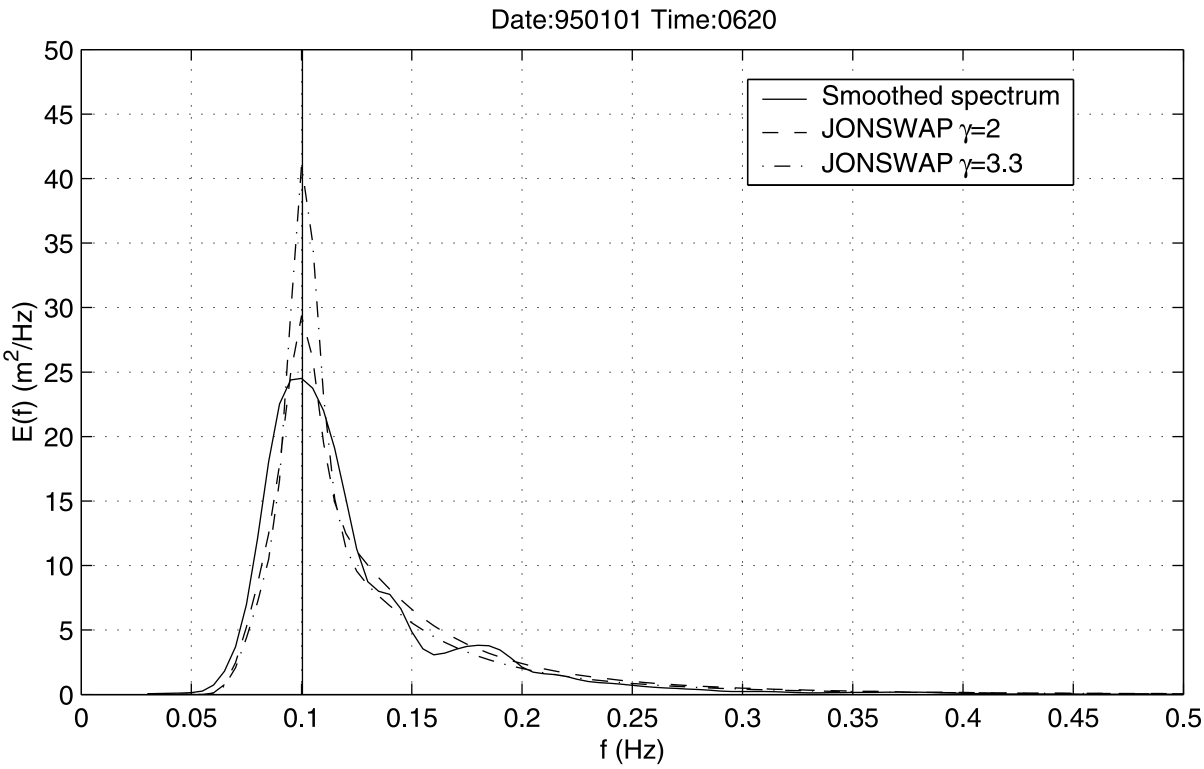

Measured, smoothed and JONSWAP spectra vertical line indicates position of $1/T_{pb}$	storms 1995	ELD
	Measurements Petten Sea Defence	
WL | DELFT HYDRAULICS & ALKYON HYDRAULIC CONSULTANCY & RESEARCH	H4197/A1044	Fig. F−6

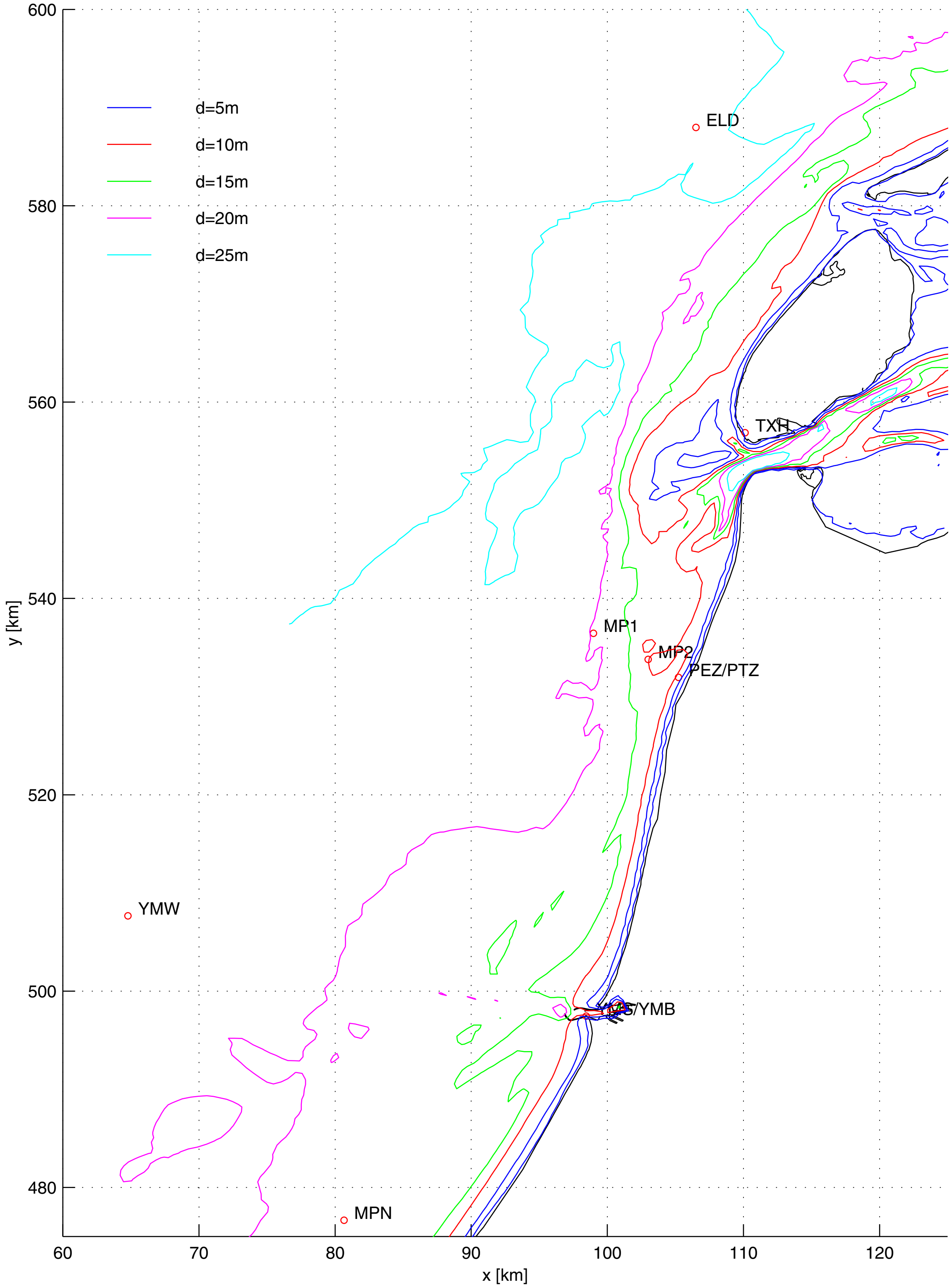

Location of measurement stations (water level, wind and waves)	Measurements Petten Sea Defence	
WL | DELFT HYDRAULICS –– ALKYON HYDRAULIC CONSULTANCY & RESEARCH	H4197/A1044	Fig. F–1a

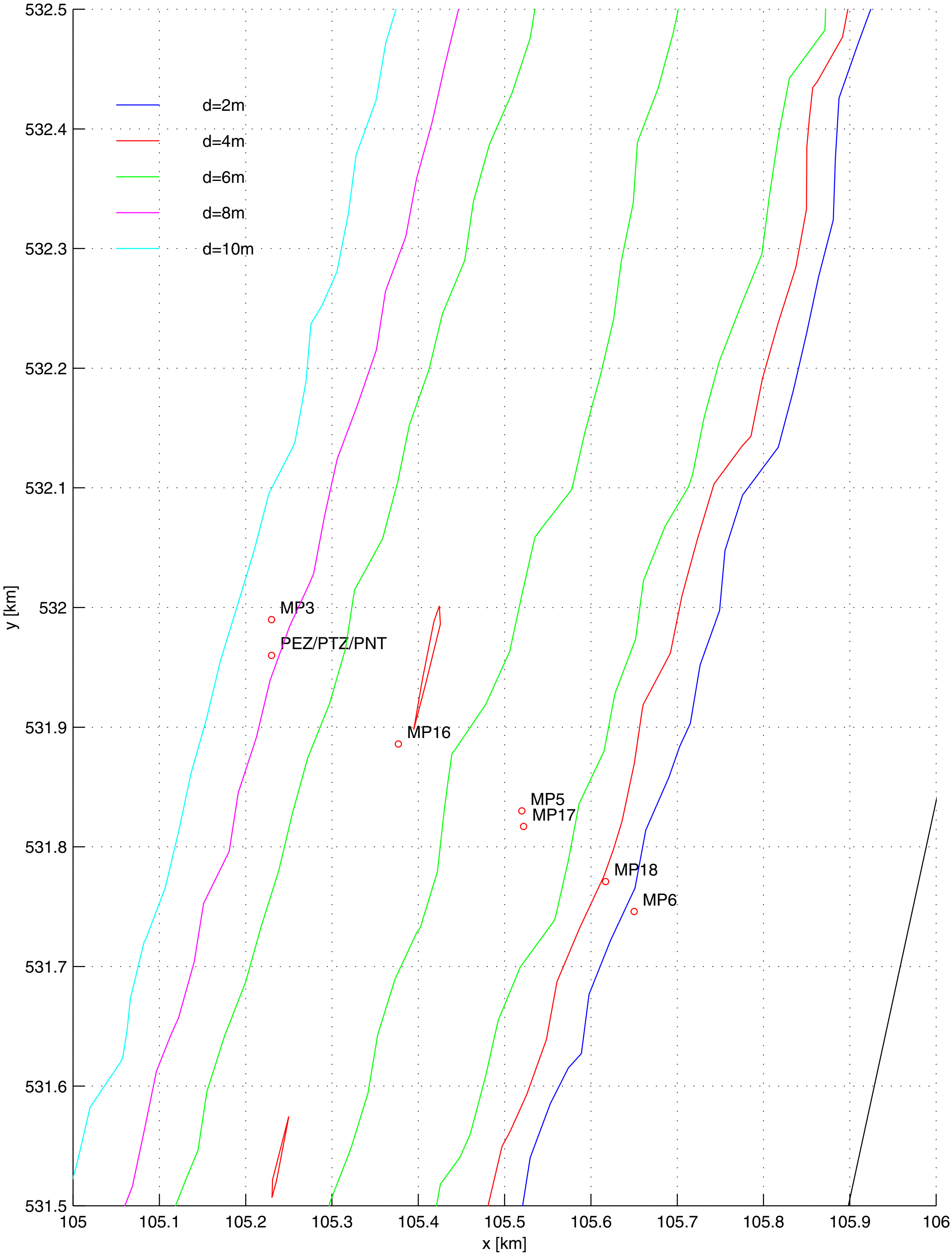

Location of measurement stations (water level, wind and waves) near Petten

Measurements Petten Sea Defence

WL | DELFT HYDRAULICS –– ALKYON HYDRAULIC CONSULTANCY & RESEARCH

H4197/A1044

Fig. F–1b

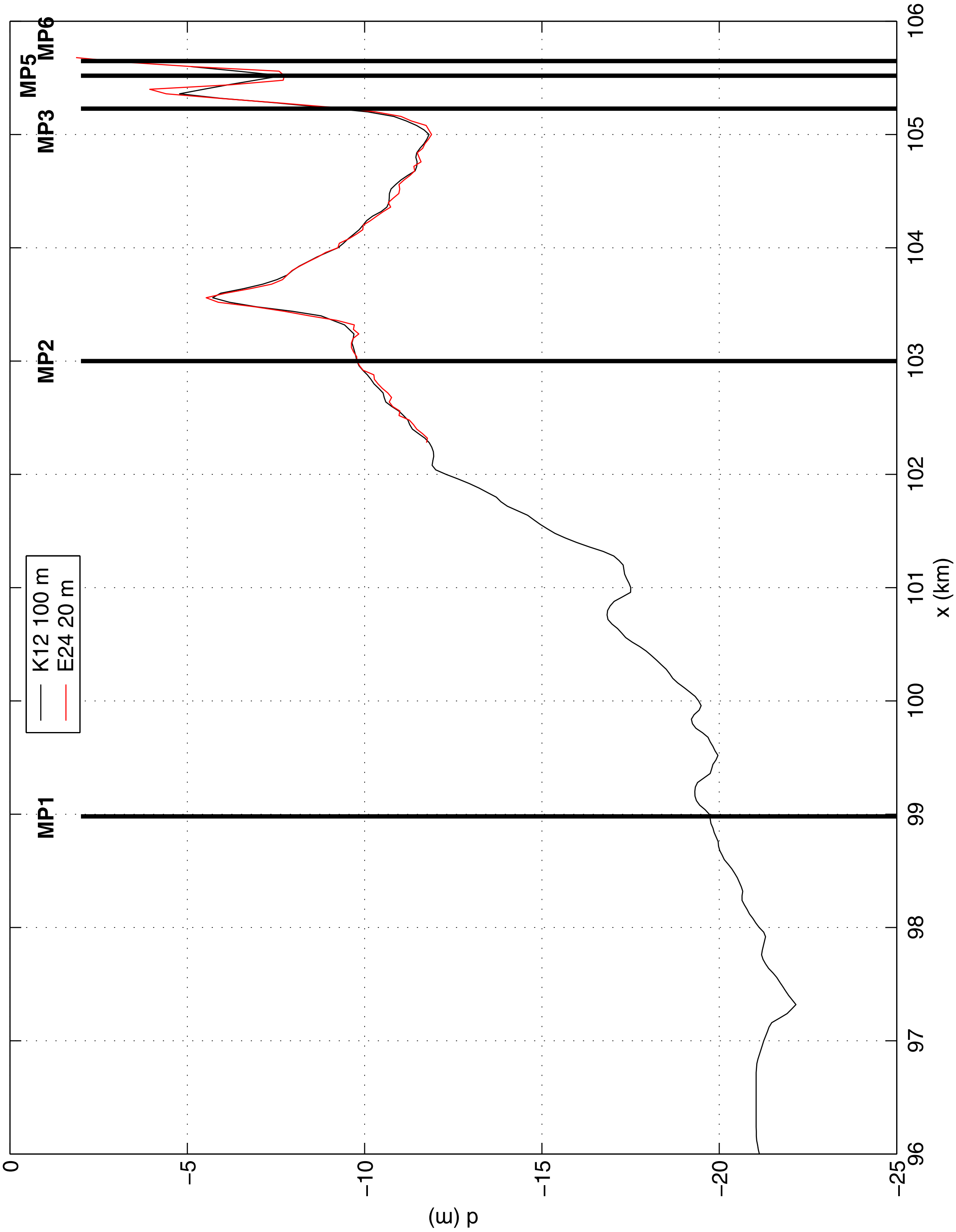

Bottom profile in Petten ray in 1995

Measurements Petten Sea Defence

WL | DELFT HYDRAULICS & ALKYON HYDRAULIC CONSULTANCY & RESEARCH

H4197/A1044

Fig. F−1c

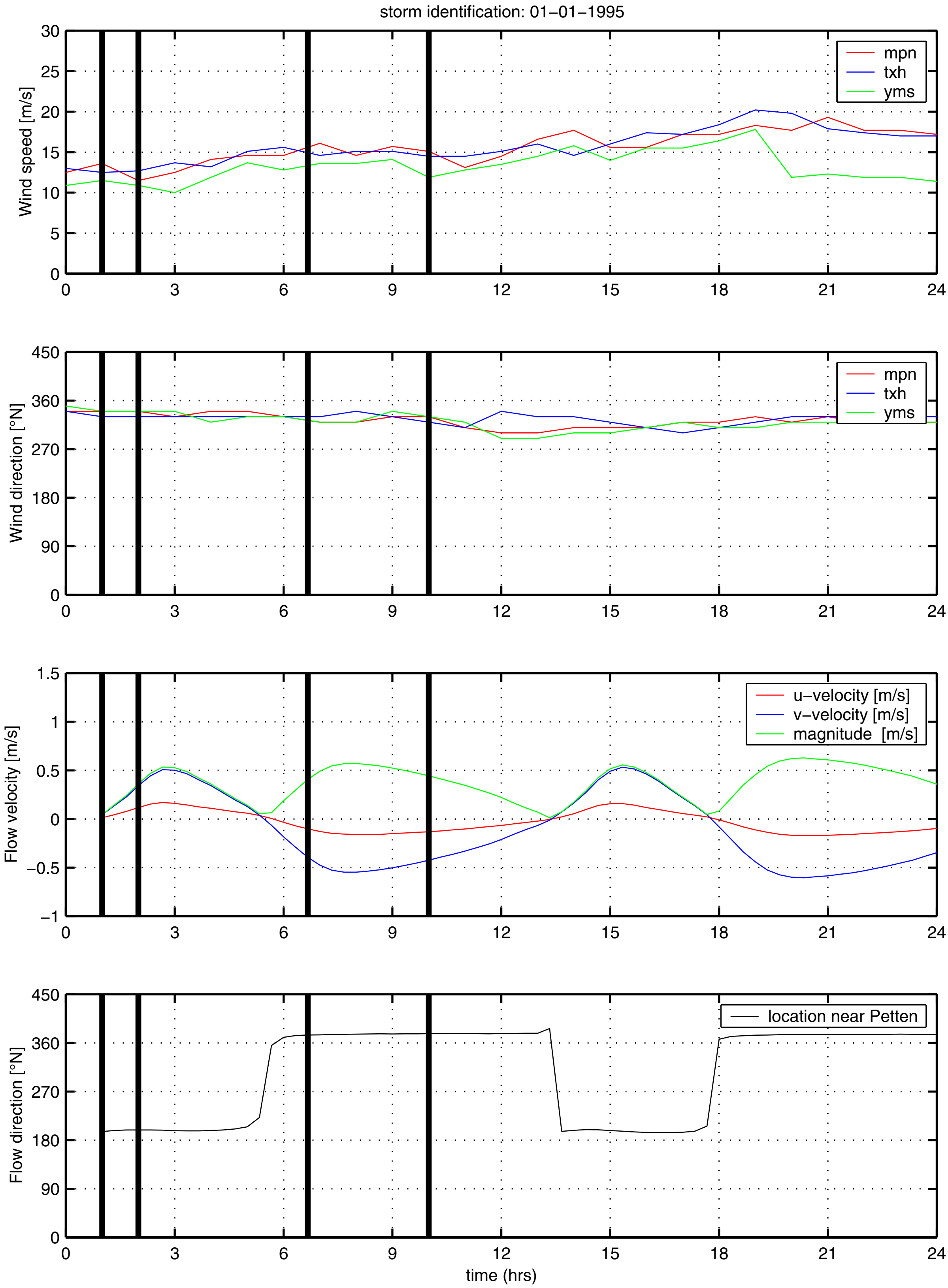

Time signals of computed flow characteristics and measured wind characteristics	storm: 01−01−1995	
	Measurements Petten Sea Defence	
WL I DELFT HYDRAULICS −− ALKYON HYDRAULIC CONSULTANCY & RESEARCH	H4197/A1044	Fig. F−2.a

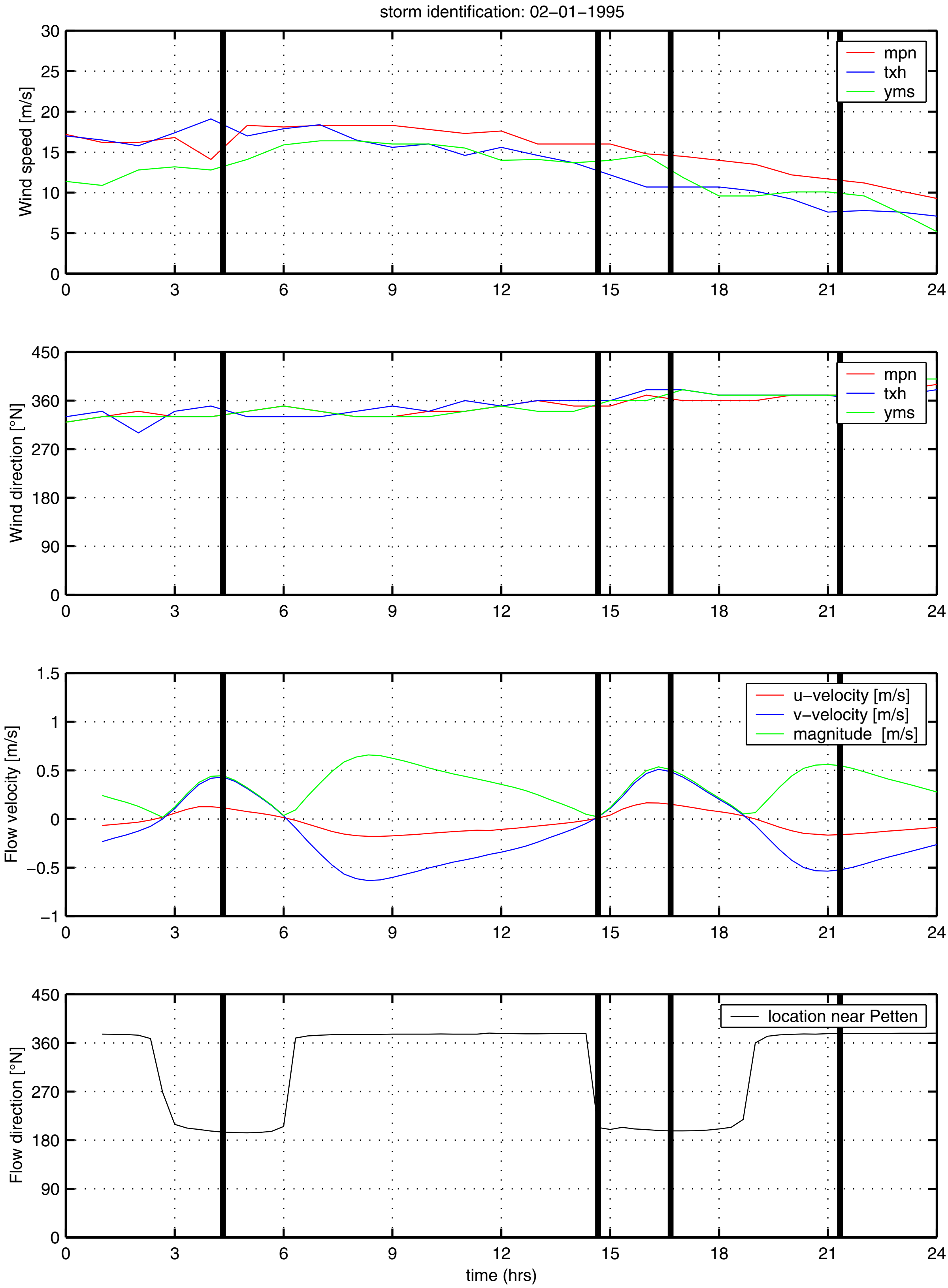

Time signals of computed flow characteristics and measured wind characteristics	storm: 02–01–1995	
	Measurements Petten Sea Defence	
WL | DELFT HYDRAULICS –– ALKYON HYDRAULIC CONSULTANCY & RESEARCH	H4197/A1044	Fig. F–2.b

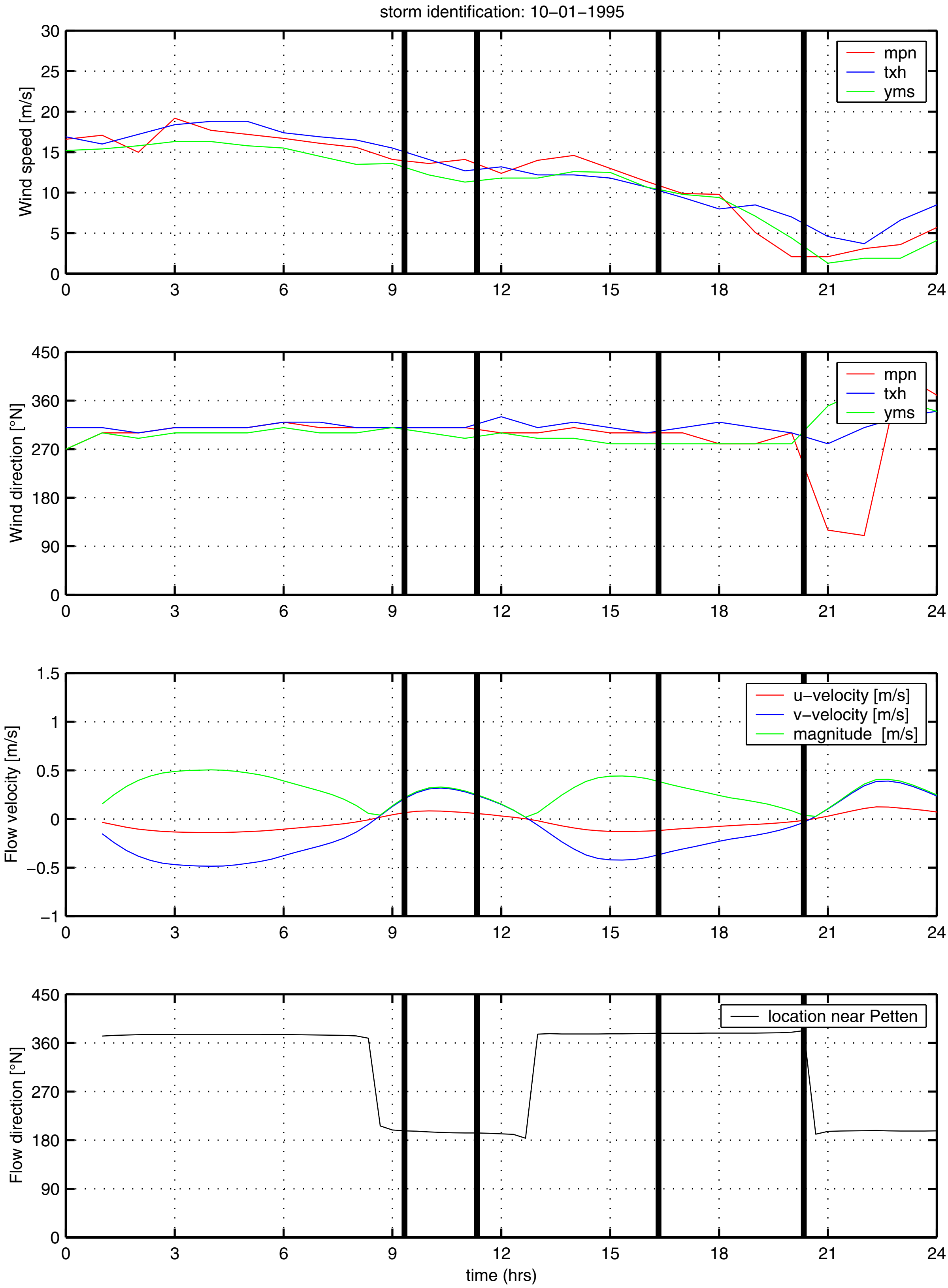

Time signals of computed flow characteristics and measured wind characteristics	storm: 10–01–1995	
	Measurements Petten Sea Defence	
WL | DELFT HYDRAULICS –– ALKYON HYDRAULIC CONSULTANCY & RESEARCH	H4197/A1044	Fig. F–2.c

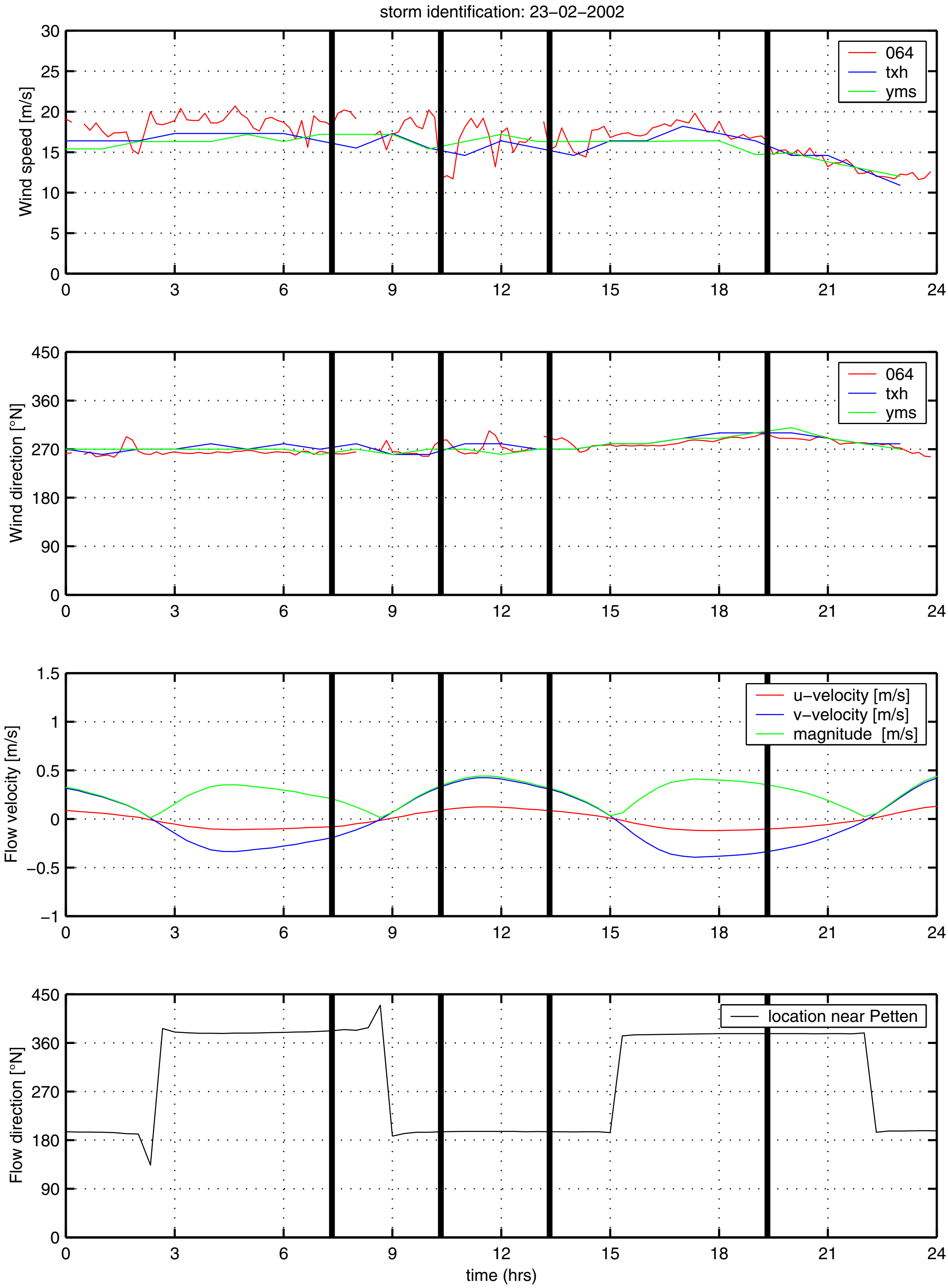

Time signals of computed flow characteristics and measured wind characteristics	storm: 23−02−2002	
	Measurements Petten Sea Defence	
WL I DELFT HYDRAULICS −− ALKYON HYDRAULIC CONSULTANCY & RESEARCH	H4197/A1044	Fig. F−2.d

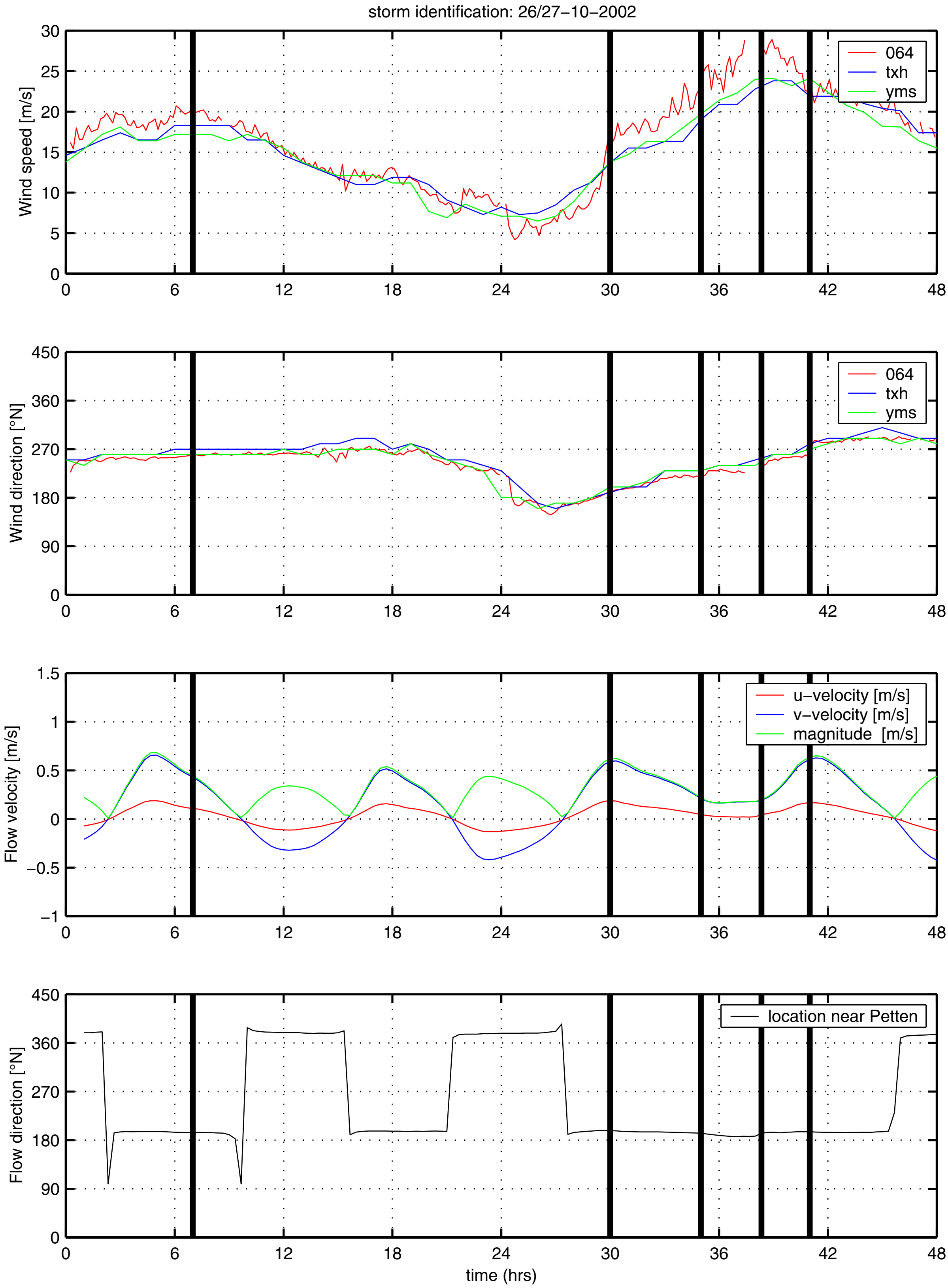

Time signals of computed flow characteristics and measured wind characteristics	storm: 26/27−10−2002	
	Measurements Petten Sea Defence	
WL I DELFT HYDRAULICS −− ALKYON HYDRAULIC CONSULTANCY & RESEARCH	H4197/A1044	Fig. F−2.e

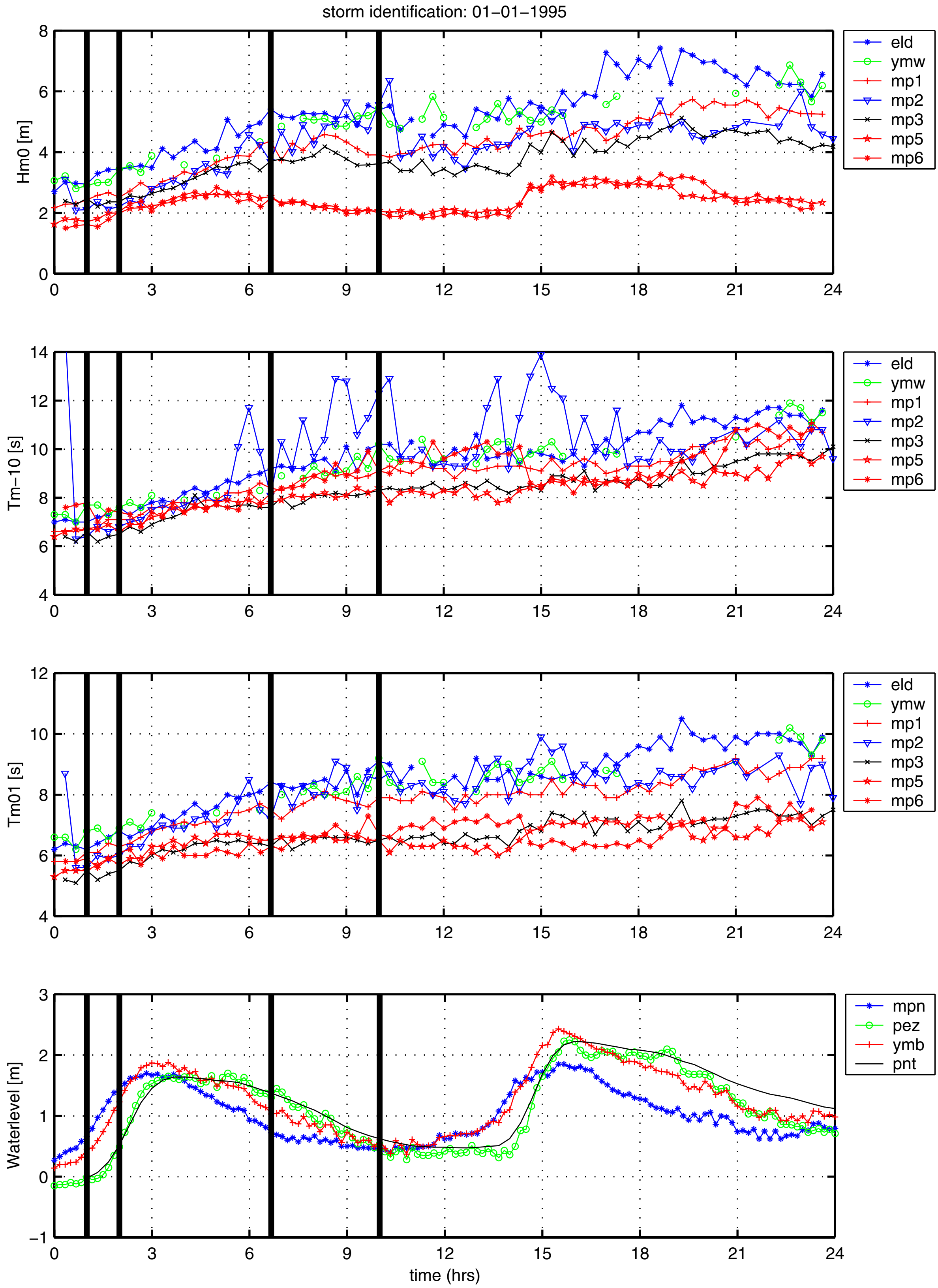

Time signals of measured spectral parameters and water level (computed at ptn)	storm: 01−01−1995	
	Measurements Petten Sea Defence	
WL | DELFT HYDRAULICS −− ALKYON HYDRAULIC CONSULTANCY & RESEARCH	H4197/A1044	Fig. F−3.a

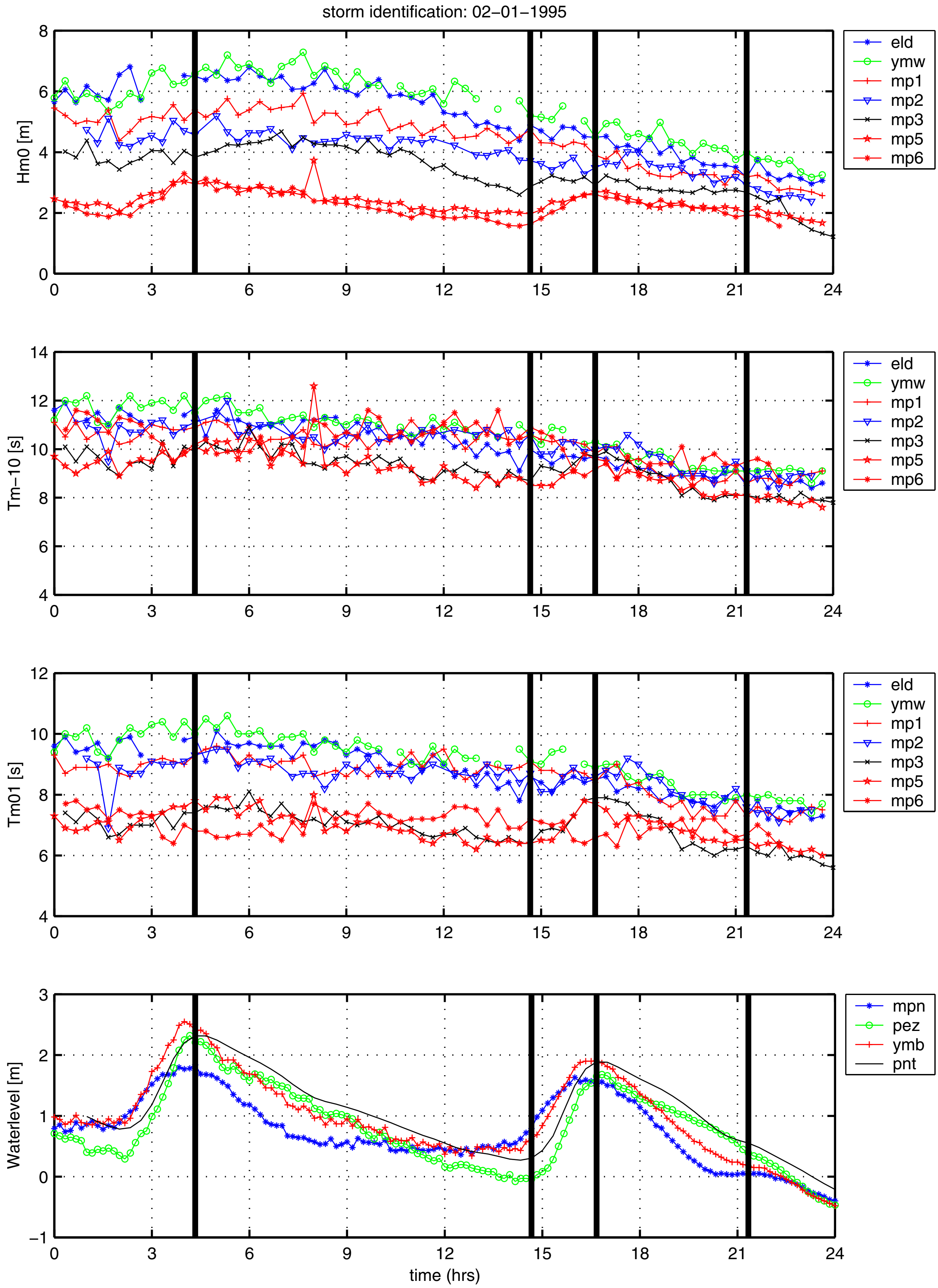

Time signals of measured spectral parameters and water level (computed at ptn)	storm: 02−01−1995	
	Measurements Petten Sea Defence	
**WL	DELFT HYDRAULICS –– ALKYON HYDRAULIC CONSULTANCY & RESEARCH**	H4197/A1044	Fig. F−3.b

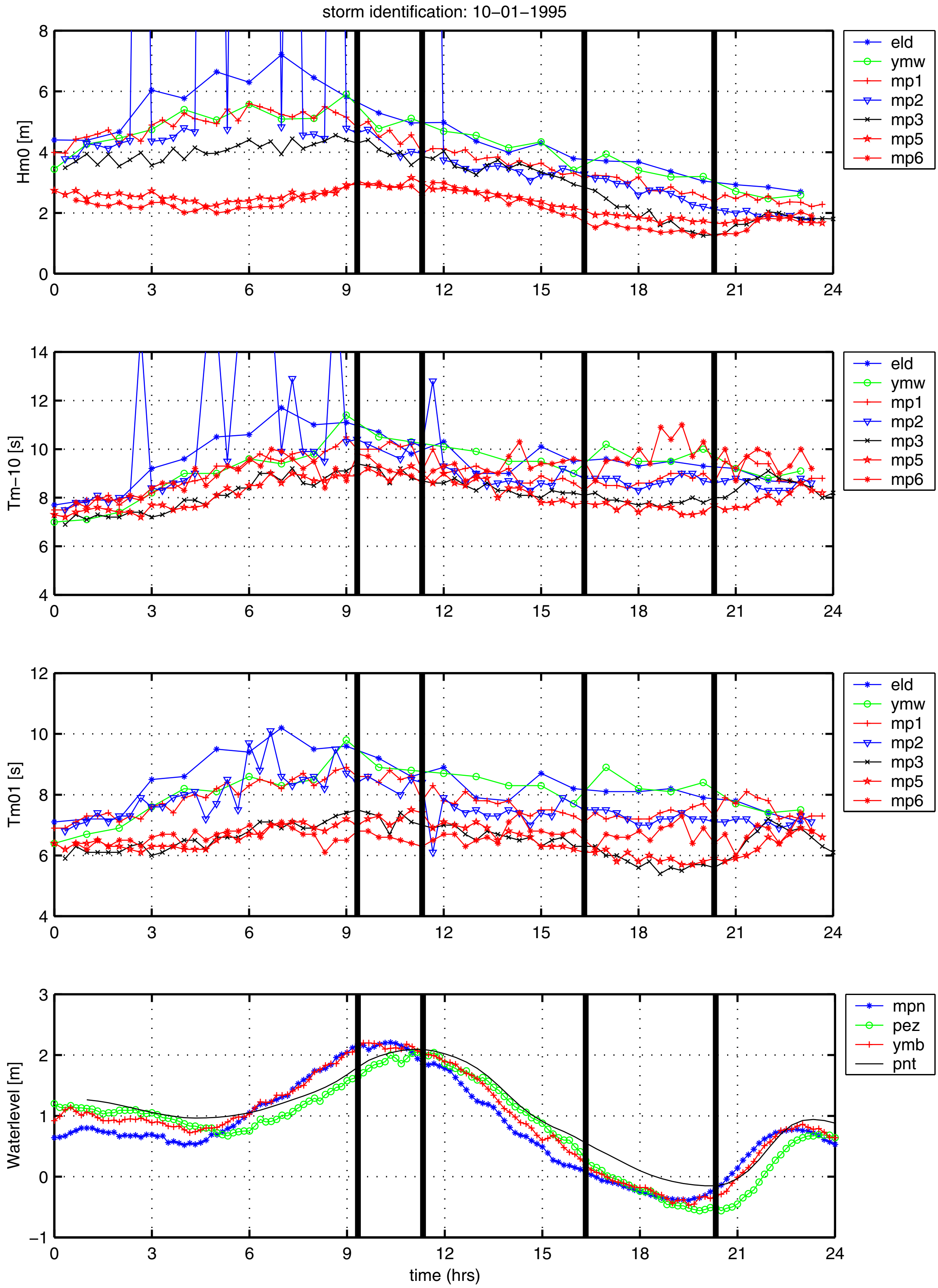

Time signals of measured spectral parameters and water level (computed at ptn)	storm: 10–01–1995	
	Measurements Petten Sea Defence	
WL | DELFT HYDRAULICS –– ALKYON HYDRAULIC CONSULTANCY & RESEARCH	H4197/A1044	Fig. F–3.c

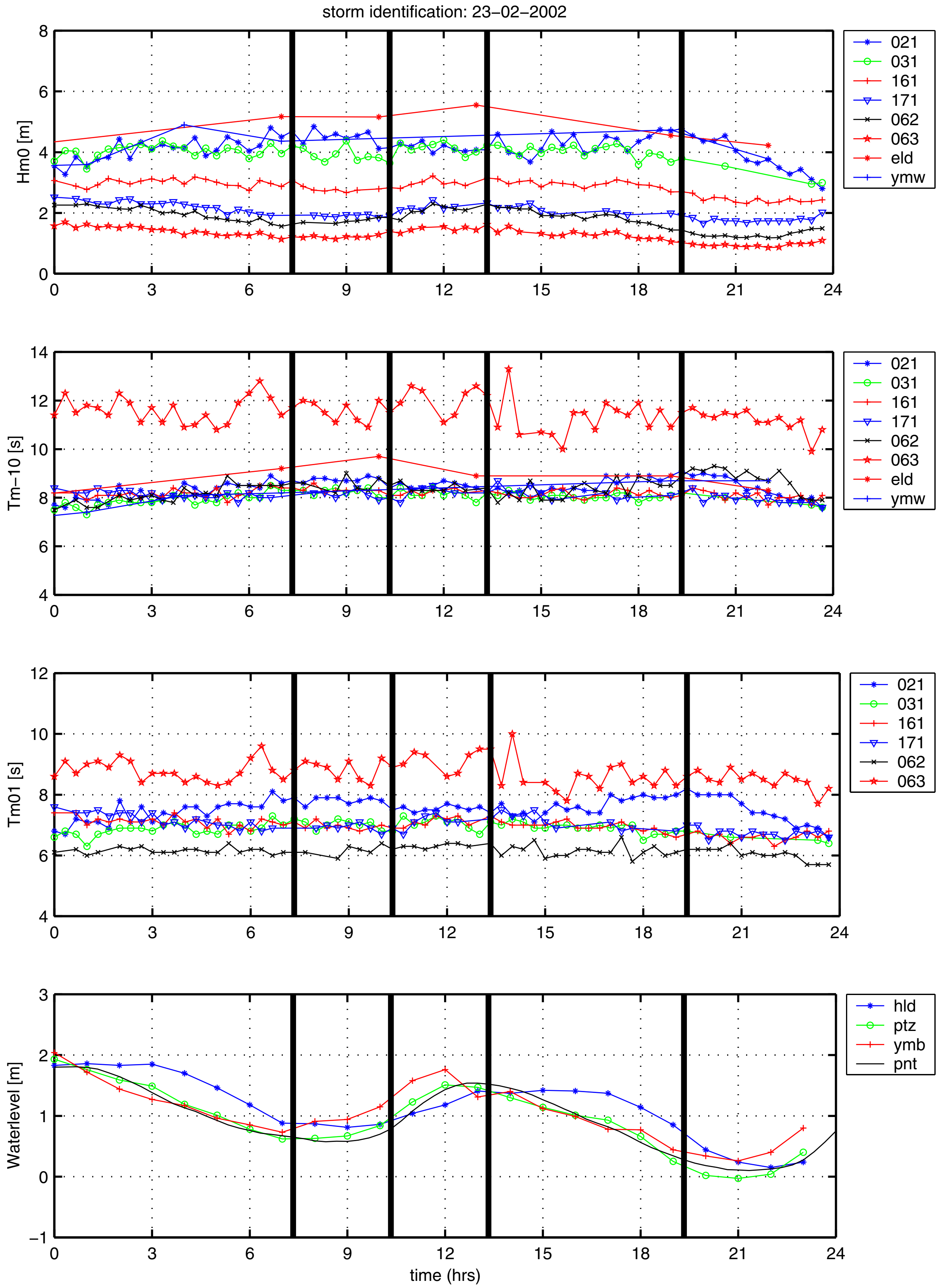

Time signals of measured spectral parameters and water level (computed at ptn)

storm: 23−02−2002	
Measurements Petten Sea Defence	

WL I DELFT HYDRAULICS −− ALKYON HYDRAULIC CONSULTANCY & RESEARCH	H4197/A1044	Fig. F−3.d

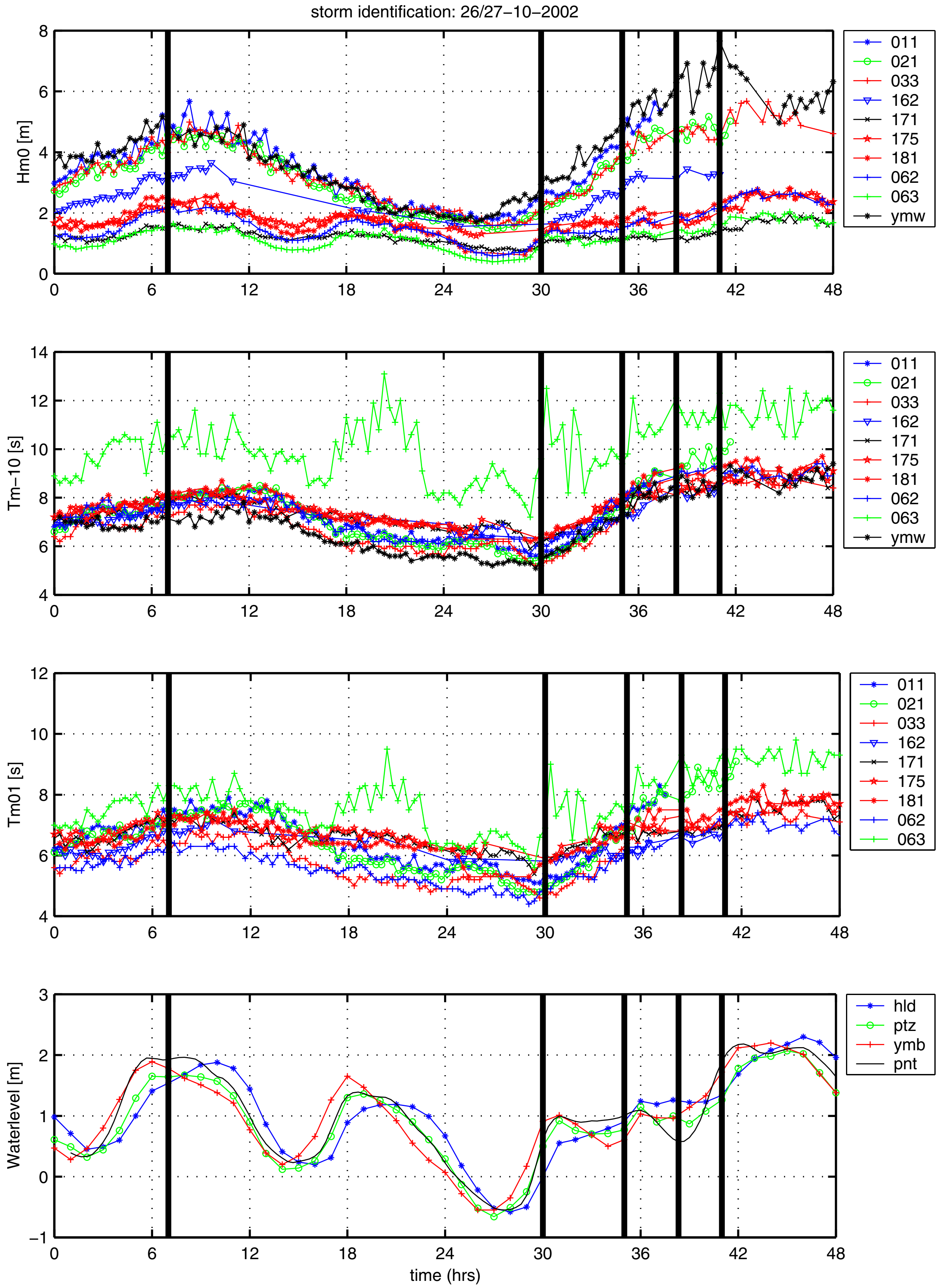

Time signals of measured spectral parameters and water level (computed at ptn)	storm: 26/27−10−2002	
	Measurements Petten Sea Defence	
WL | DELFT HYDRAULICS −− ALKYON HYDRAULIC CONSULTANCY & RESEARCH	H4197/A1044	Fig. F−3.e

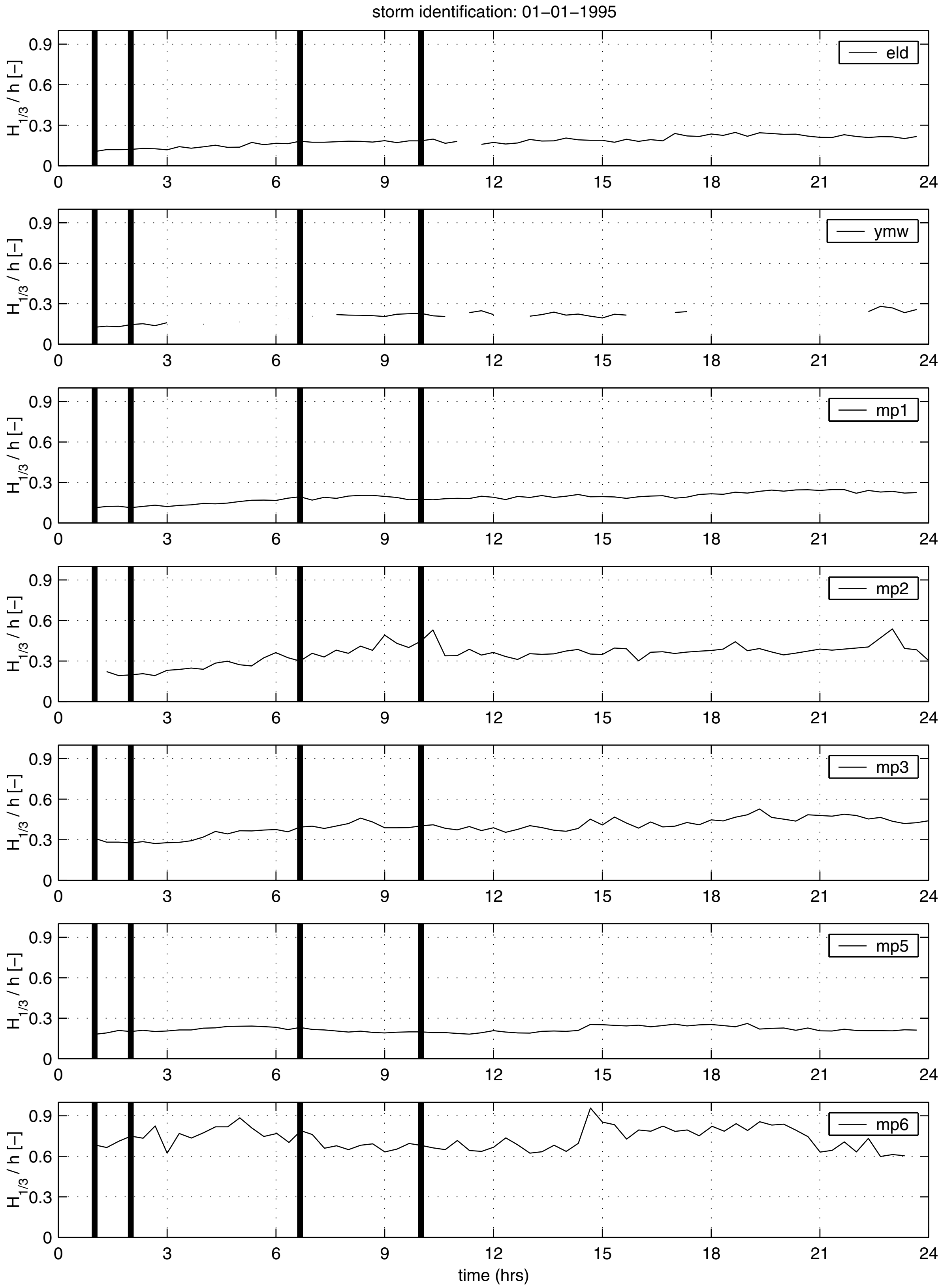

Time signals of ratio $H_{1/3}$ and total water depth	storm: 01−01−1995
	Measurements Petten Sea Defence
WL | DELFT HYDRAULICS −− ALKYON HYDRAULIC CONSULTANCY & RESEARCH	H4197/A1044 — Fig. F−4.a

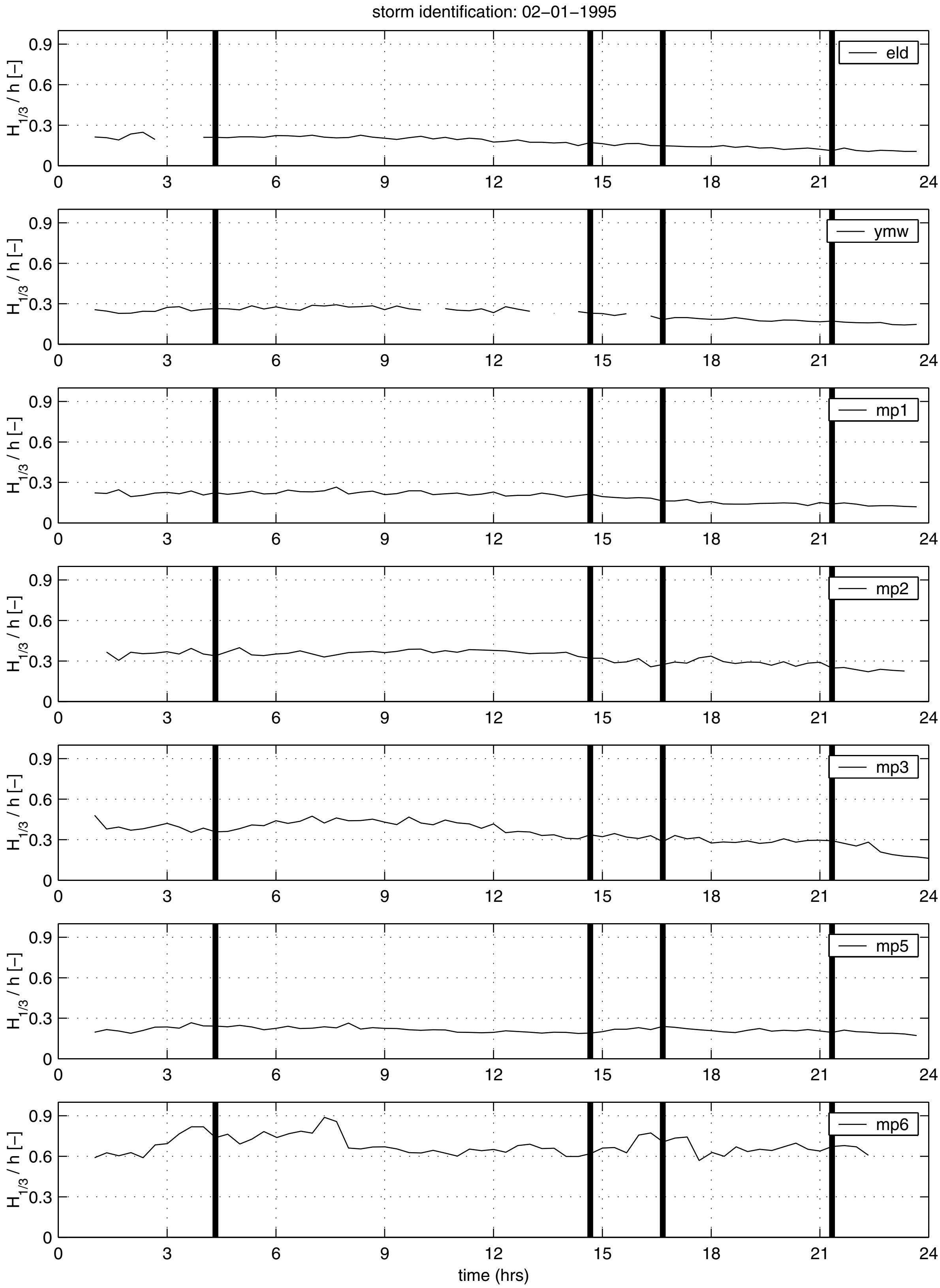

Time signals of ratio $H_{1/3}$ and total water depth	storm: 02−01−1995	
	Measurements Petten Sea Defence	
WL | DELFT HYDRAULICS −− ALKYON HYDRAULIC CONSULTANCY & RESEARCH	H4197/A1044	Fig. F−4.b

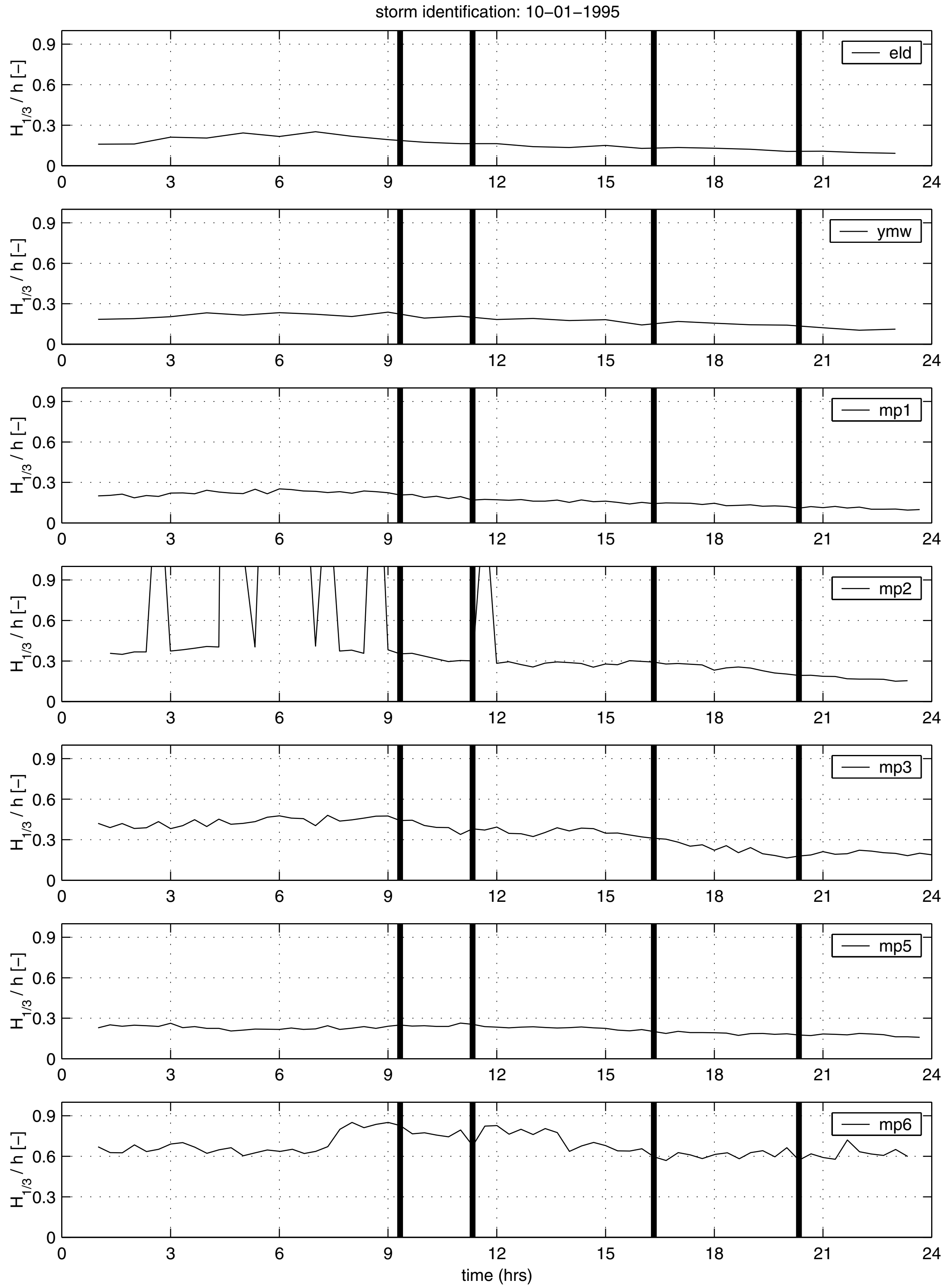

Time signals of ratio $H_{1/3}$ and total water depth	storm: 10−01−1995	
	Measurements Petten Sea Defence	
WL | DELFT HYDRAULICS –– ALKYON HYDRAULIC CONSULTANCY & RESEARCH	H4197/A1044	Fig. F−4.c

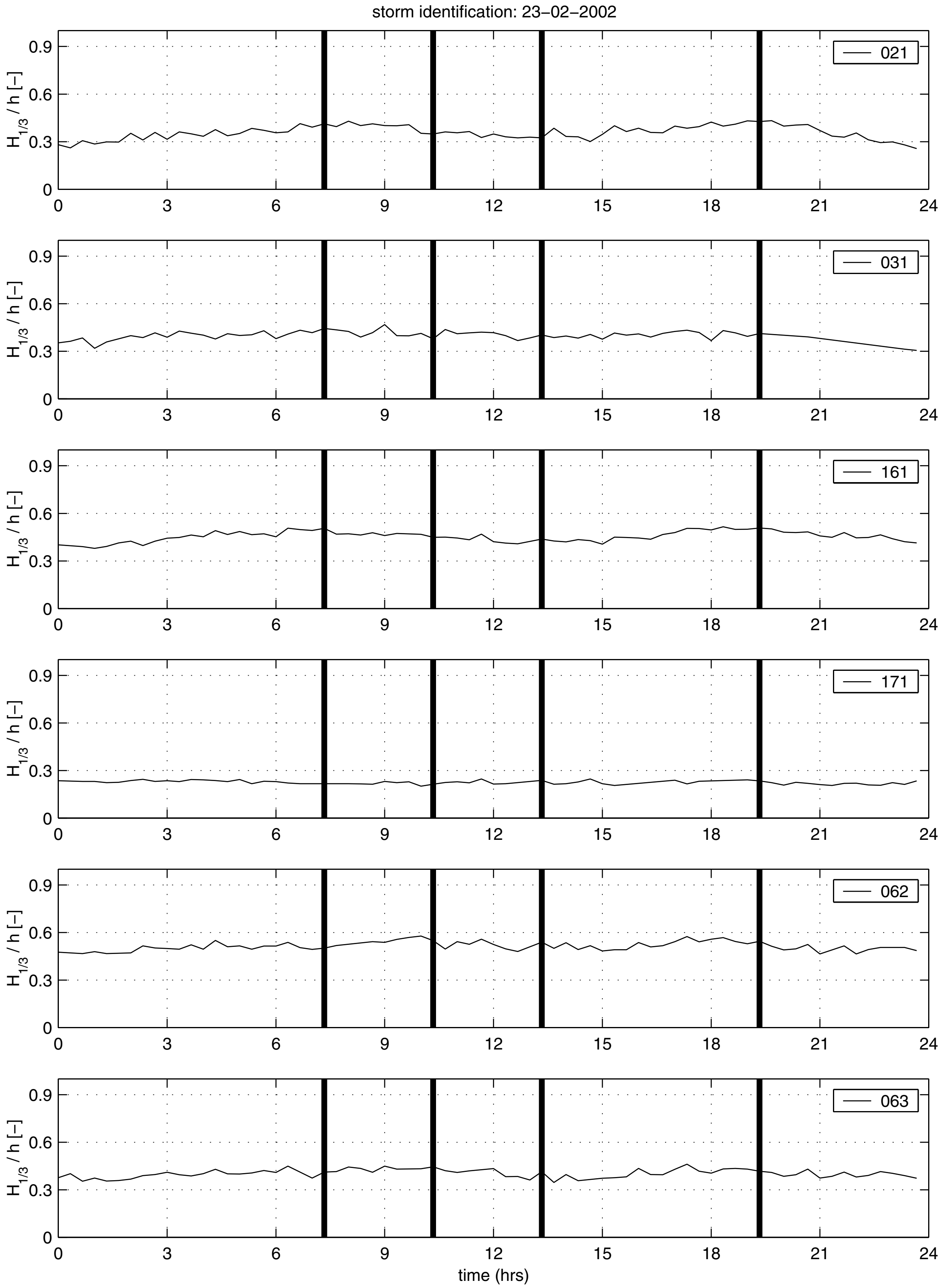

Time signals of ratio $H_{1/3}$ and total water depth	storm: 23−02−2002	
	Measurements Petten Sea Defence	
WL | DELFT HYDRAULICS −− ALKYON HYDRAULIC CONSULTANCY & RESEARCH	H4197/A1044	Fig. F−4.d

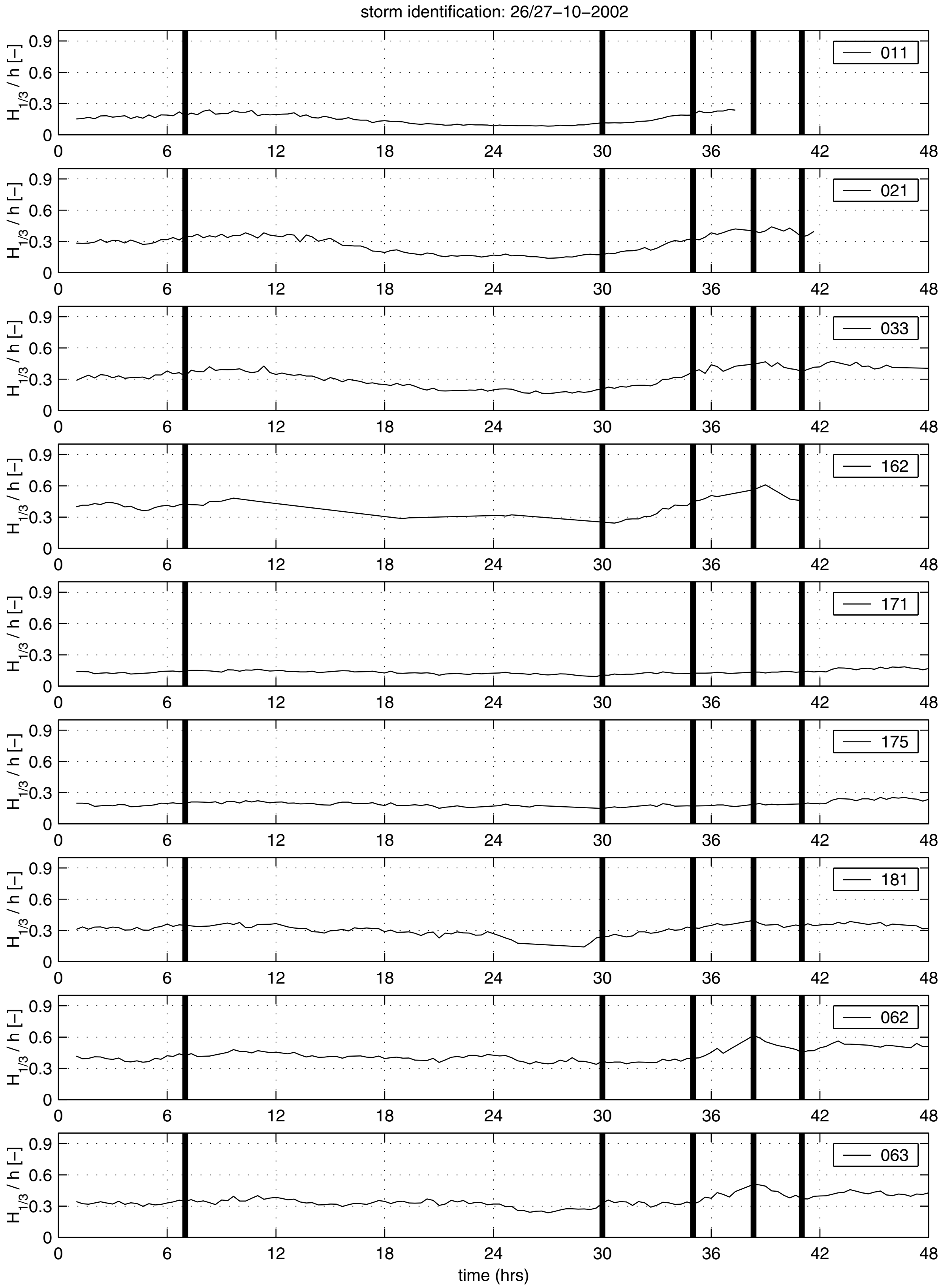

Time signals of ratio $H_{1/3}$ and total water depth

storm: 26/27−10−2002

Measurements Petten Sea Defence

WL | DELFT HYDRAULICS −− ALKYON HYDRAULIC CONSULTANCY & RESEARCH

H4197/A1044

Fig. F−4.e

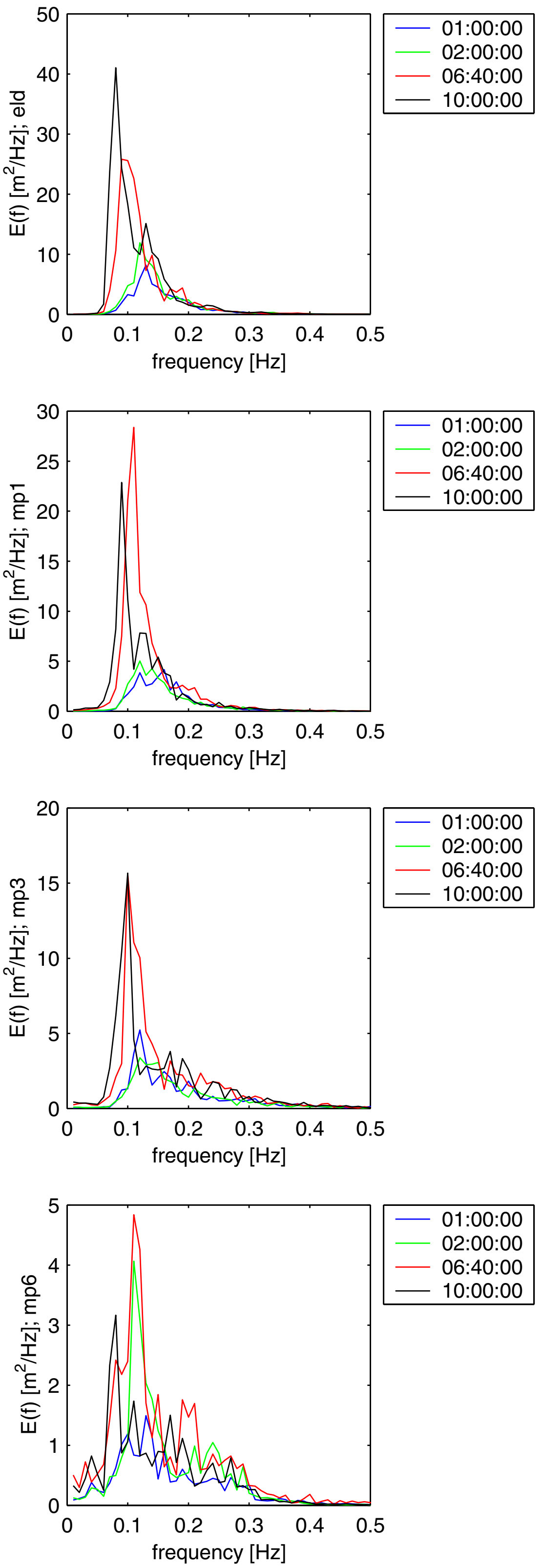

measured wave energy spectra per location (name of location on vertical axis)	storm: 01–01–1995	
	Measurements Petten Sea Defence	
WL | DELFT HYDRAULICS –– ALKYON HYDRAULIC CONSULTANCY & RESEARCH	H4197/A1044	Fig. F–5.a

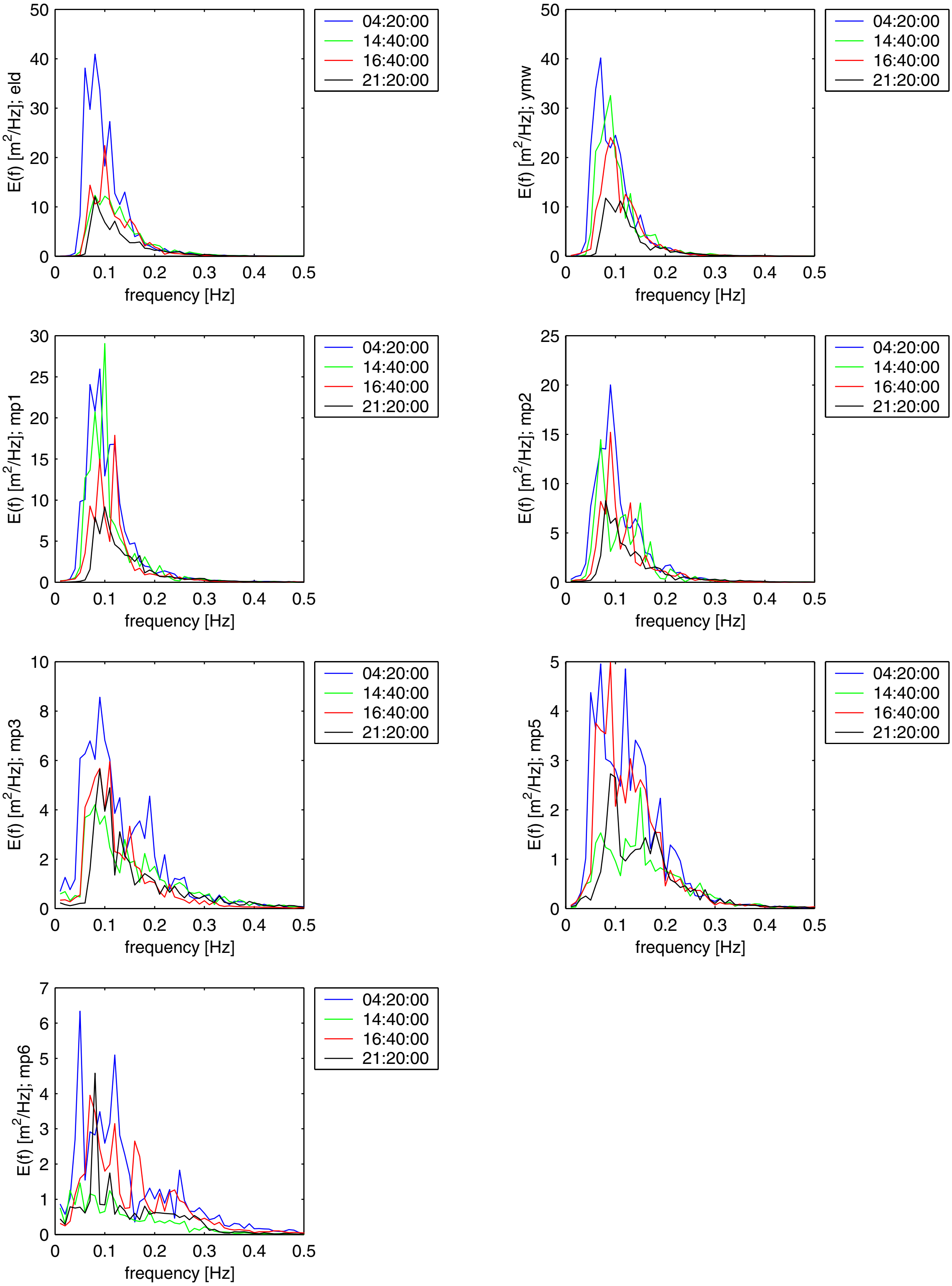

measured wave energy spectra per location (name of location on vertical axis)	storm: 02–01–1995	
	Measurements Petten Sea Defence	
WL | DELFT HYDRAULICS –– ALKYON HYDRAULIC CONSULTANCY & RESEARCH	H4197/A1044	Fig. F–5.b

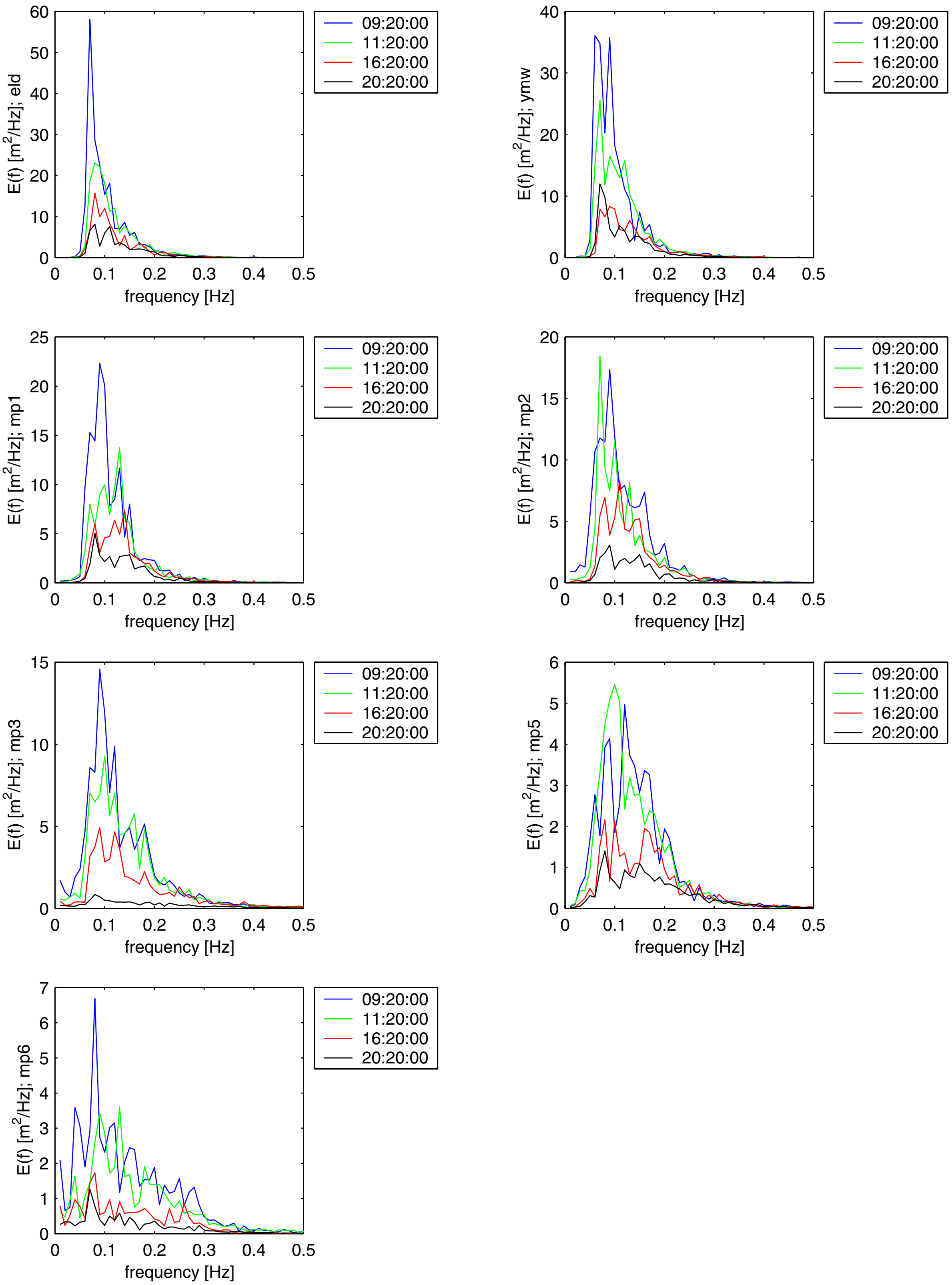

measured wave energy spectra per location (name of location on vertical axis)	storm: 10–01–1995	
	Measurements Petten Sea Defence	
WL | DELFT HYDRAULICS –– ALKYON HYDRAULIC CONSULTANCY & RESEARCH	H4197/A1044	Fig. F–5.c

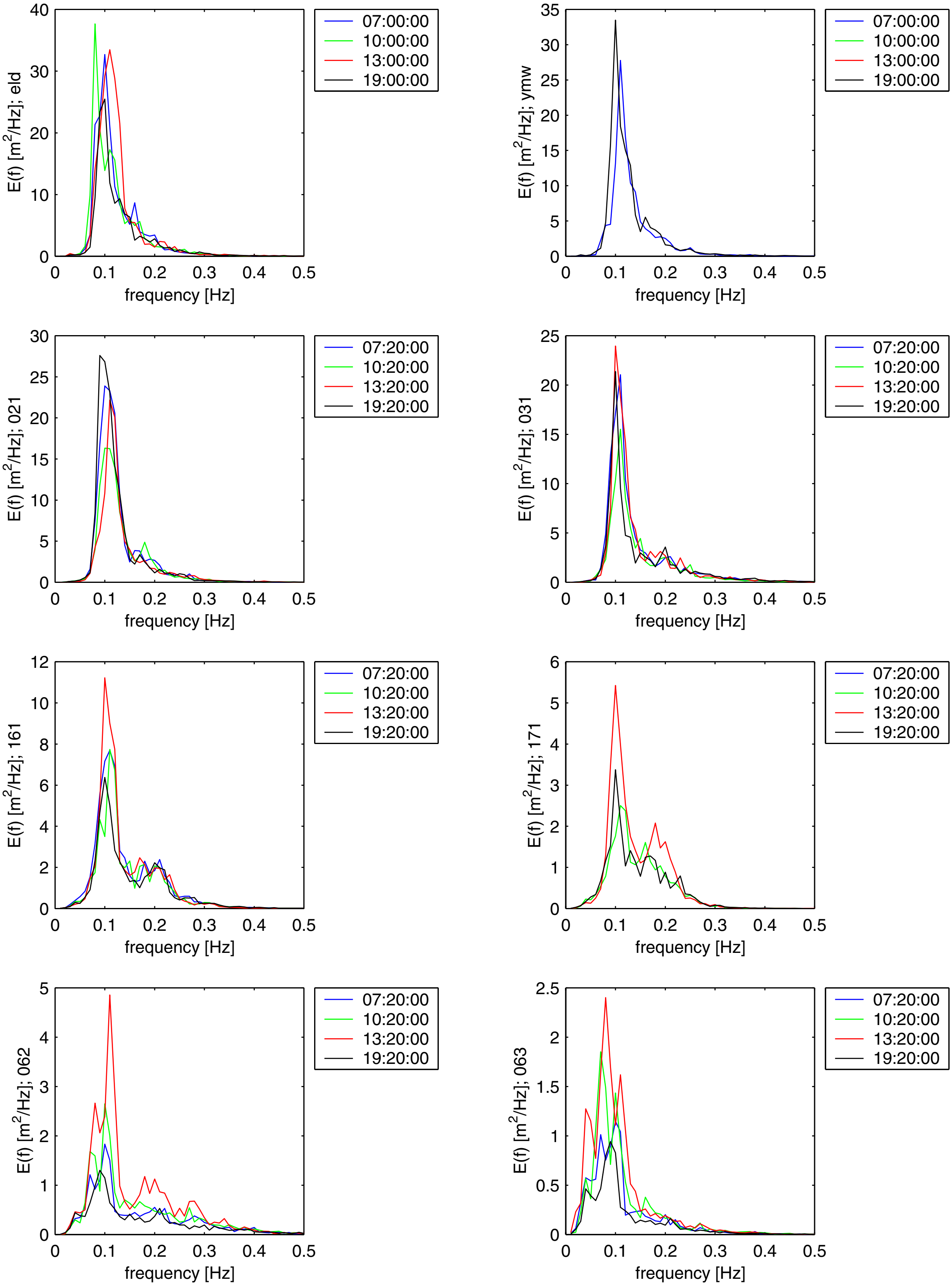

measured wave energy spectra per location (name of location on vertical axis)

storm: 23–02–2002	
Measurements Petten Sea Defence	

WL I DELFT HYDRAULICS –– ALKYON HYDRAULIC CONSULTANCY & RESEARCH	H4197/A1044	Fig. F–5.d

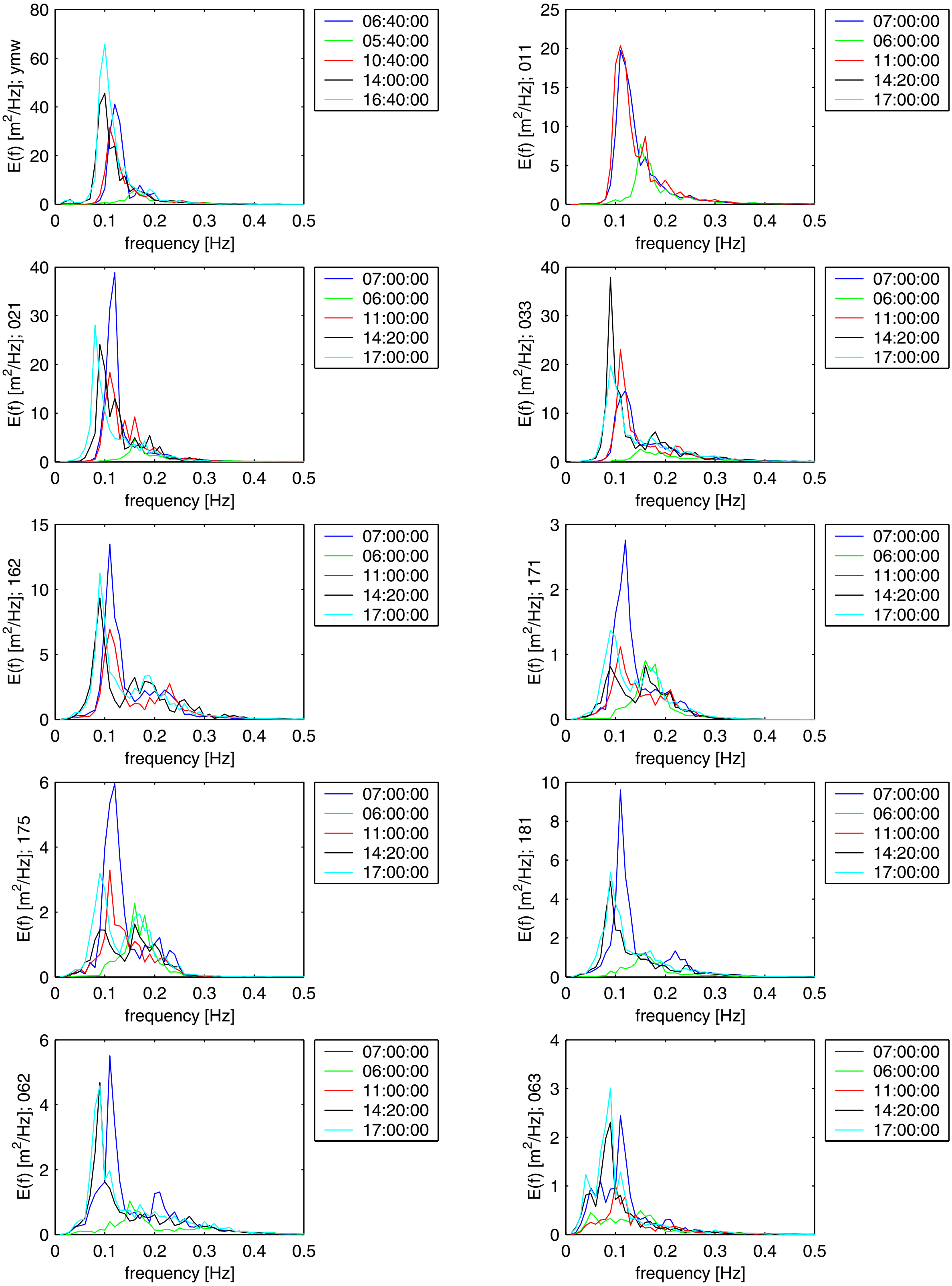

measured wave energy spectra per location (name of location on vertical axis)	storm: 26/27−10−2002	
	Measurements Petten Sea Defence	
WL I DELFT HYDRAULICS −− ALKYON HYDRAULIC CONSULTANCY & RESEARCH	H4197/A1044	Fig. F−5.e

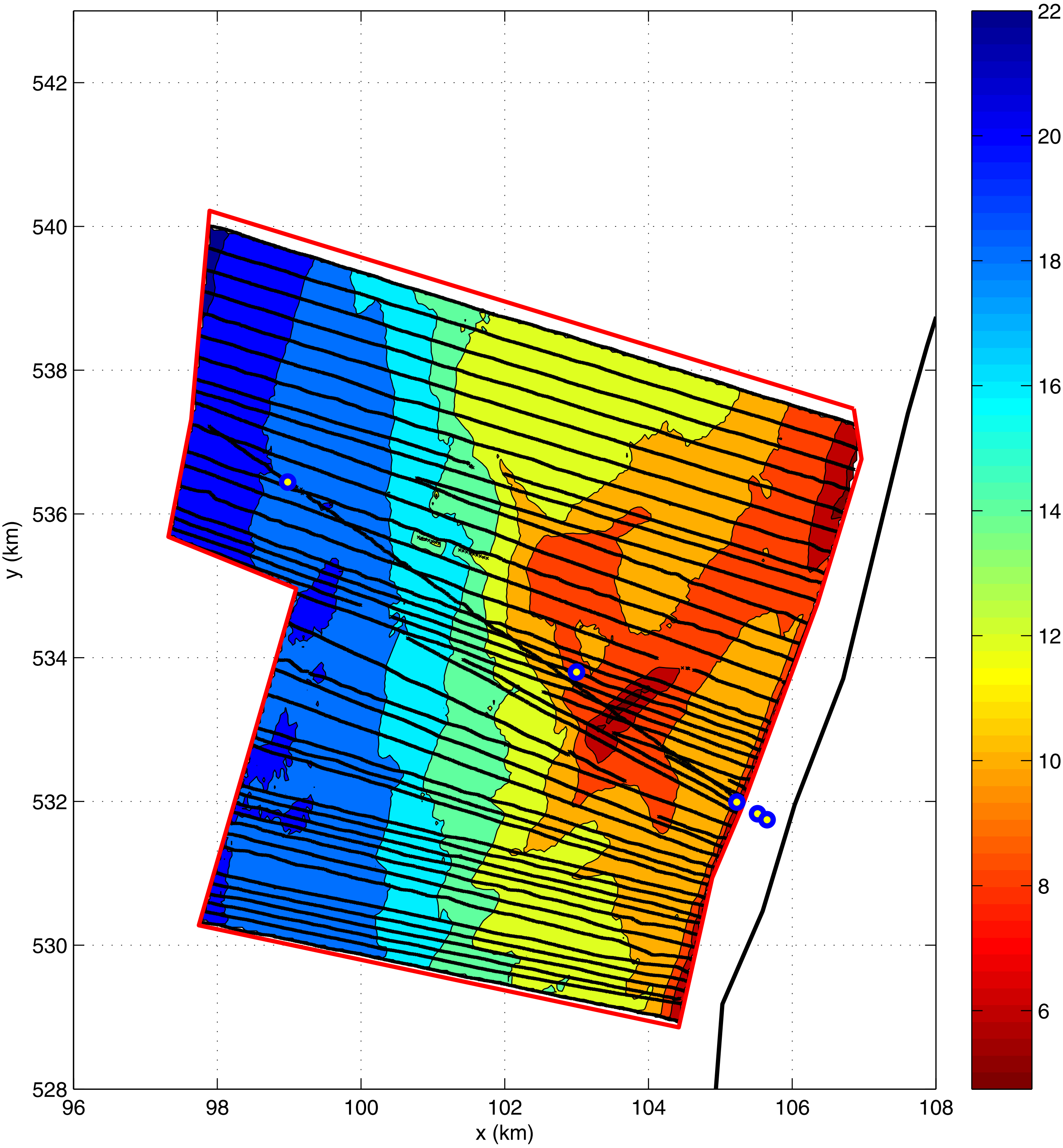

Bottom rays and interpolated bottom original configuration, depth in m	year 1994	
	Measurements Petten Sea Defence	
WL | DELFT HYDRAULICS & ALKYON HYDRAULIC CONSULTANCY & RESEARCH	H4197/A1044	Fig. F–7

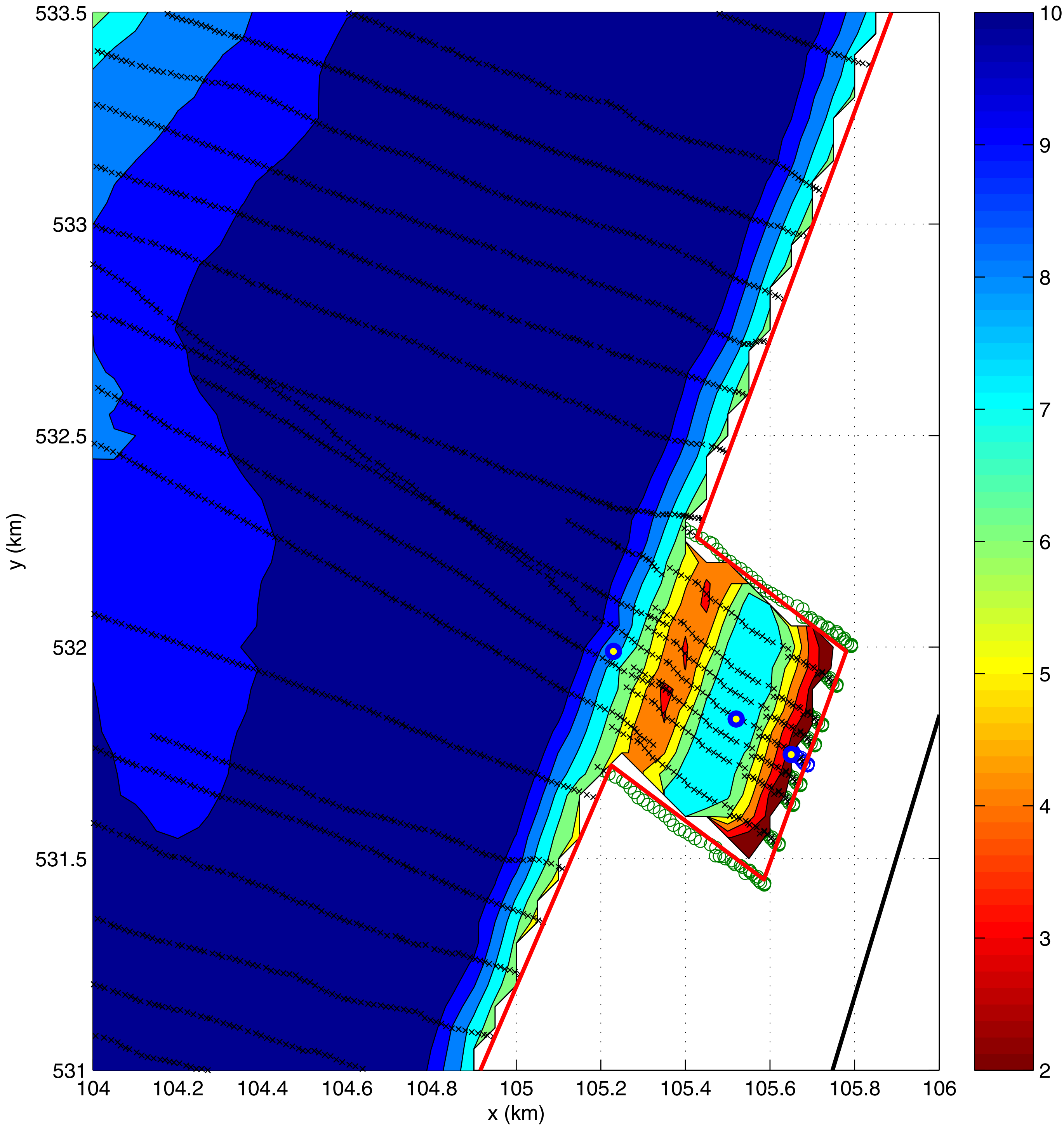

Bottom rays and interpolated bottom Extended along Petten ray, depth in m	year 1994	
	Measurements Petten Sea Defence	
WL I DELFT HYDRAULICS & ALKYON HYDRAULIC CONSULTANCY & RESEARCH	H4197/A1044	Fig. F–8

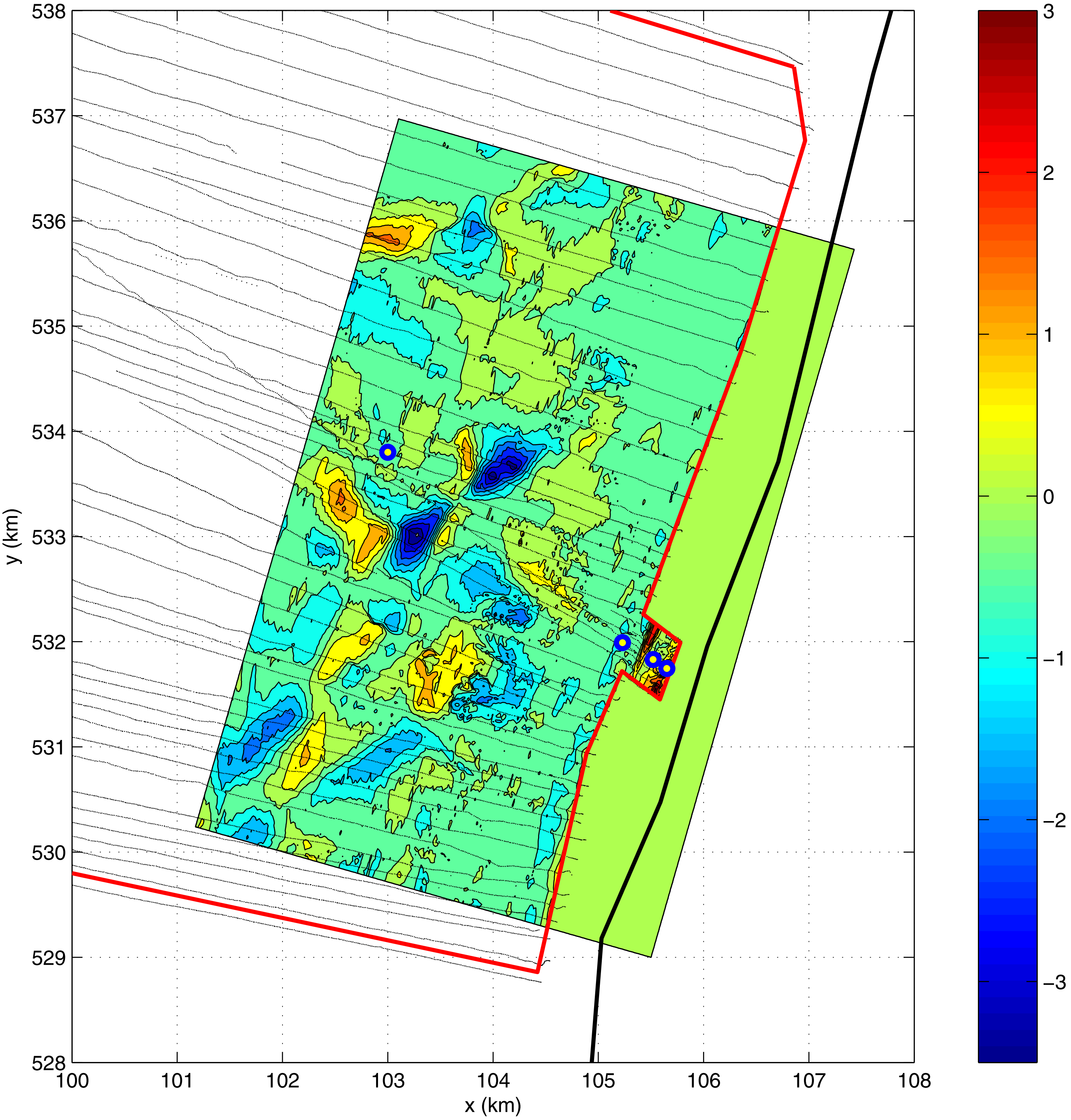

Difference in bottom for grid E24 $dz=z_{new}-z_{old}$, scale in m dz>0 corresponds to lower bottom	year 1994	
	Measurements Petten Sea Defence	
WL | DELFT HYDRAULICS & ALKYON HYDRAULIC CONSULTANCY & RESEARCH	H4197/A1044	Fig. F−9

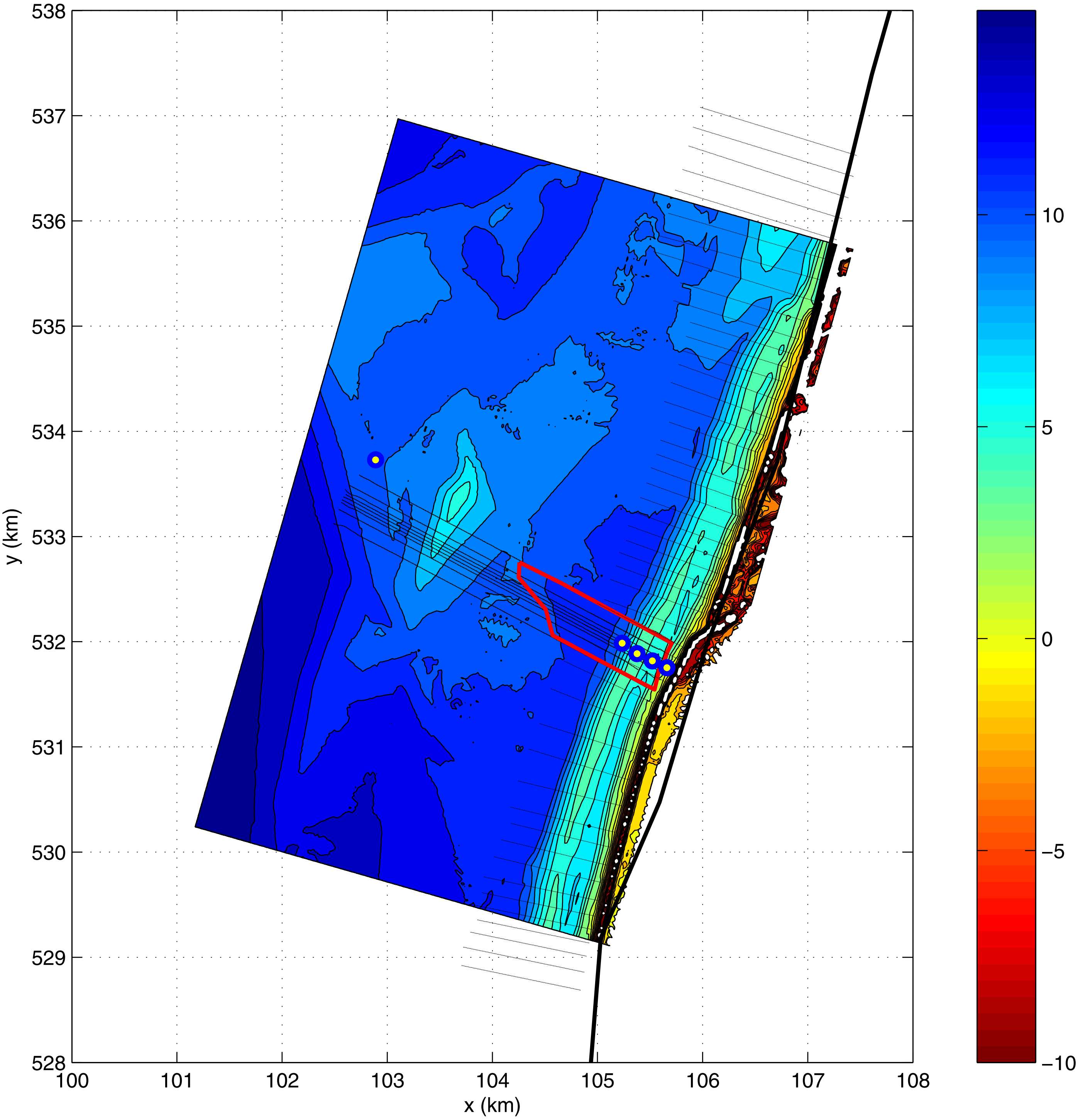

Updated bottom topography for grid e24 based on Jarkus 2002 rays and 9 Pettemer rays depth in m	year 2002	November
	Measurements Petten Sea Defence	
WL I DELFT HYDRAULICS & ALKYON HYDRAULIC CONSULTANCY & RESEARCH	H4197/A1044	Fig. F−10

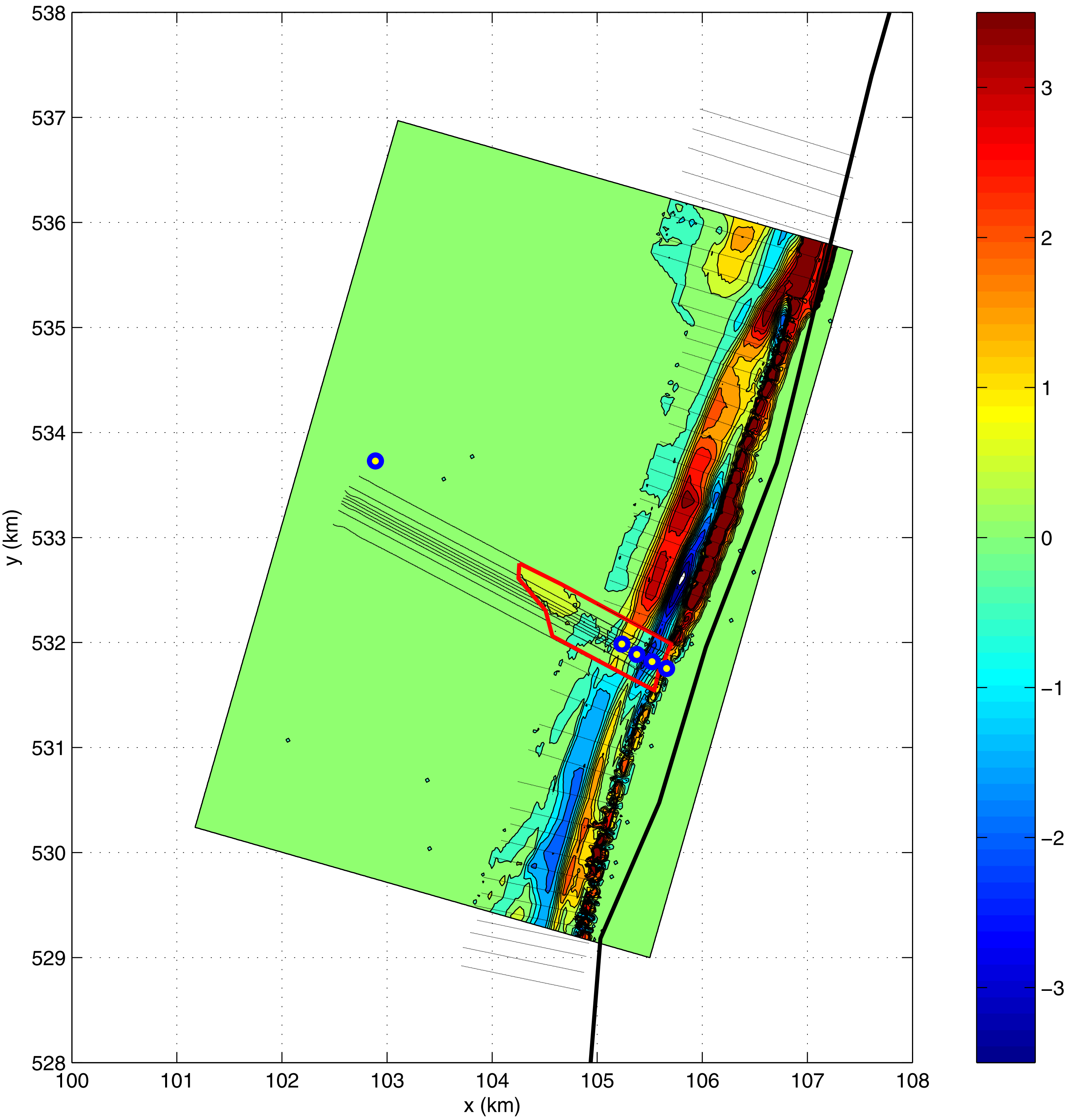

Difference in bottom for grid e24, scale in m $dz=z_{new}-z_{old}$, dz>0 corresponds to lower bottom based on Jarkus 2002 rays and 9 Pettemer rays	year 2002	November
	Measurements Petten Sea Defence	
WL | DELFT HYDRAULICS & ALKYON HYDRAULIC CONSULTANCY & RESEARCH	H4197/A1044	Fig. F−11

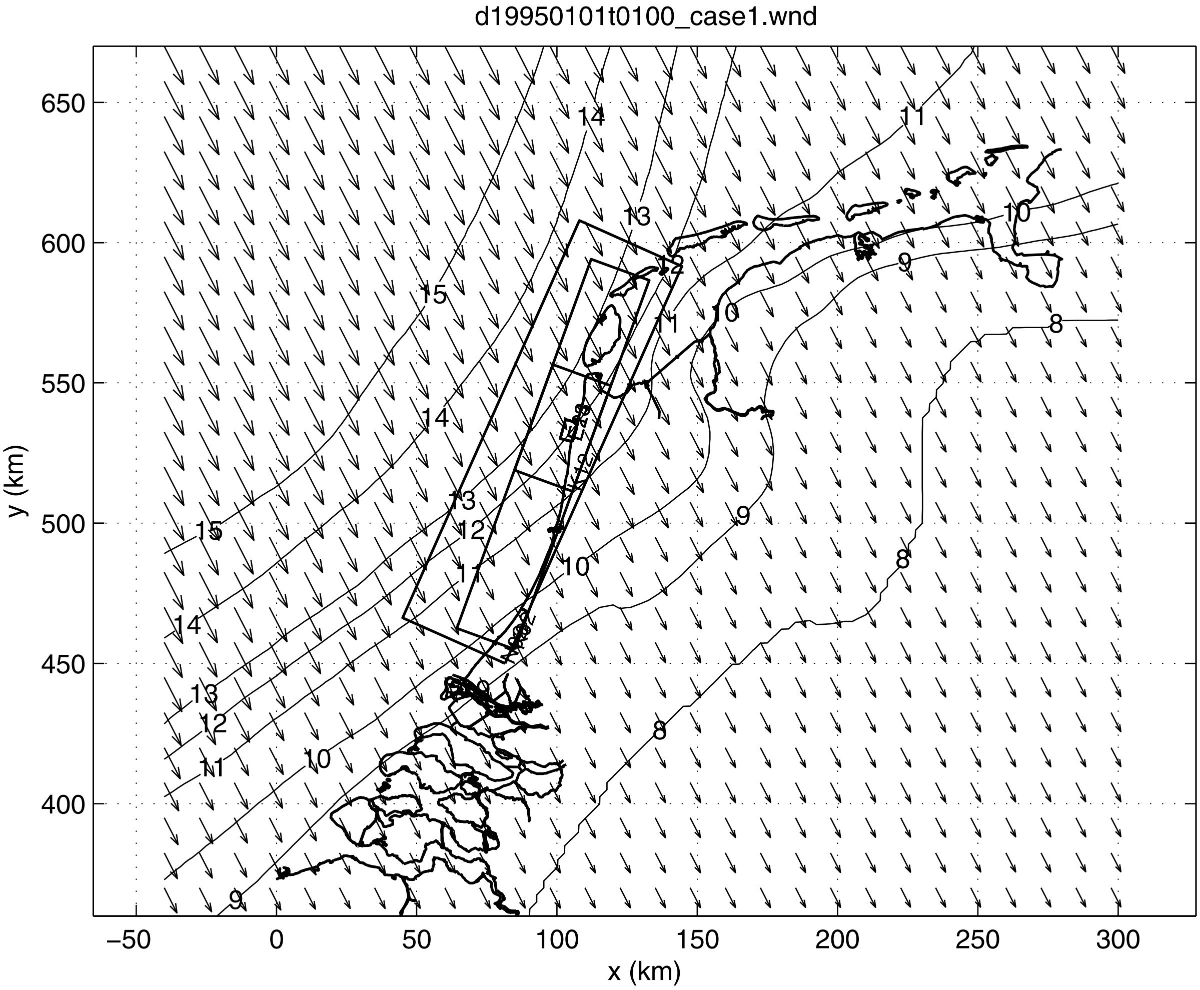

Wind field for d19950101t0100_case1.wnd	1995 storms	
	Measurements Petten Sea Defence	
WL | DELFT HYDRAULICS & ALKYON HYDRAULIC CONSULTANCY & RESEARCH	H4197/A1044	Fig. F–12

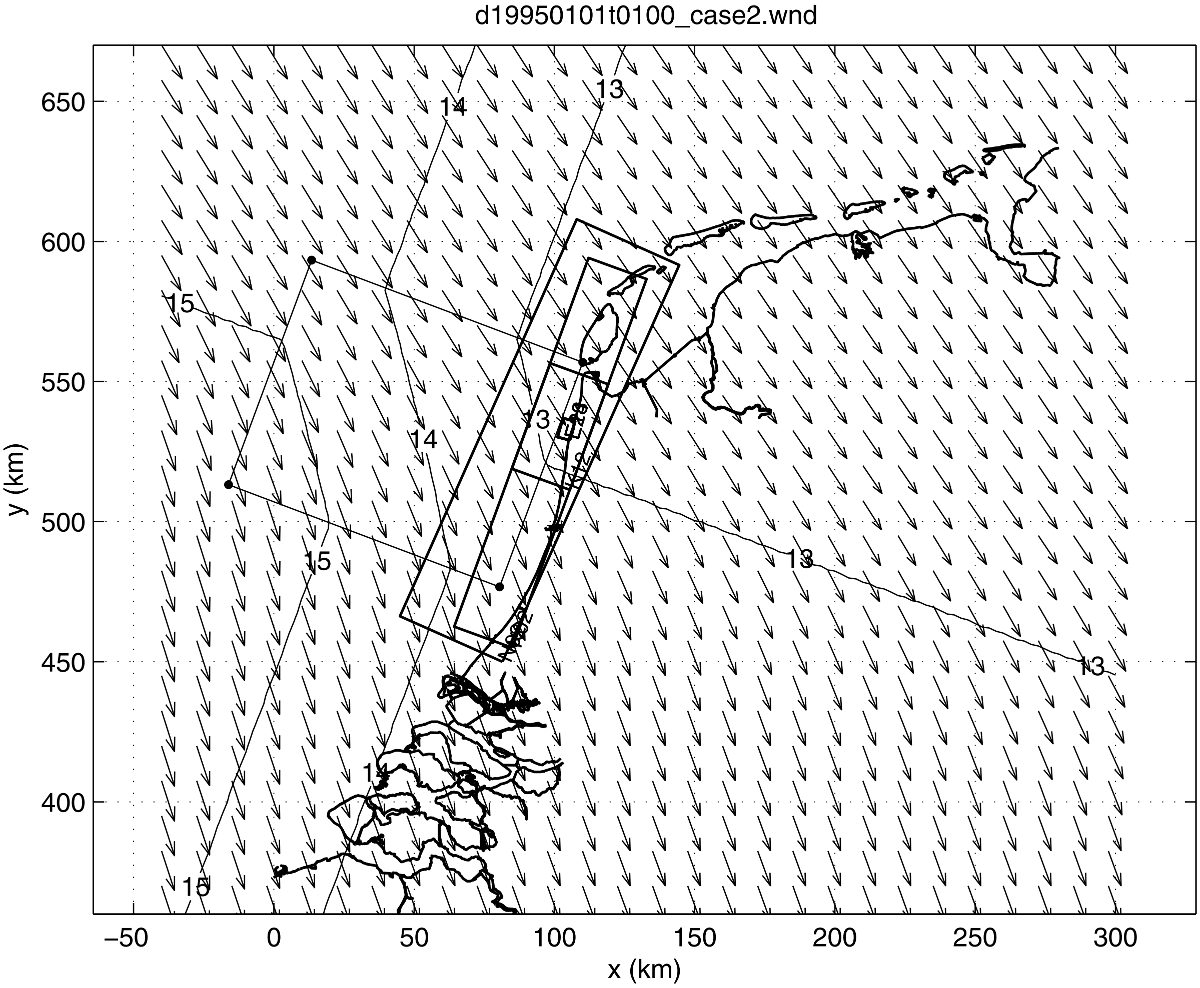

Wind field for d19950101t0100_case2.wnd	1995 storms	
	Measurements Petten Sea Defence	
WL | DELFT HYDRAULICS & ALKYON HYDRAULIC CONSULTANCY & RESEARCH	H4197/A1044	Fig. F−13

d20020223t1920_case2.wnd

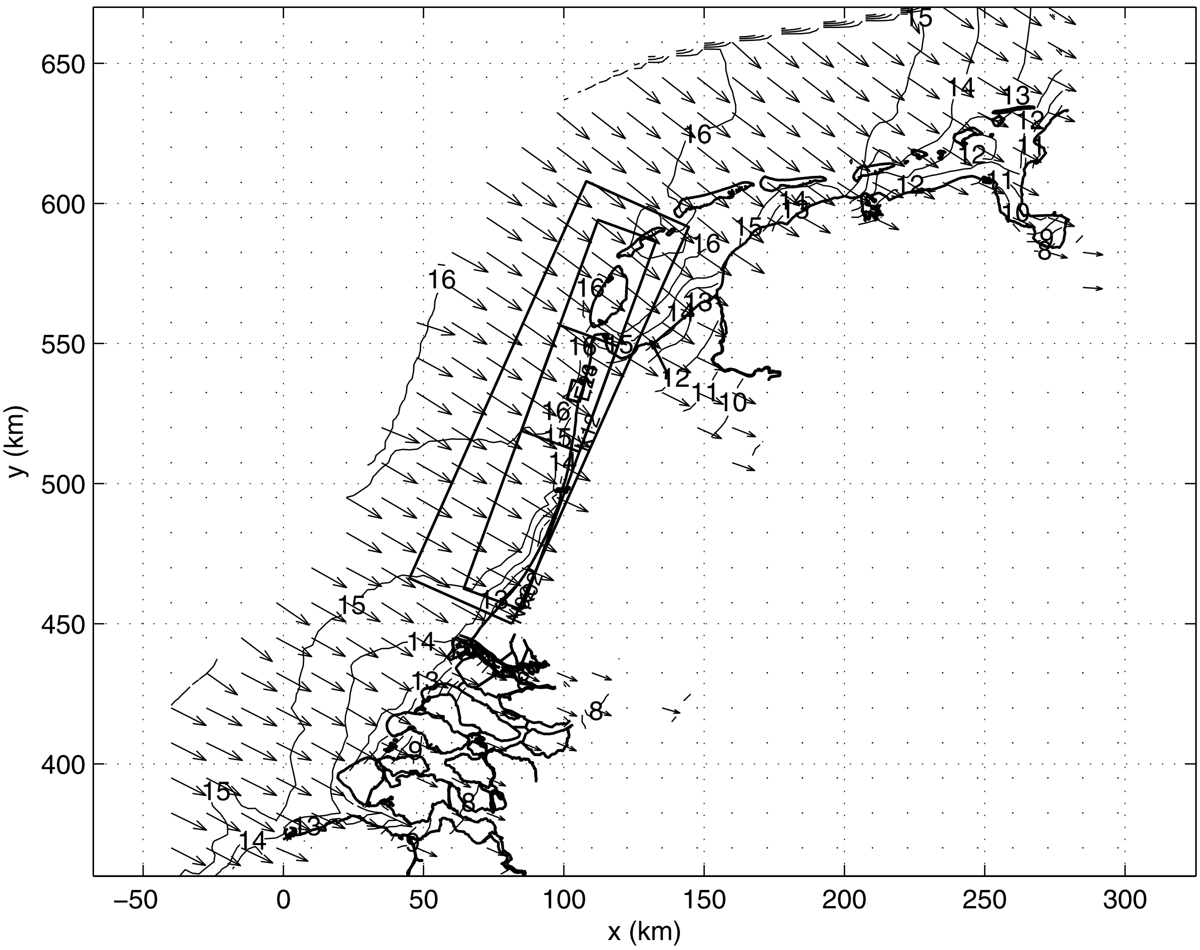

Wind field for d20020223t1920_case2.wnd	2002 storms	
	Measurements Petten Sea Defence	
WL | DELFT HYDRAULICS & ALKYON HYDRAULIC CONSULTANCY & RESEARCH	H4197/A1044	Fig. F−14

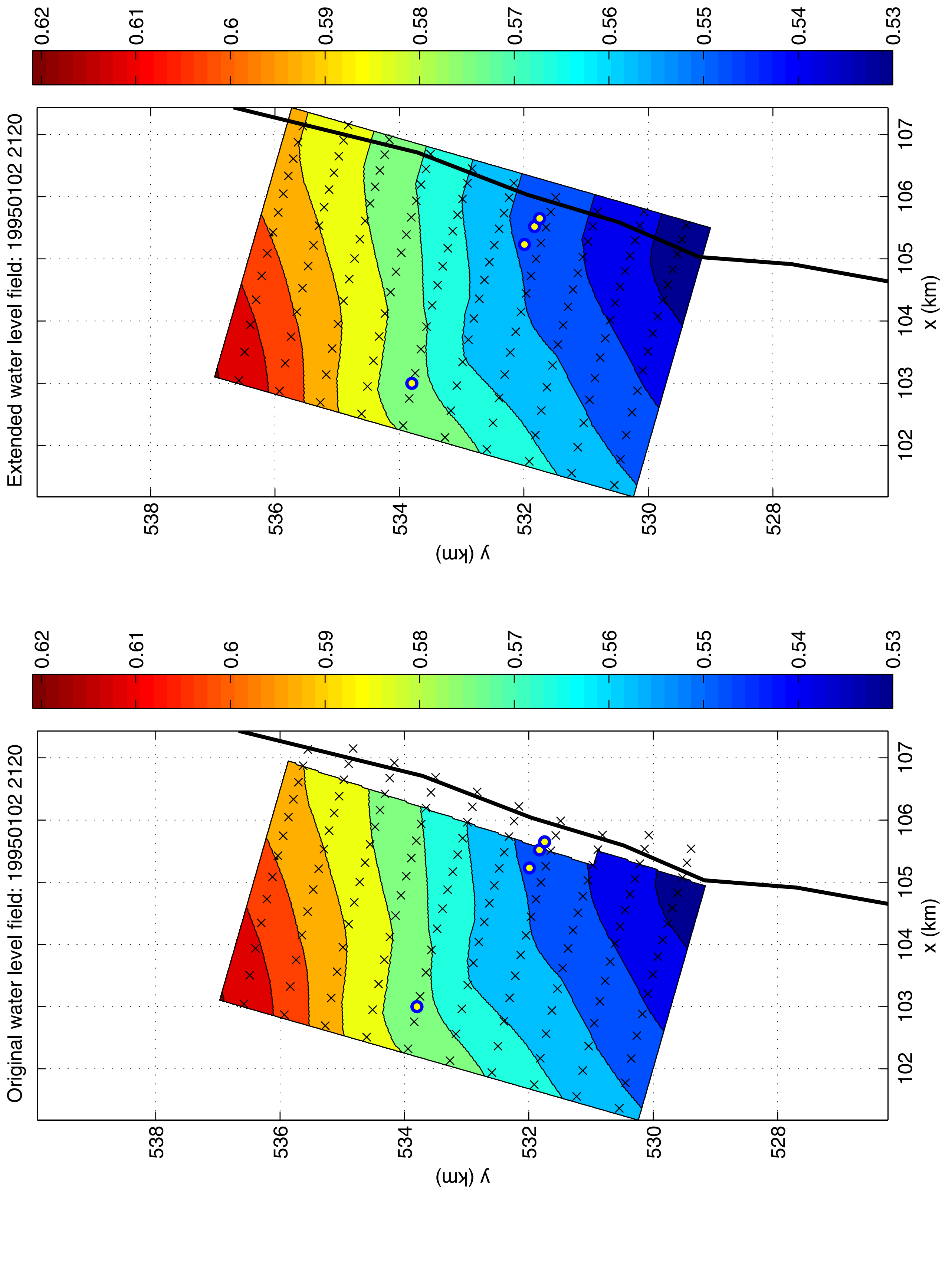

Water level field, basic (left) and extended (right)

e24	19950102 2120
Measurements Petten Sea Defence	

WL | DELFT HYDRAULICS & ALKYON HYDRAULIC CONSULTANCY & RESEARCH

H4197/A1044	Fig. F–15

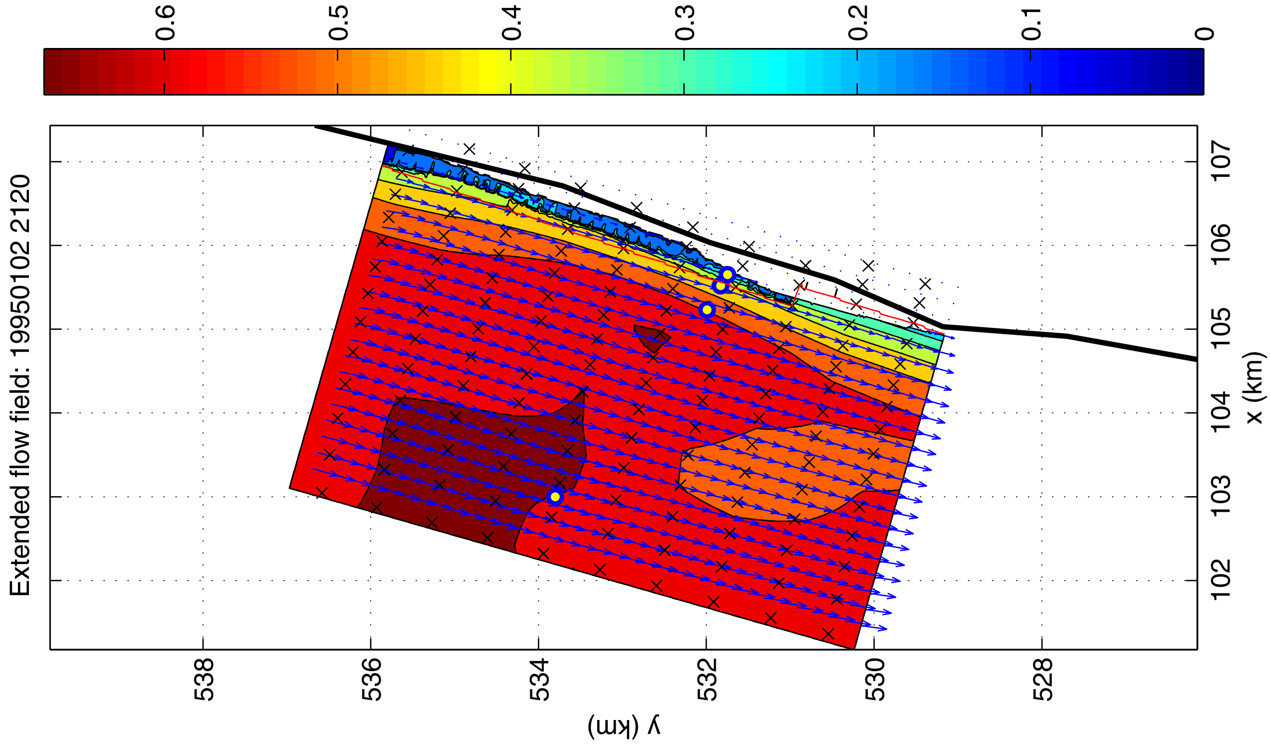

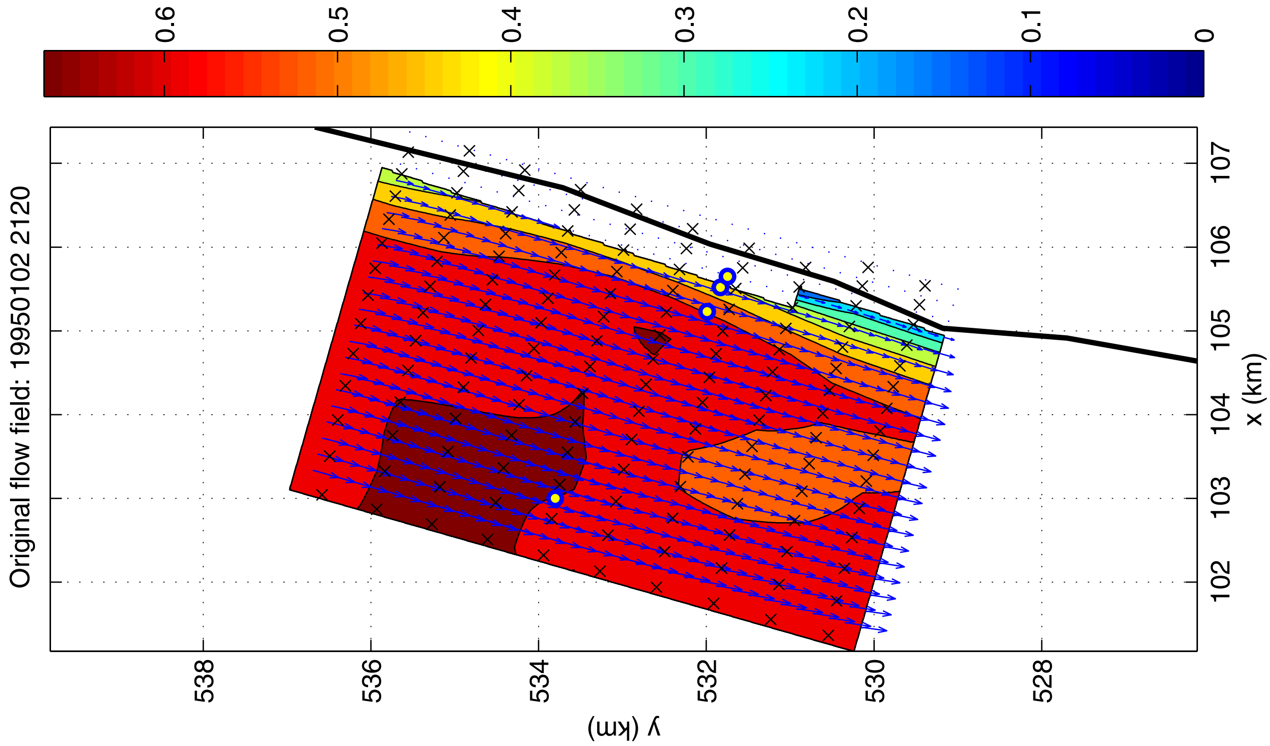

Current field, basic (left) and extended (right)	e24	19950102 2120
	Measurements Petten Sea Defence	
WL | DELFT HYDRAULICS & ALKYON HYDRAULIC CONSULTANCY & RESEARCH	H4197/A1044	Fig. F−16

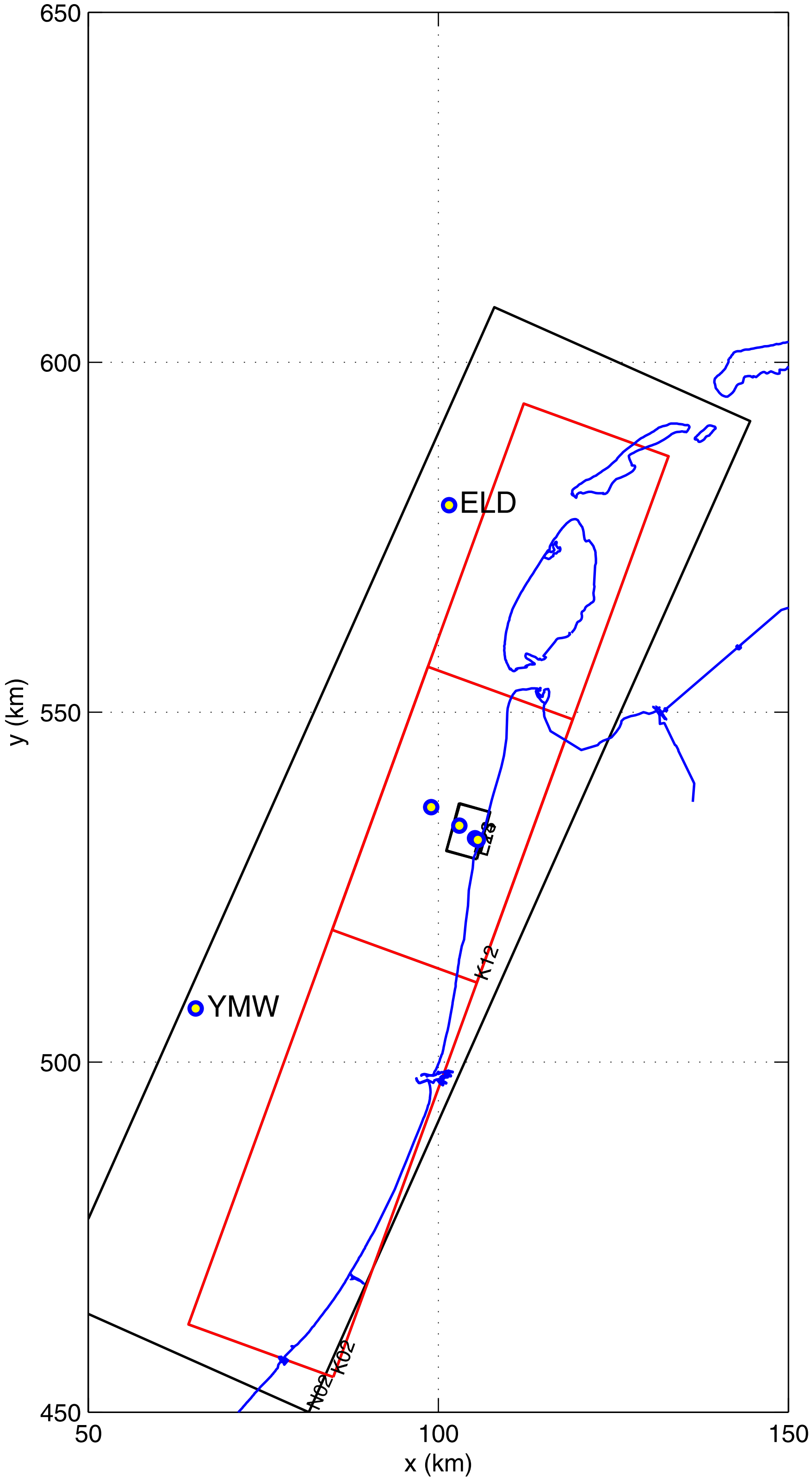

Computational grids and output locations	storms 1995	
	Measurements Petten Sea Defence	
WL | DELFT HYDRAULICS & ALKYON HYDRAULIC CONSULTANCY & RESEARCH	H4197/A1044	Fig. F–17

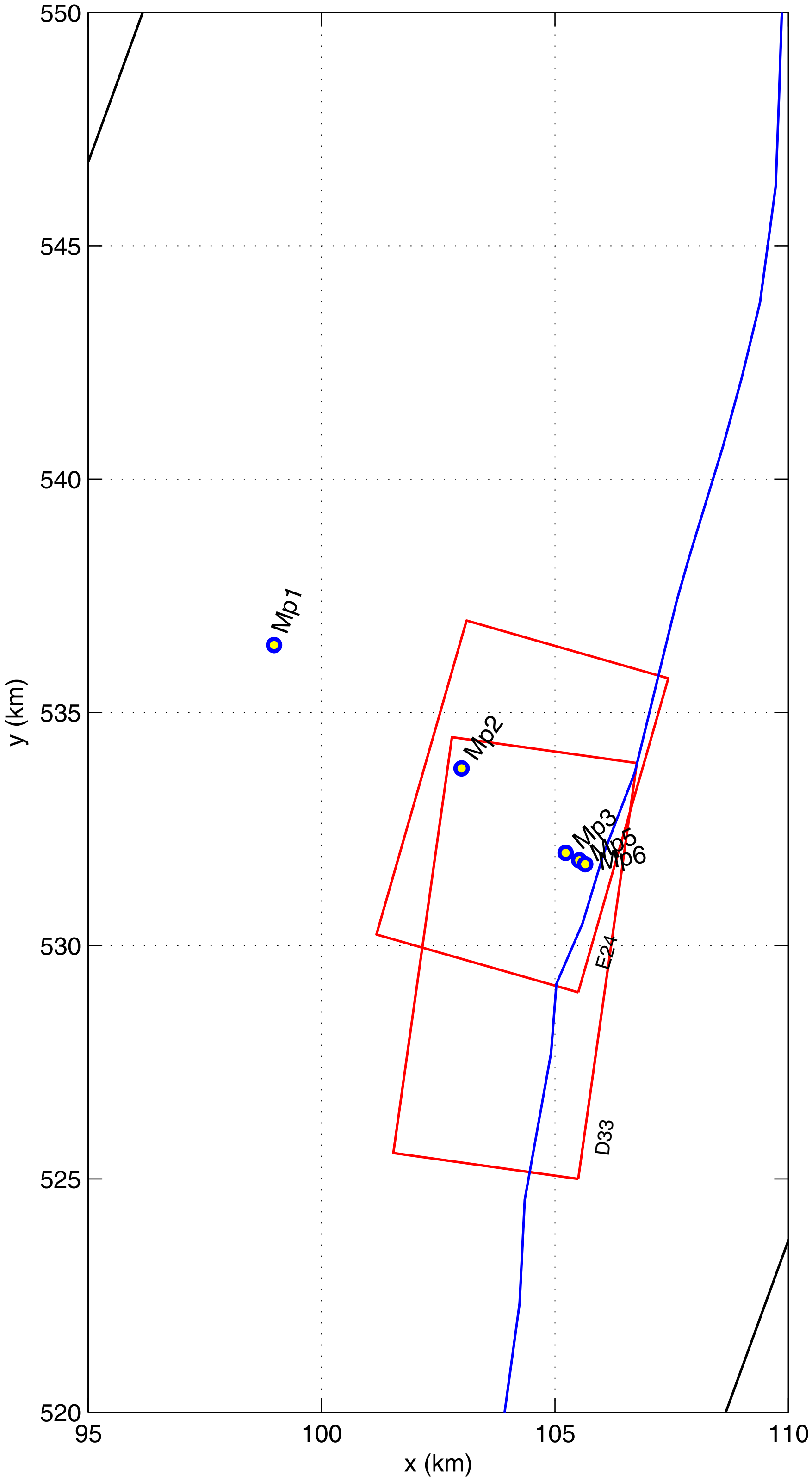

Detailed computational grids and output locations	storms 1995	
	Measurements Petten Sea Defence	
WL	DELFT HYDRAULICS & ALKYON HYDRAULIC CONSULTANCY & RESEARCH	H4197/A1044	Fig. F–18

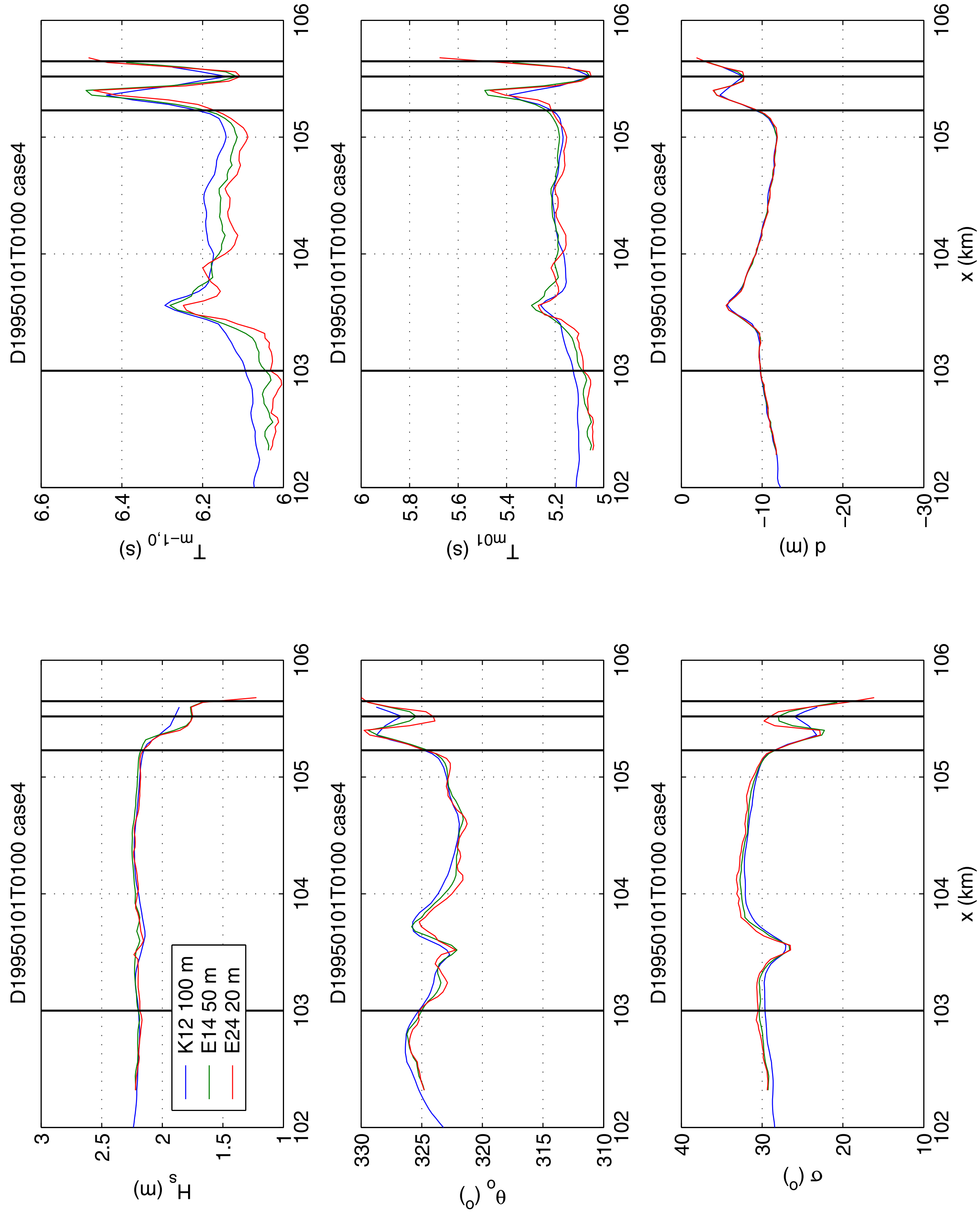

Spatial variation of integral wave parameters along Petten ray
for grid resolutions of 100 m, 50 m and 20 m

storms 1995	
Measurements Petten Sea Defence	

WL | DELFT HYDRAULICS & ALKYON HYDRAULIC CONSULTANCY & RESEARCH

H4197/A1044	Fig. F−19

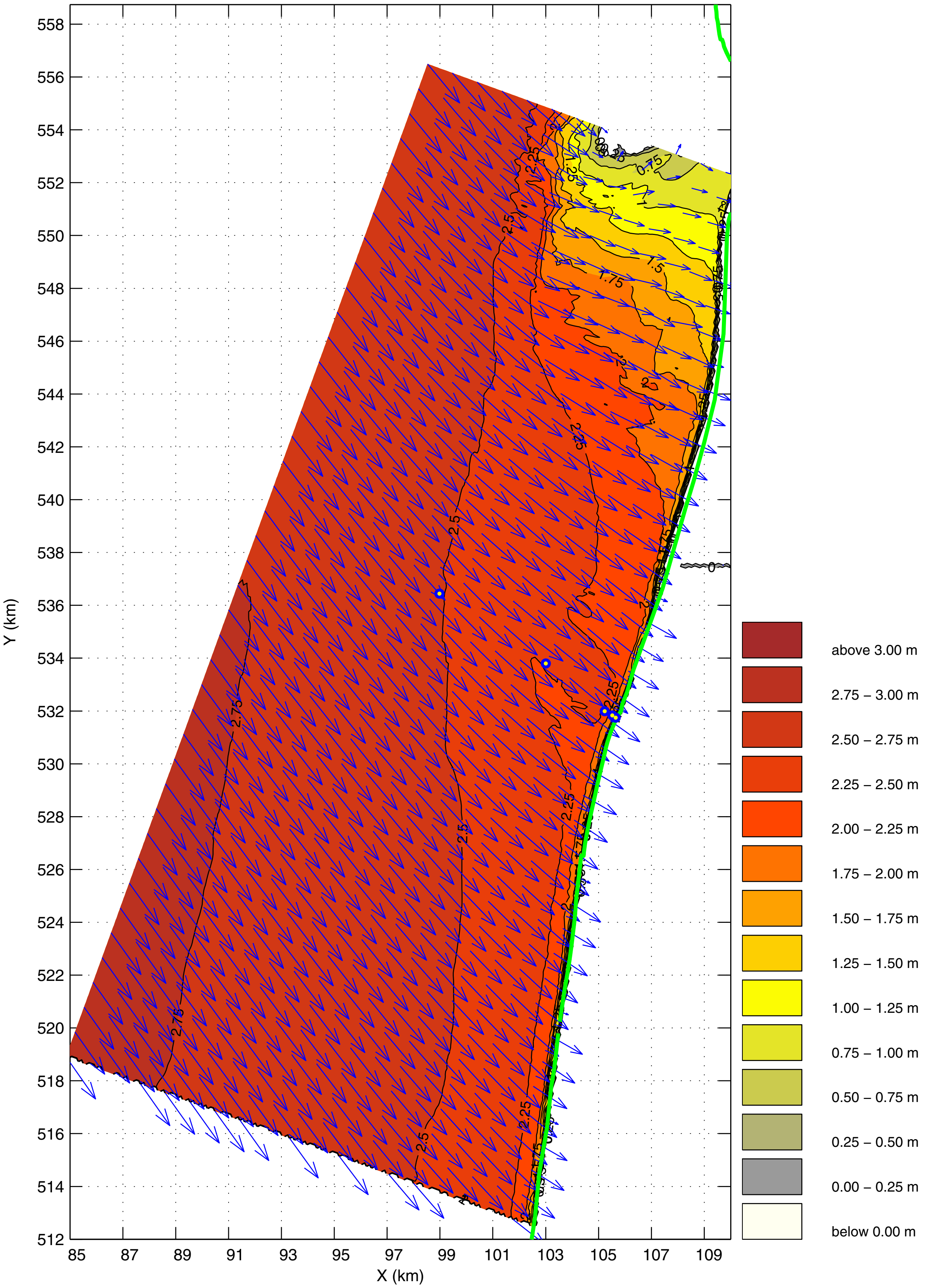

Spatial variation of significant wave height
Grid K12
Date, time, case and parameter: D19950101T0100_case2 HS

Measurements Petten Sea Defence

WLIDELFT HYDRAULICS –– ALKYON HYDRAULIC CONSULTANCY & RESEARCH

H4197/A1044

Fig. F–20

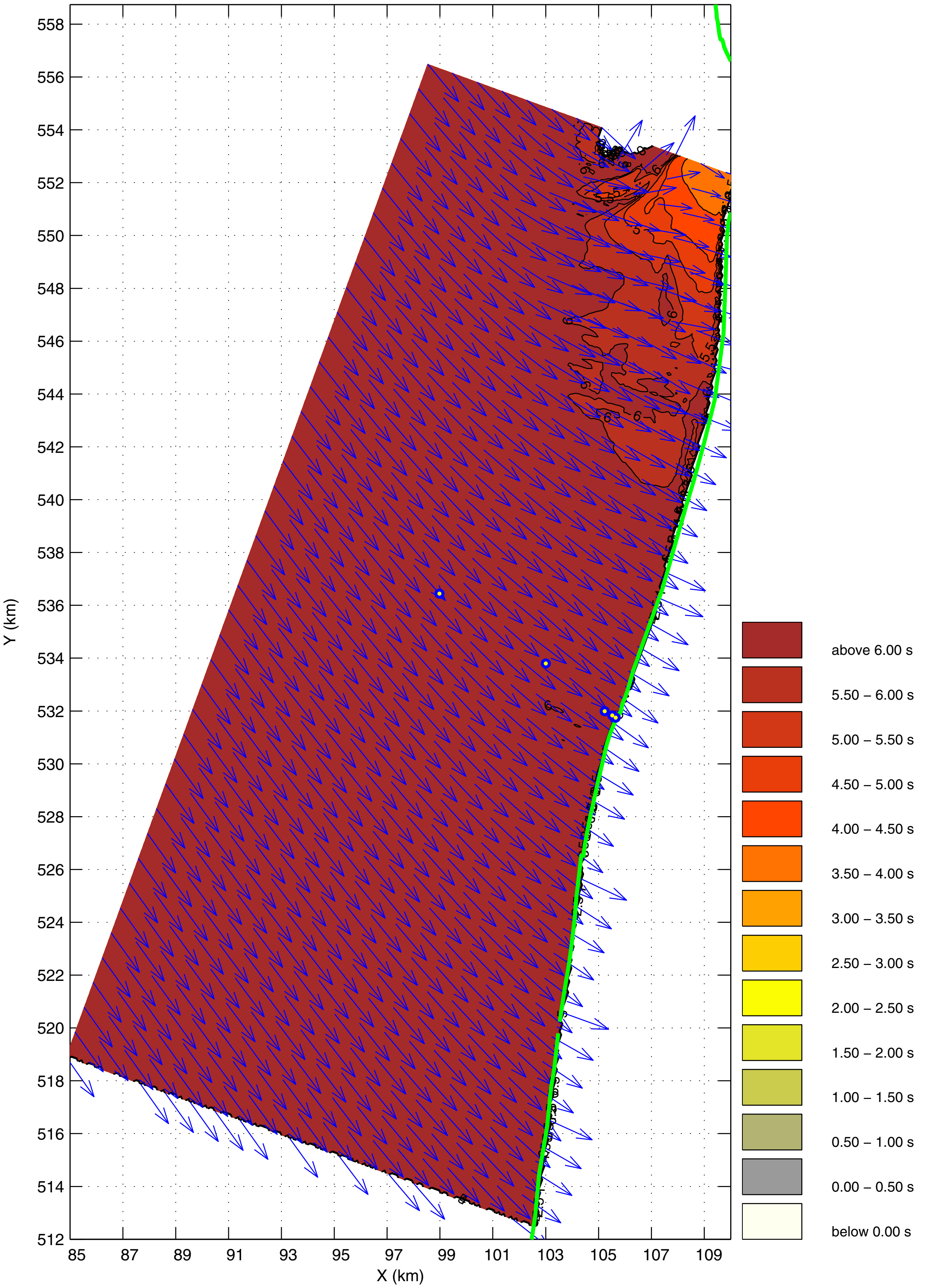

Spatial variation of mean wave period $T_{M-1,0}$ (s) Grid K12 Date, time, case and parameter: D19950101T0100_case2 T0	Measurements Petten Sea Defence	
WLIDELFT HYDRAULICS –– ALKYON HYDRAULIC CONSULTANCY & RESEARCH	H4197/A1044	Fig. F–21

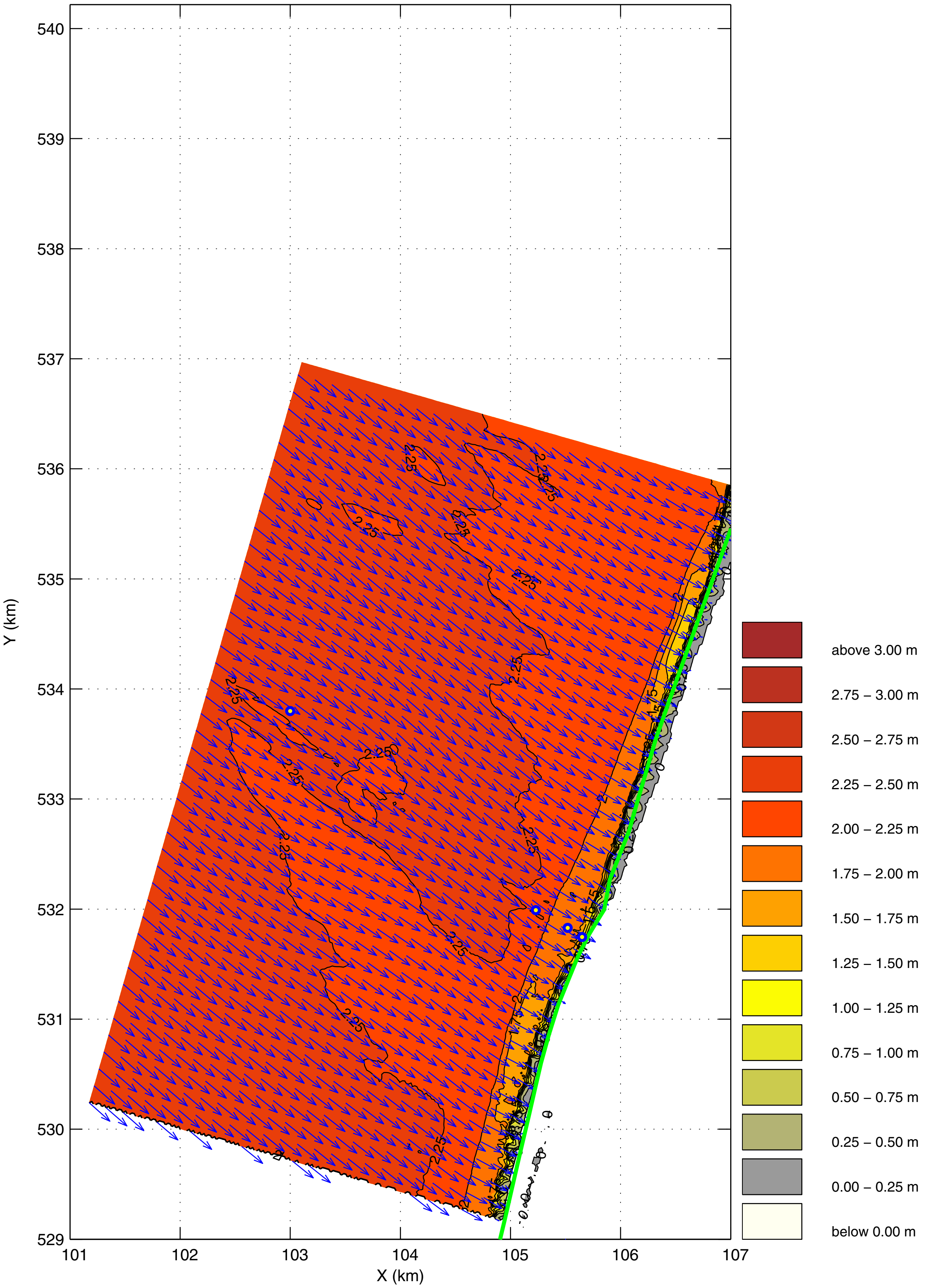

Spatial variation of significant wave height Grid E24 Date, time, case and parameter: D19950101T0100_case2 HS		
	Measurements Petten Sea Defence	
WLIDELFT HYDRAULICS –– ALKYON HYDRAULIC CONSULTANCY & RESEARCH	H4197/A1044	Fig. F–22

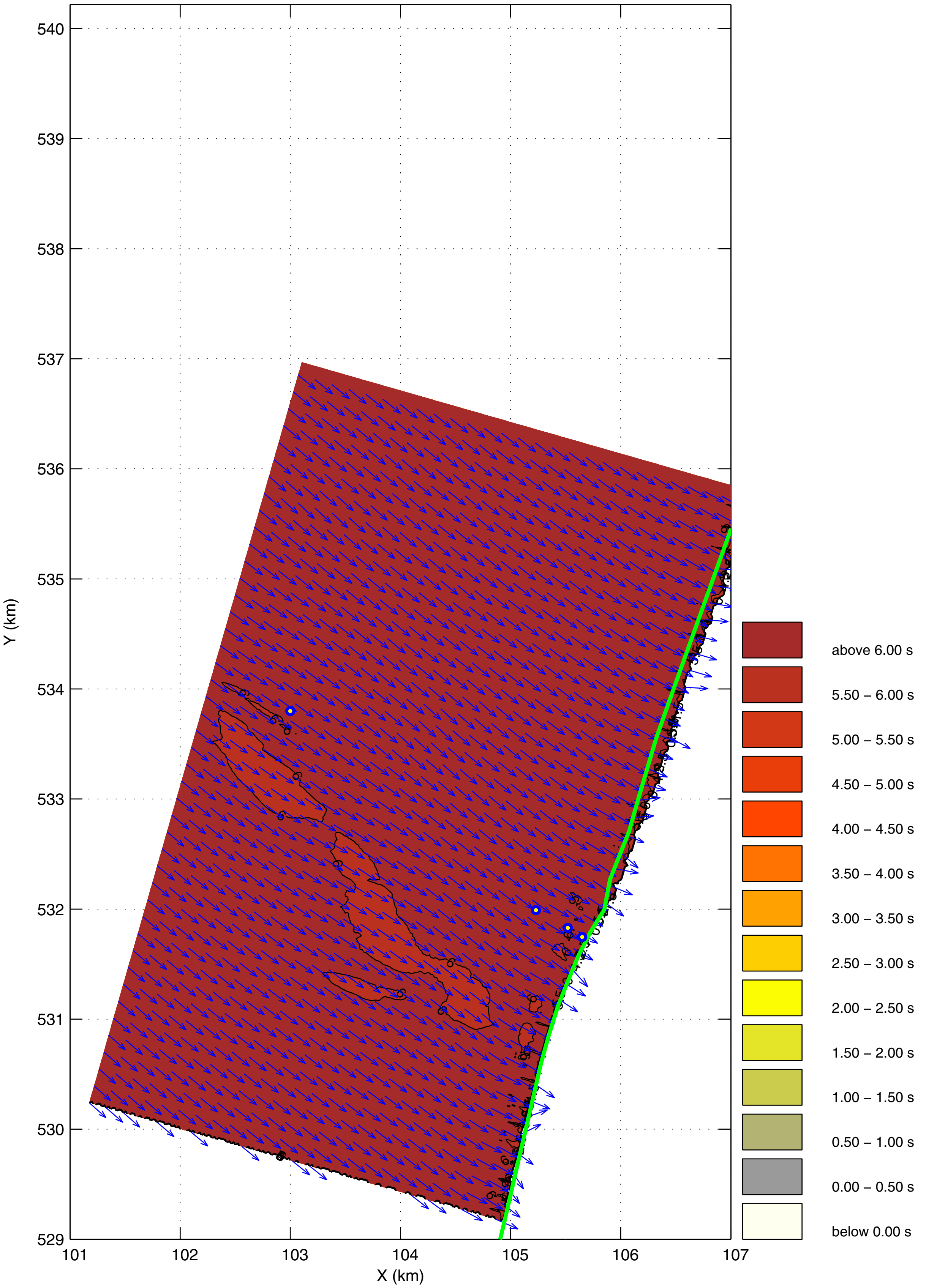

Spatial variation of mean wave period $T_{M-1,0}$ (s)
Grid E24
Date, time, case and parameter: D19950101T0100_case2 T0

Measurements Petten Sea Defence

WLIDELFT HYDRAULICS –– ALKYON HYDRAULIC CONSULTANCY & RESEARCH

H4197/A1044

Fig. F–23

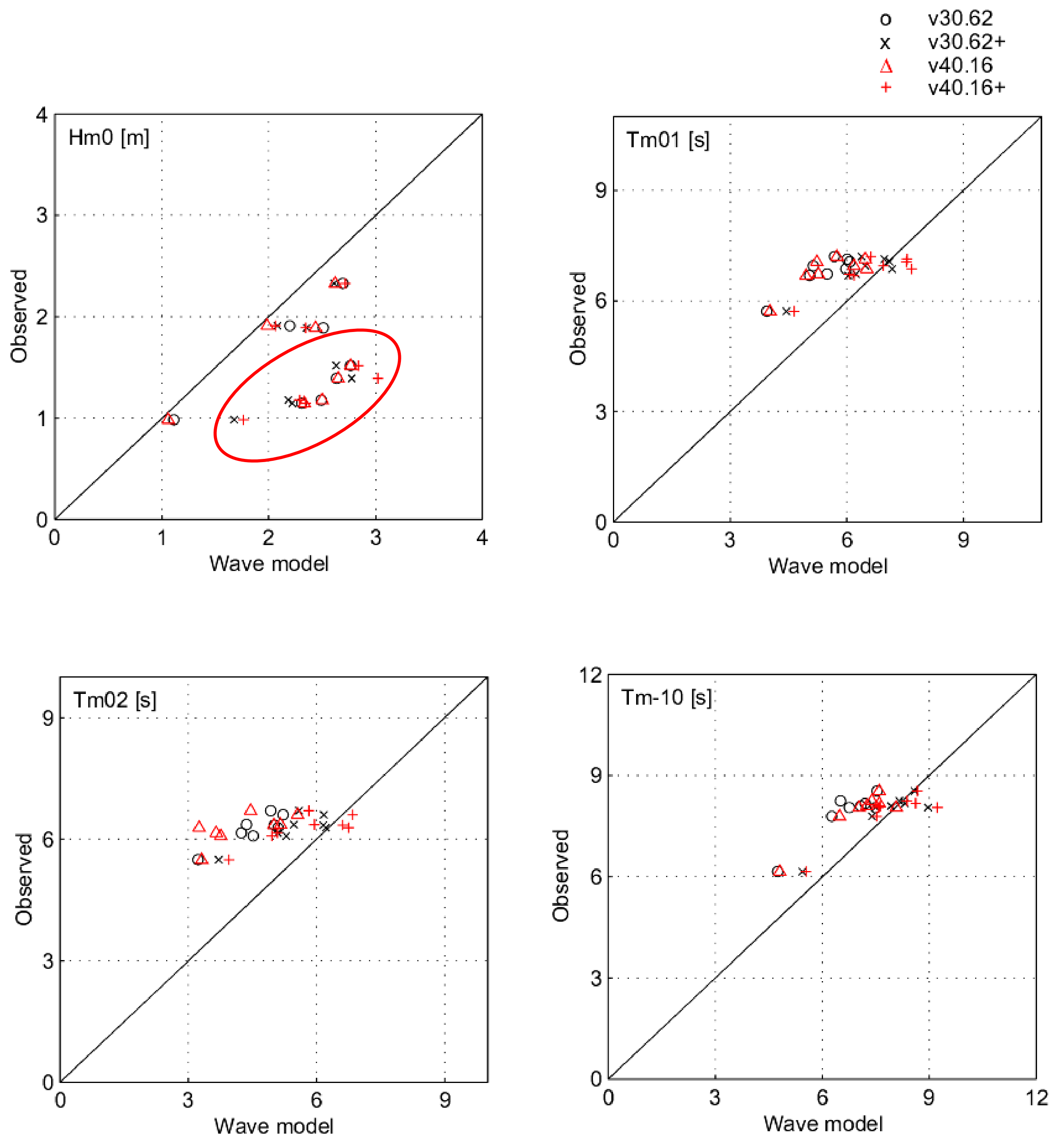

WL | Delft Hydraulics

Alkyon Hydraulic Consultancy & Research

H4197/A1044

Wave model: SWAN 30.62/40.16

Reliability of SWAN at the Petten Sea Defence

Loc. 171

Fig. F - 24

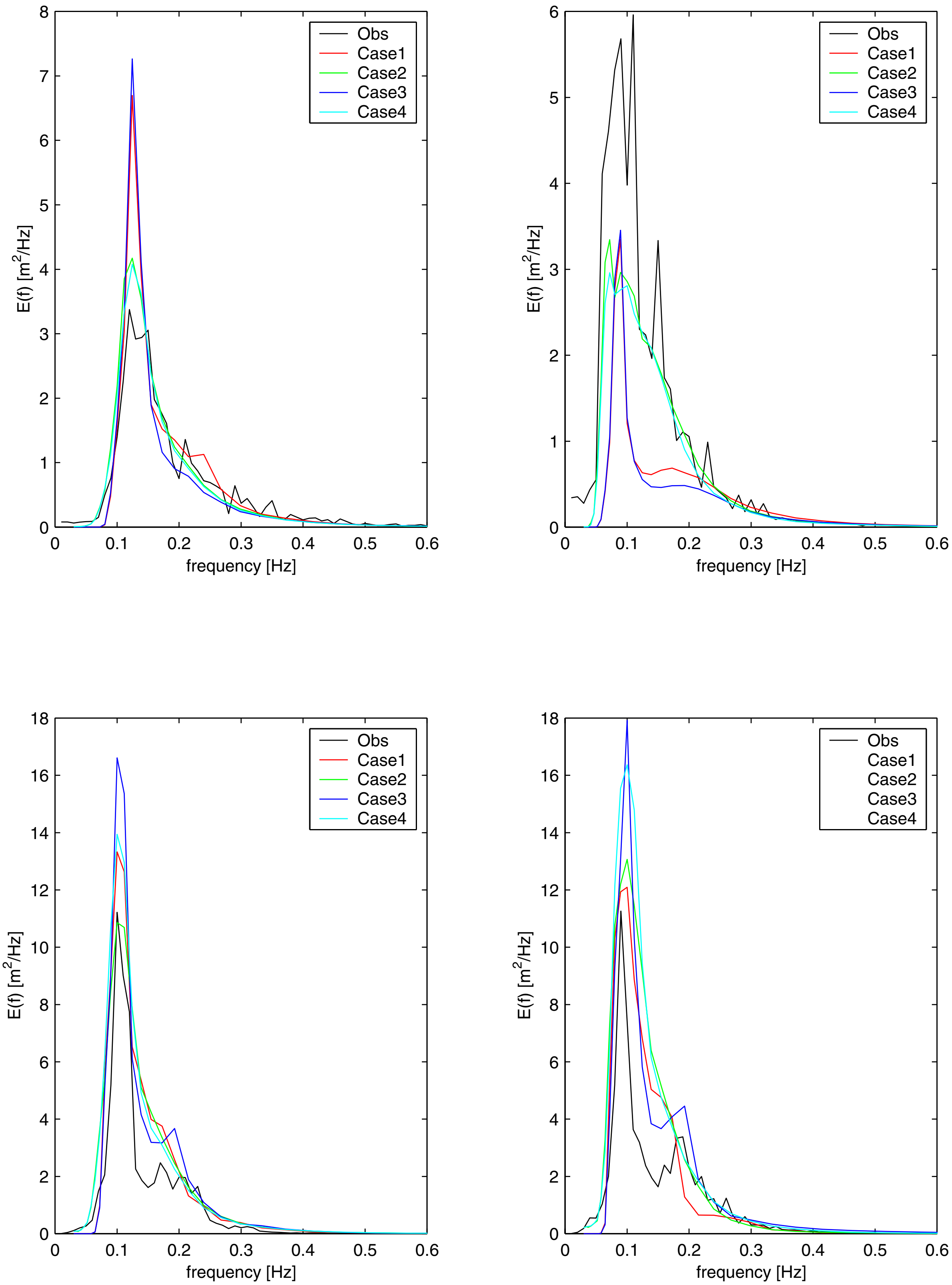

measured and computed wave energy spectra at 1 Jan 1995, 2:00hr (upper left), 2 Jan 1995, 16:40hr (upper right), 23 Feb 2002, 13:20hr (lower left), 27 Oct 2002, 17:00hr (lower right)

Loc. MP3/031/033		
Measurements Petten Sea Defence		
WL I DELFT HYDRAULICS –– ALKYON HYDRAULIC CONSULTANCY & RESEARCH	H4197/A1044	Fig. F–25a

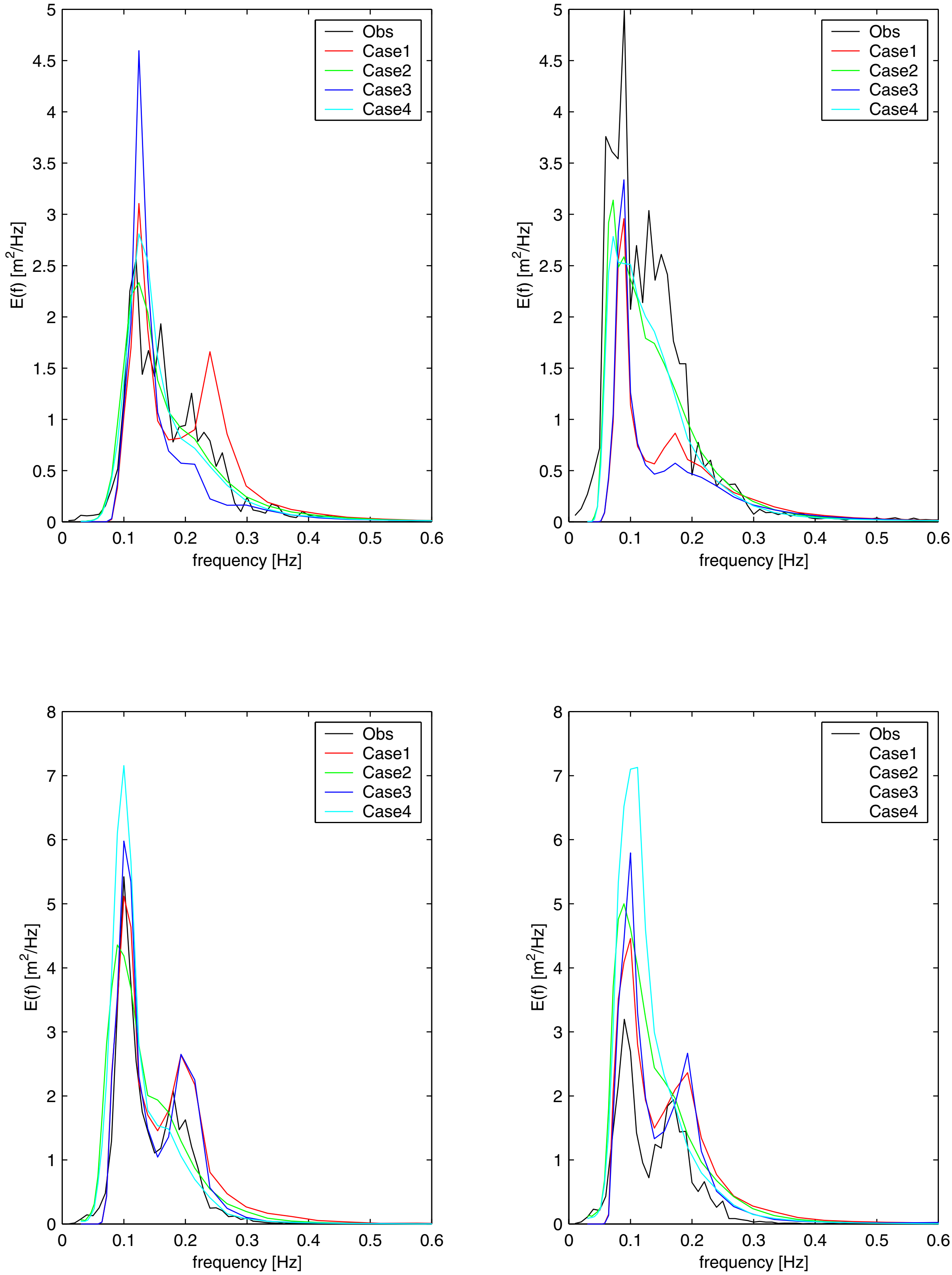

measured and computed wave energy spectra at 1 Jan 1995, 2:00hr (upper left), 2 Jan 1995, 16:40hr (upper right), 23 Feb 2002, 13:20hr (lower left), 27 Oct 2002, 17:00hr (lower right)

Loc. MP5/171/175

Measurements Petten Sea Defence

WL | DELFT HYDRAULICS –– ALKYON HYDRAULIC CONSULTANCY & RESEARCH

H4197/A1044

Fig. F–25b

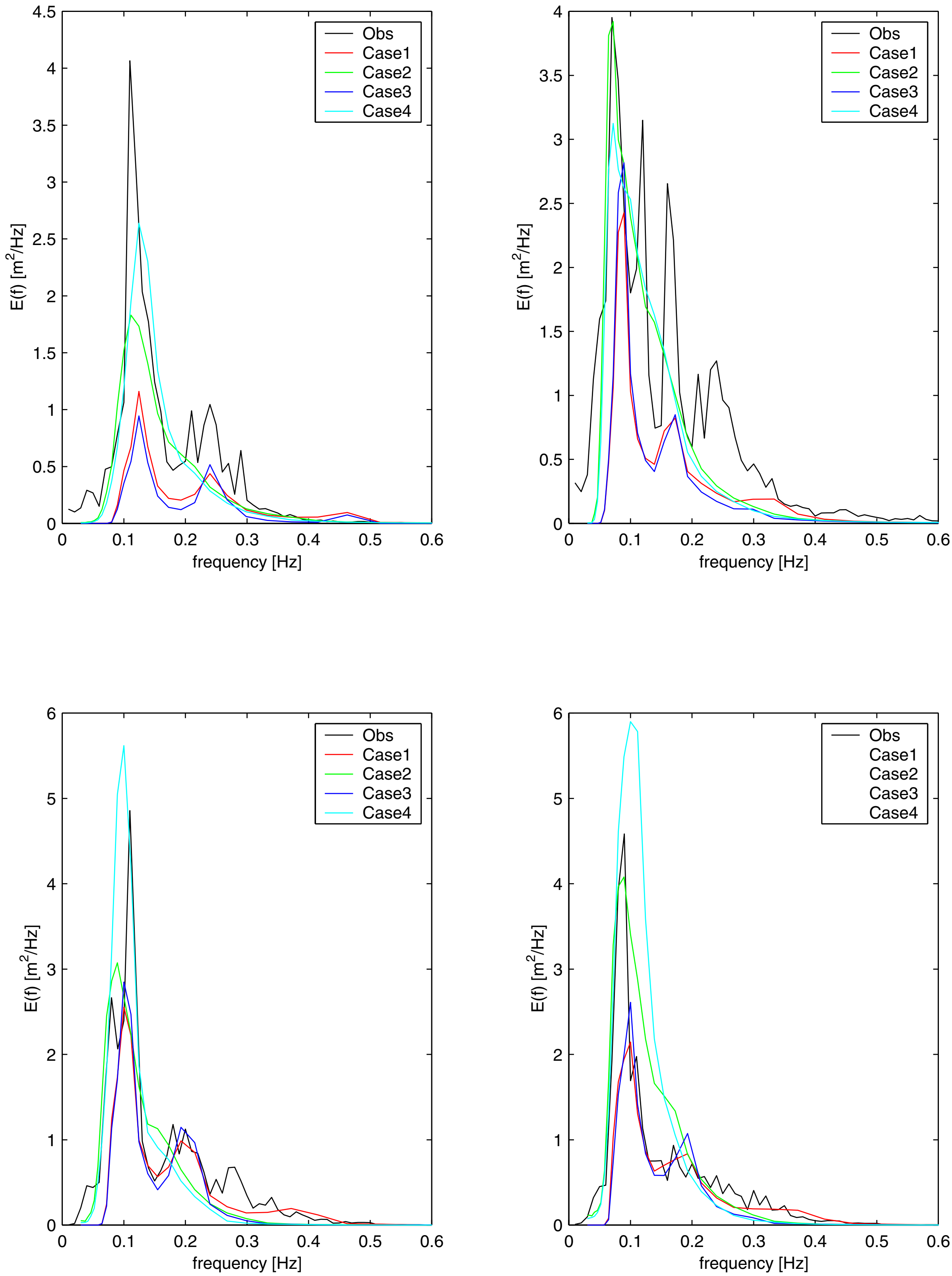

measured and computed wave energy spectra at 1 Jan 1995, 2:00hr (upper left), 2 Jan 1995, 16:40hr (upper right), 23 Feb 2002, 13:20hr (lower left), 27 Oct 2002, 17:00hr (lower right)	Loc. MP6/062	
	Measurements Petten Sea Defence	
WL I DELFT HYDRAULICS –– ALKYON HYDRAULIC CONSULTANCY & RESEARCH	H4197/A1044	Fig. F–25c

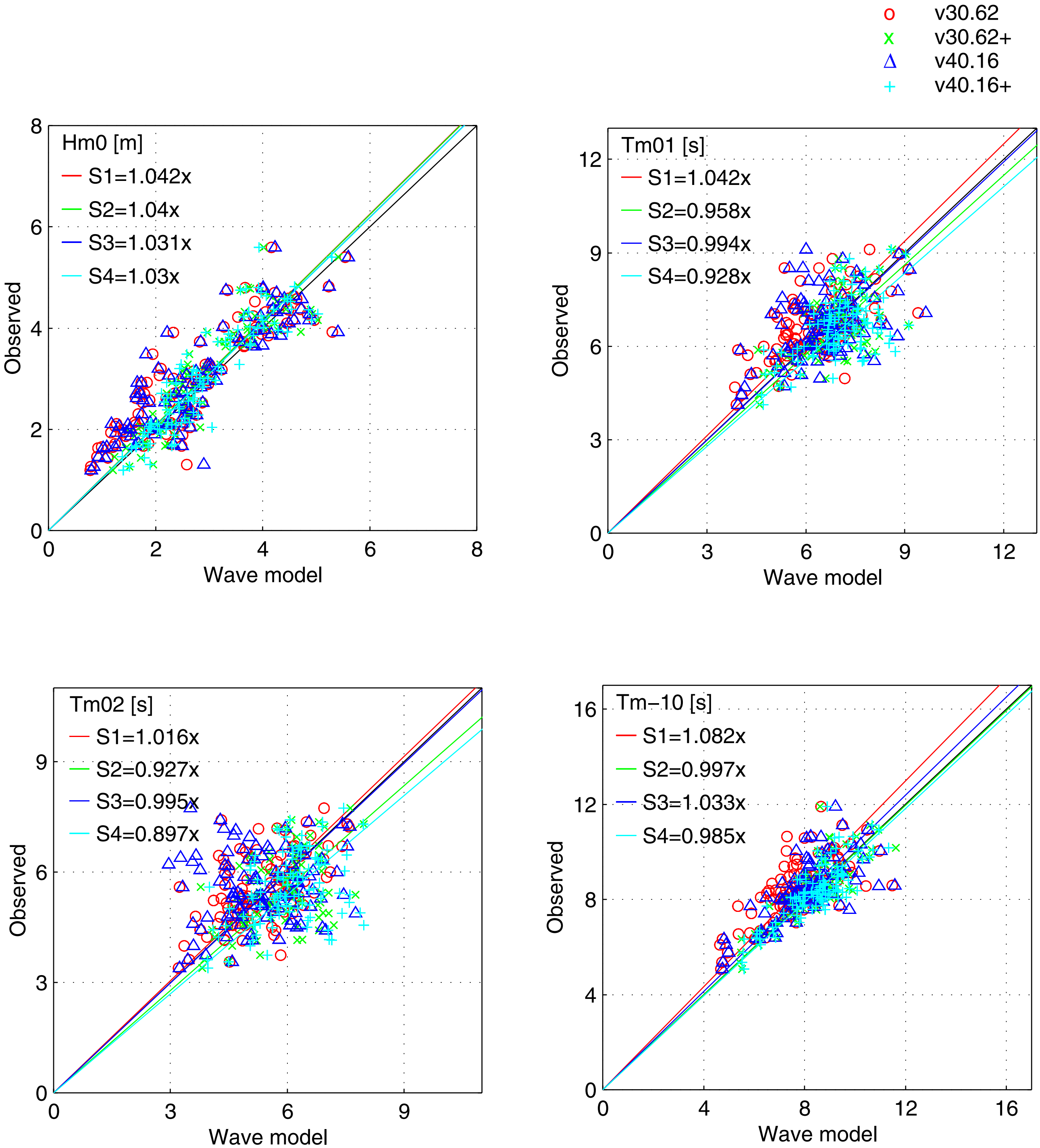

WL | Delft Hydraulics Alkyon Hydraulic Consultancy & Research	H4197/A1044
	all cases
Wave model: SWAN 30.62/40.16 Reliability of SWAN at the Petten Sea Defence	Case : **all cases** Fig. : **s00all01a.a**

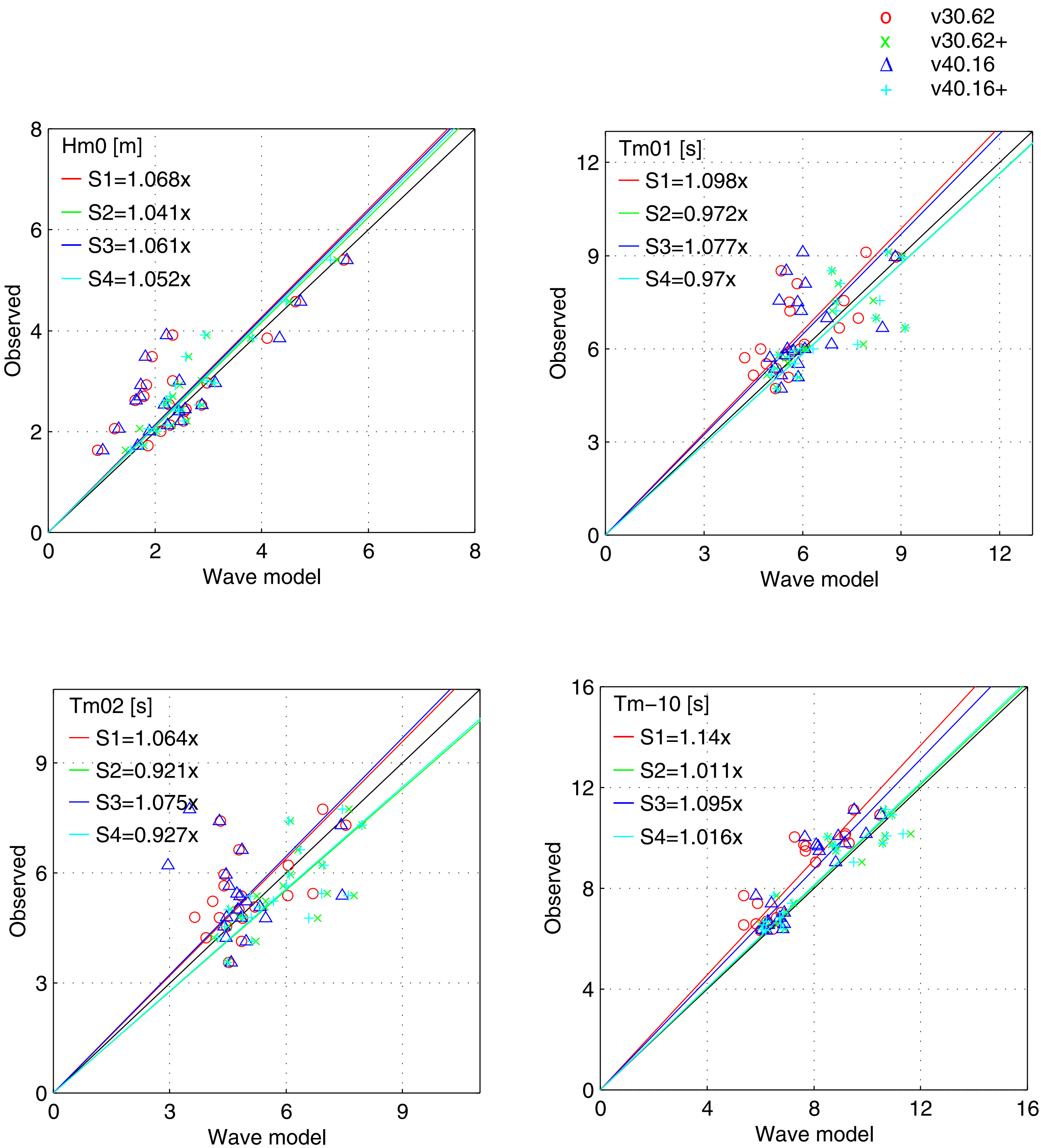

WL | Delft Hydraulics Alkyon Hydraulic Consultancy & Research	H4197/A1044
	all cases
Wave model: SWAN 30.62/40.16 Reliability of SWAN at the Petten Sea Defence	Case : **opposing current** Fig. : **s01opp01a.a**

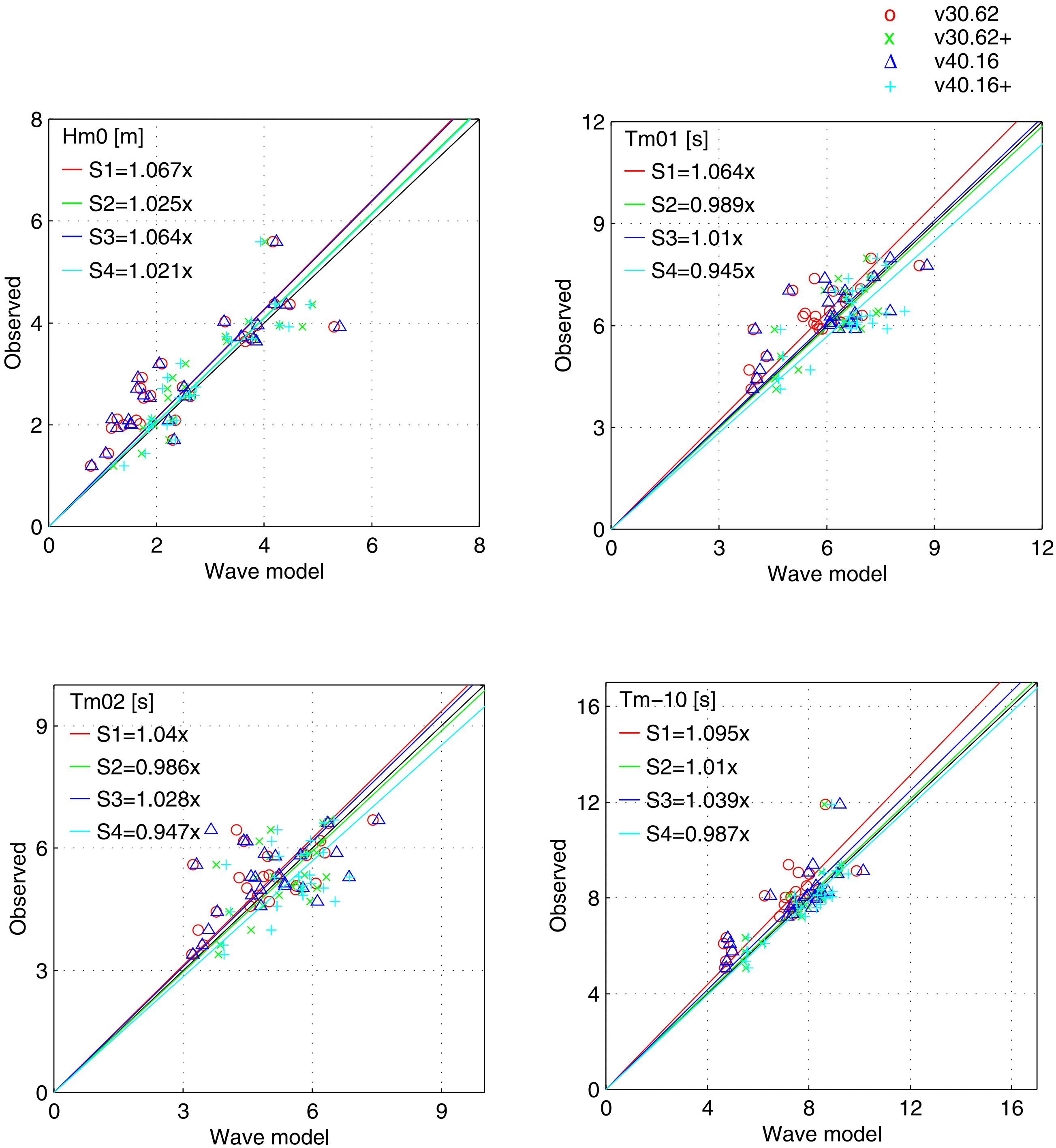

WL | Delft Hydraulics Alkyon Hydraulic Consultancy & Research	H4197/A1044
Wave model: SWAN 30.62/40.16 Reliability of SWAN at the Petten Sea Defence	all cases
	Case : **following current** Fig. : **s02par01a.a**

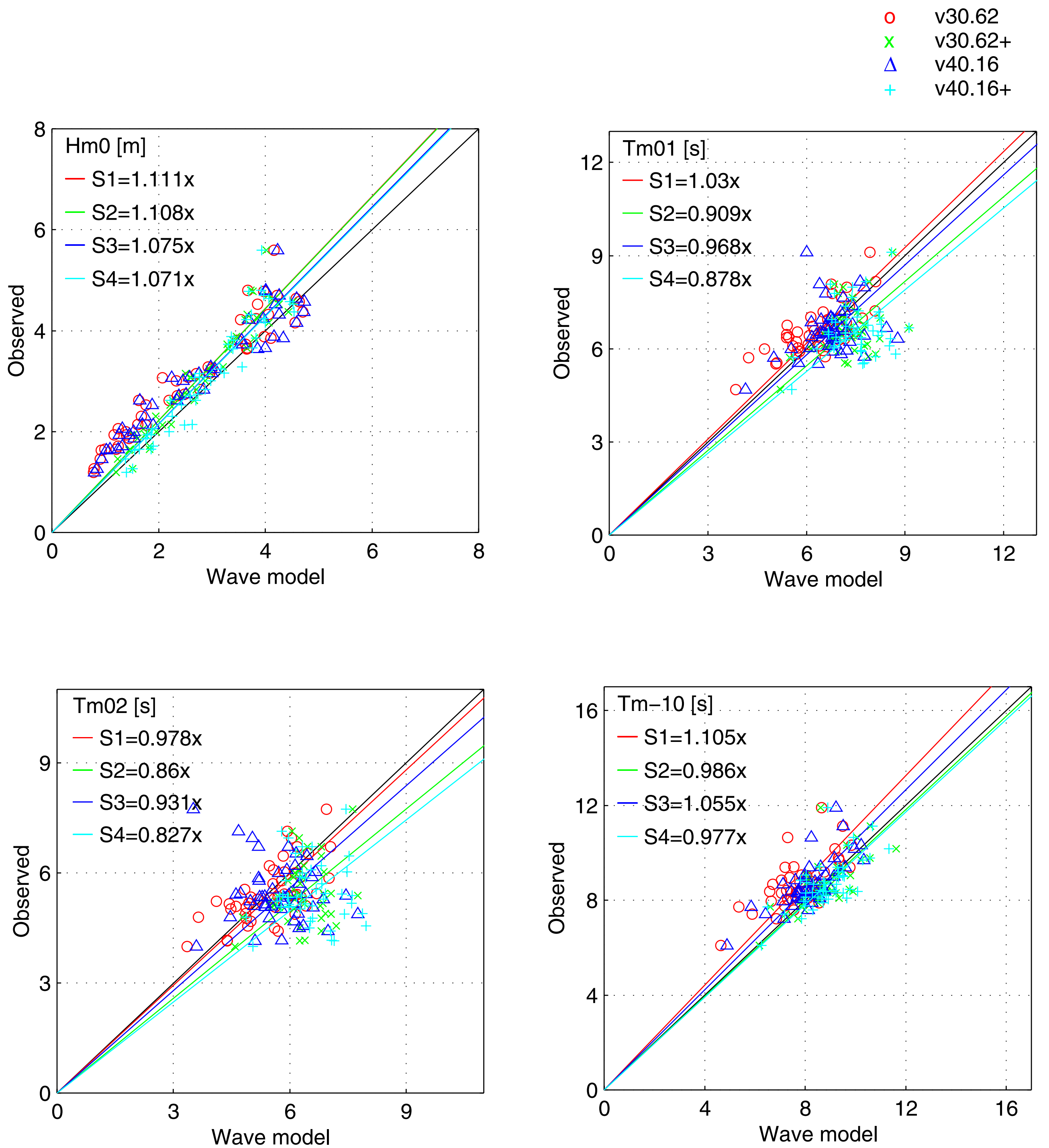

WL | Delft Hydraulics Alkyon Hydraulic Consultancy & Research	H4197/A1044
	all cases
Wave model: SWAN 30.62/40.16 Reliability of SWAN at the Petten Sea Defence	Case : **depth limited** Fig. : **s03dep01a.a**

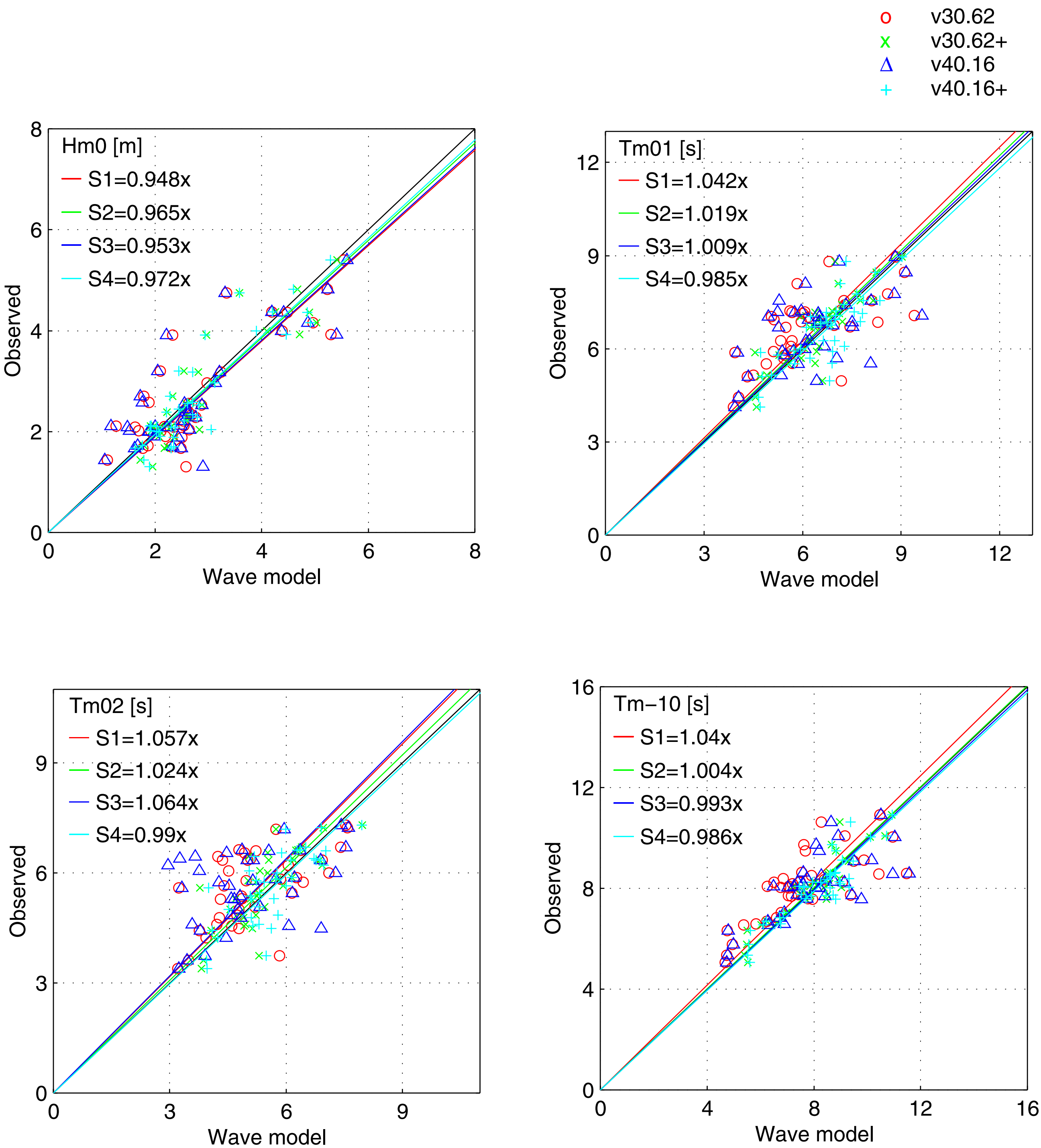

WL | Delft Hydraulics

Alkyon Hydraulic Consultancy & Research

H4197/A1044

all cases

Wave model: SWAN 30.62/40.16

Reliability of SWAN at the Petten Sea Defence

Case : **not depth limited**

Fig. : **s04nde01a.a**

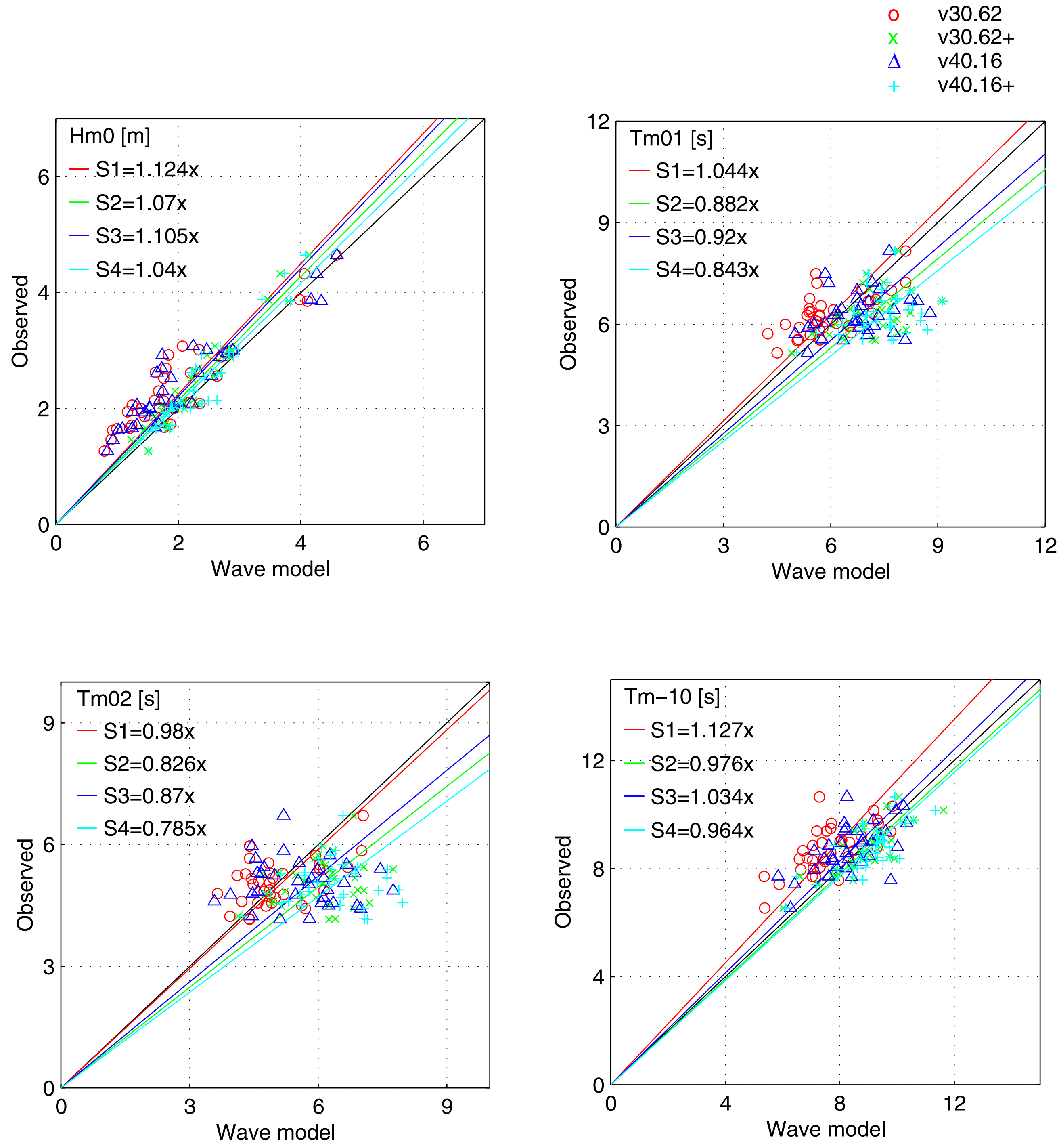

WL | Delft Hydraulics Alkyon Hydraulic Consultancy & Research	H4197/A1044
	all cases
Wave model: SWAN 30.62/40.16 Reliability of SWAN at the Petten Sea Defence	Case : **low frequency** Fig. : **s05dbl01a.a**

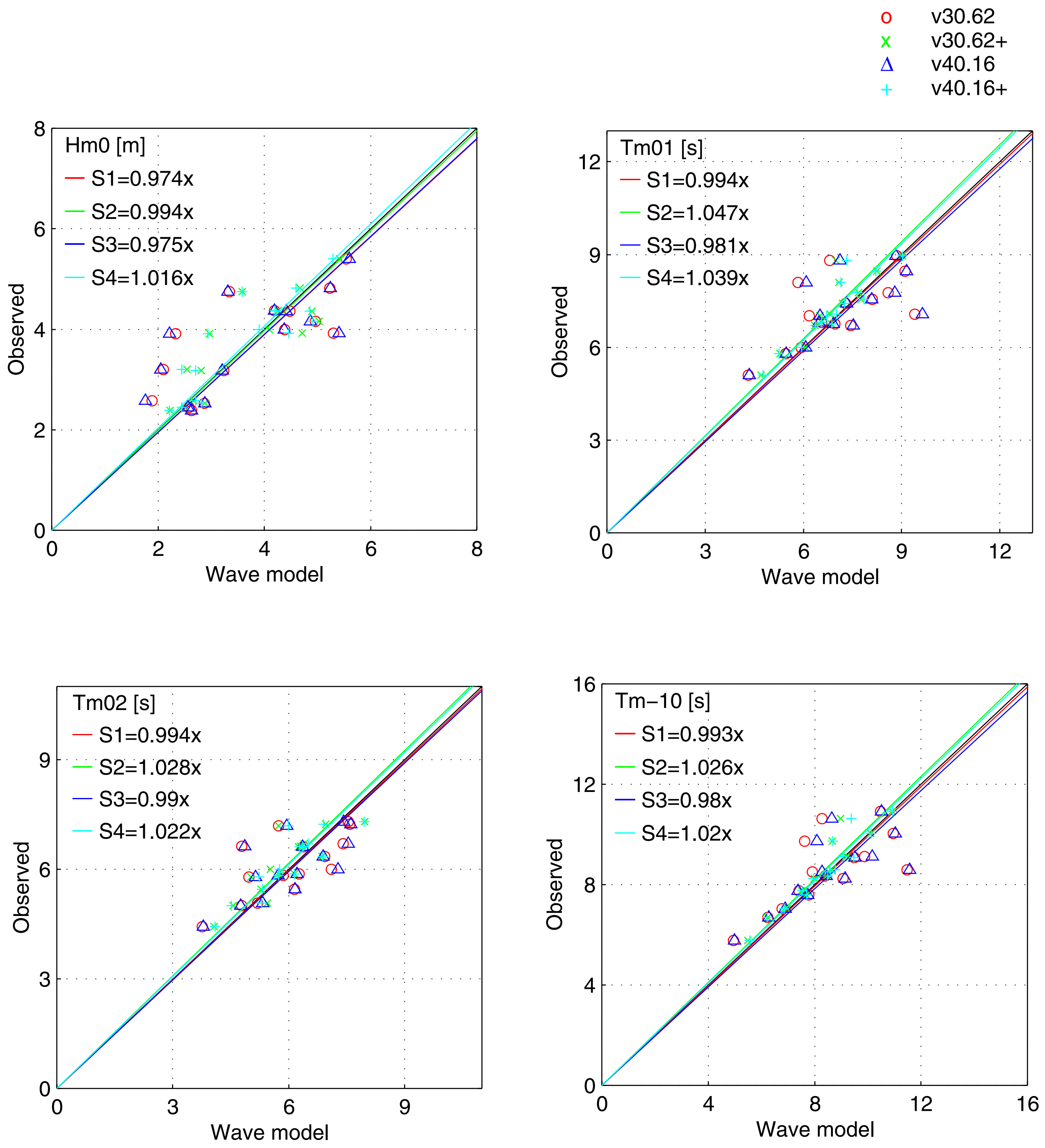

WL | Delft Hydraulics Alkyon Hydraulic Consultancy & Research	H4197/A1044
	all cases
Wave model: SWAN 30.62/40.16 Reliability of SWAN at the Petten Sea Defence	Loc. : **mp1/011** Fig. : **s06loc01a.a**

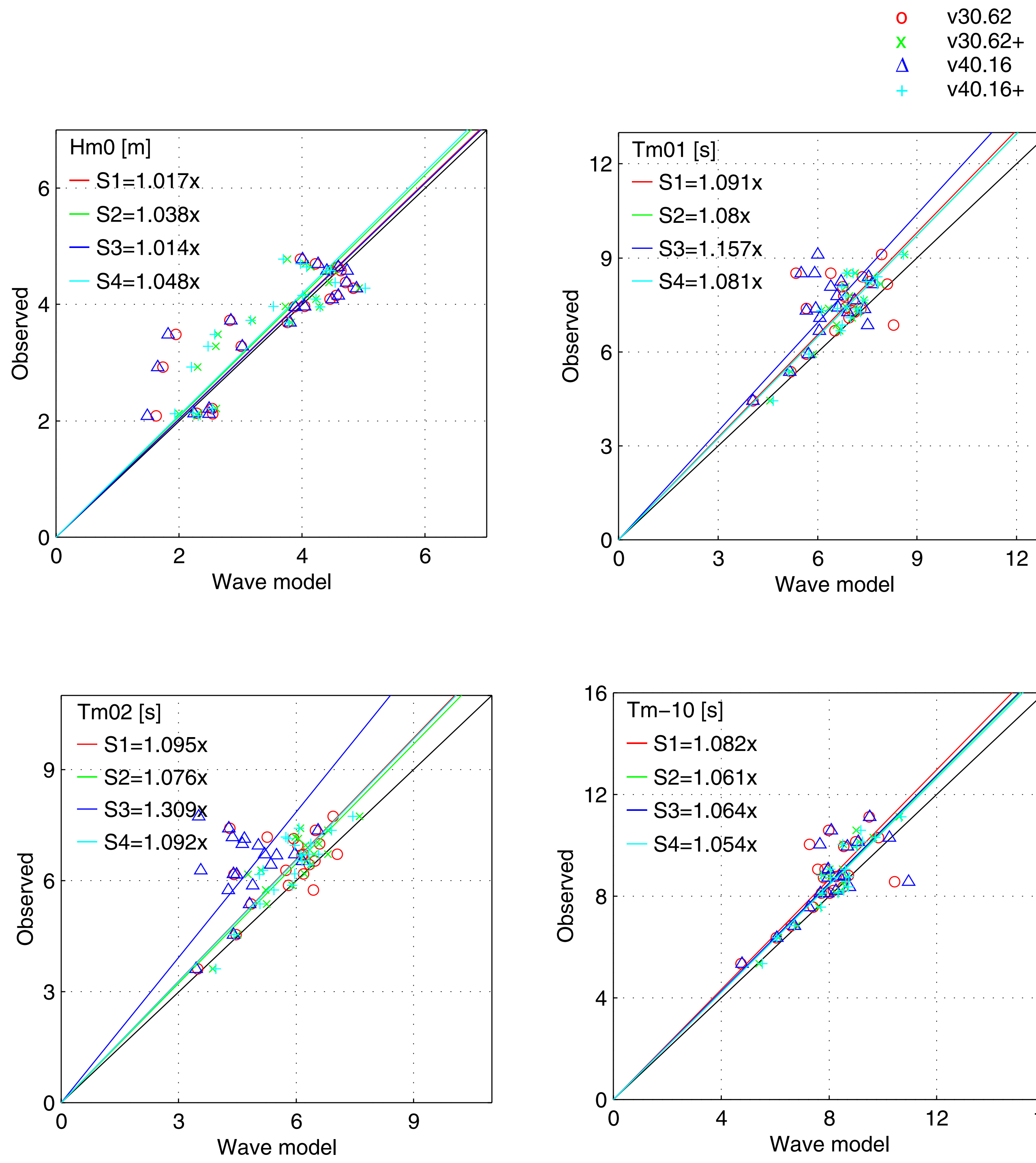

WL | Delft Hydraulics Alkyon Hydraulic Consultancy & Research	H4197/A1044
	all cases
Wave model: SWAN 30.62/40.16 Reliability of SWAN at the Petten Sea Defence	Loc. : **mp2/021** Fig. : **s07loc01a.a**

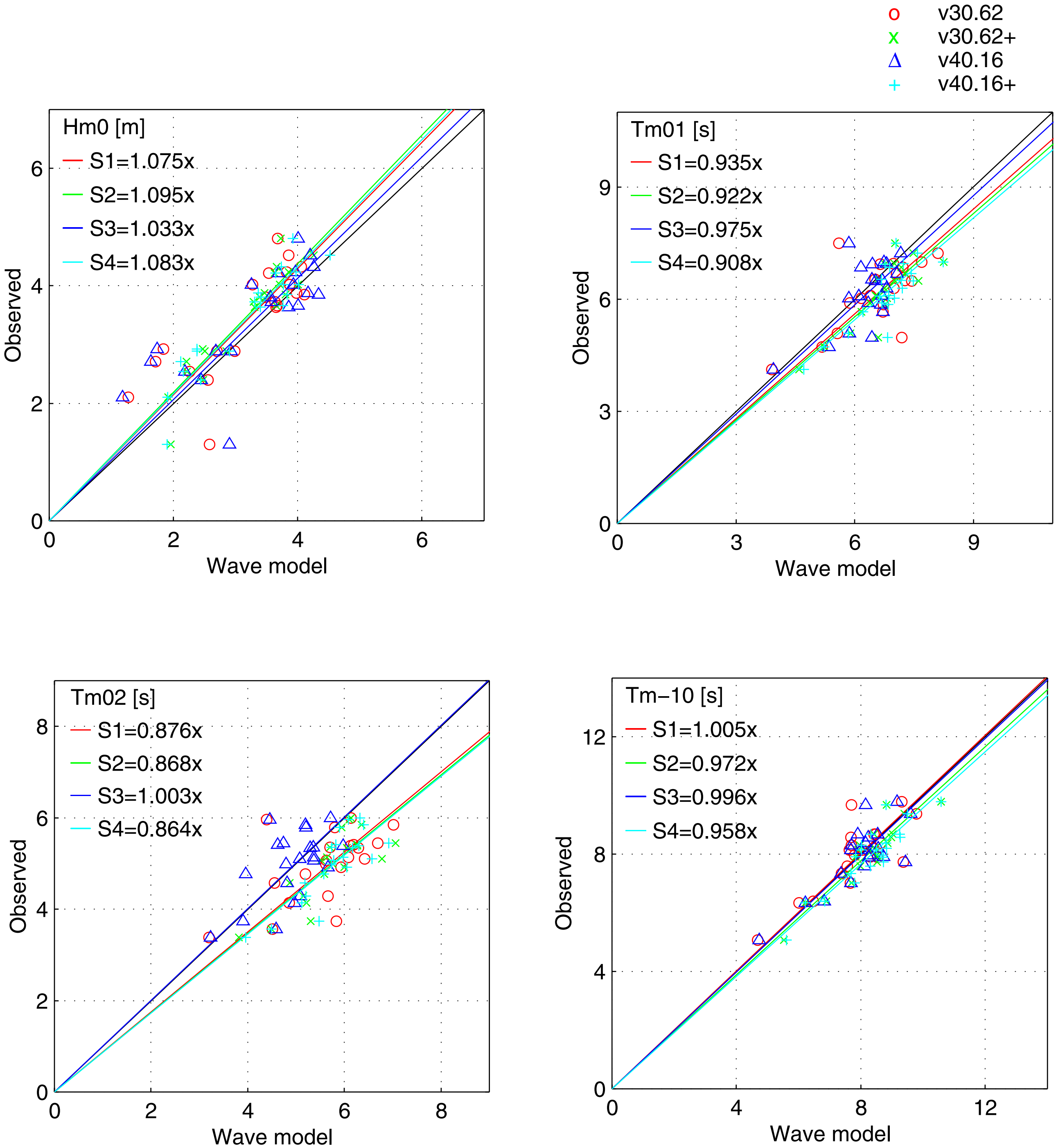

WL | Delft Hydraulics Alkyon Hydraulic Consultancy & Research	H4197/A1044
	all cases
Wave model: SWAN 30.62/40.16 Reliability of SWAN at the Petten Sea Defence	Loc. : **mp3/031/033** Fig. : **s08loc01a.a**

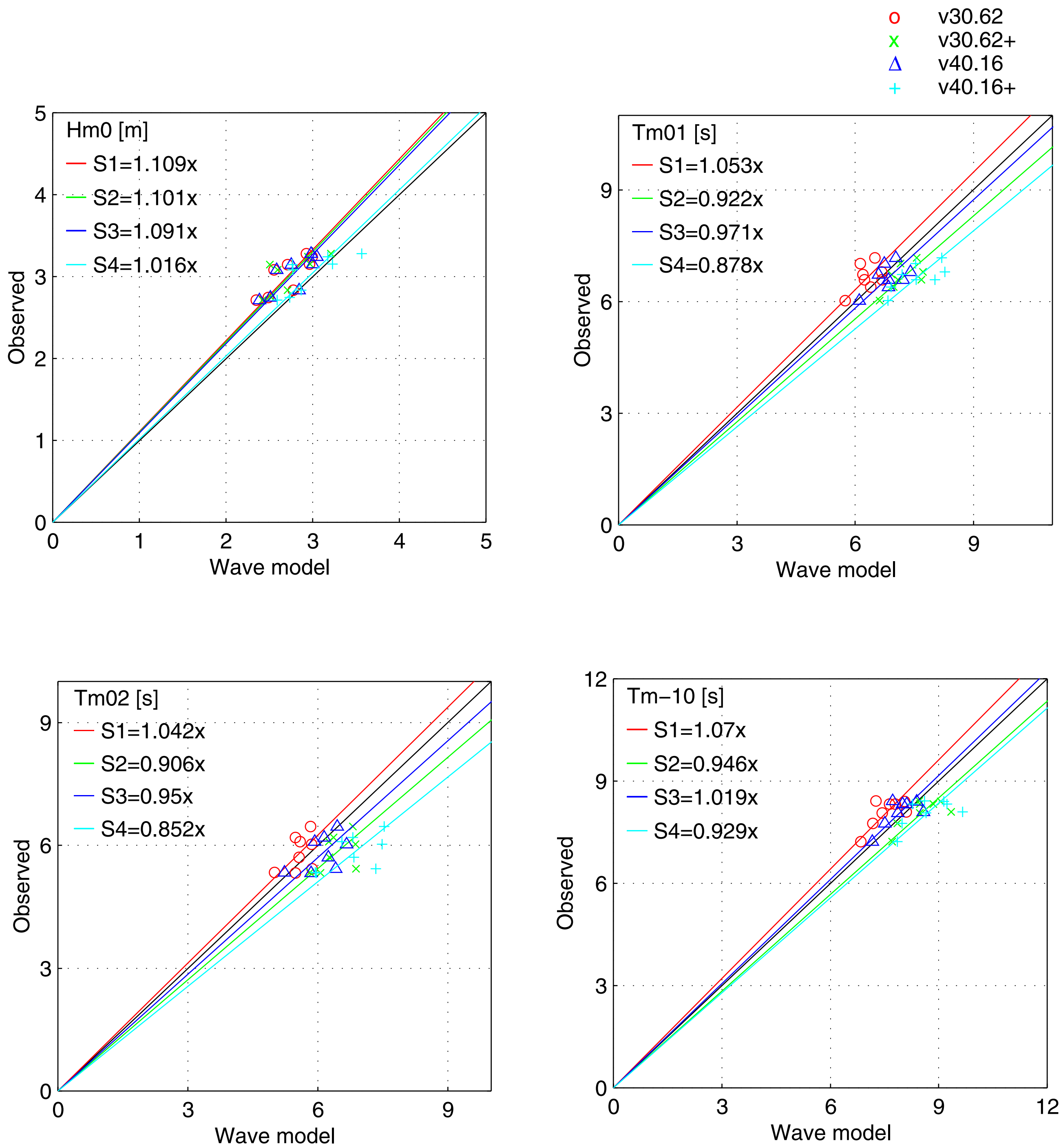

WL | Delft Hydraulics

Alkyon Hydraulic Consultancy & Research

H4197/A1044

Wave model: SWAN 30.62/40.16

Reliability of SWAN at the Petten Sea Defence

all cases

Loc. : **161/162**

Fig. : **s09loc01a.a**

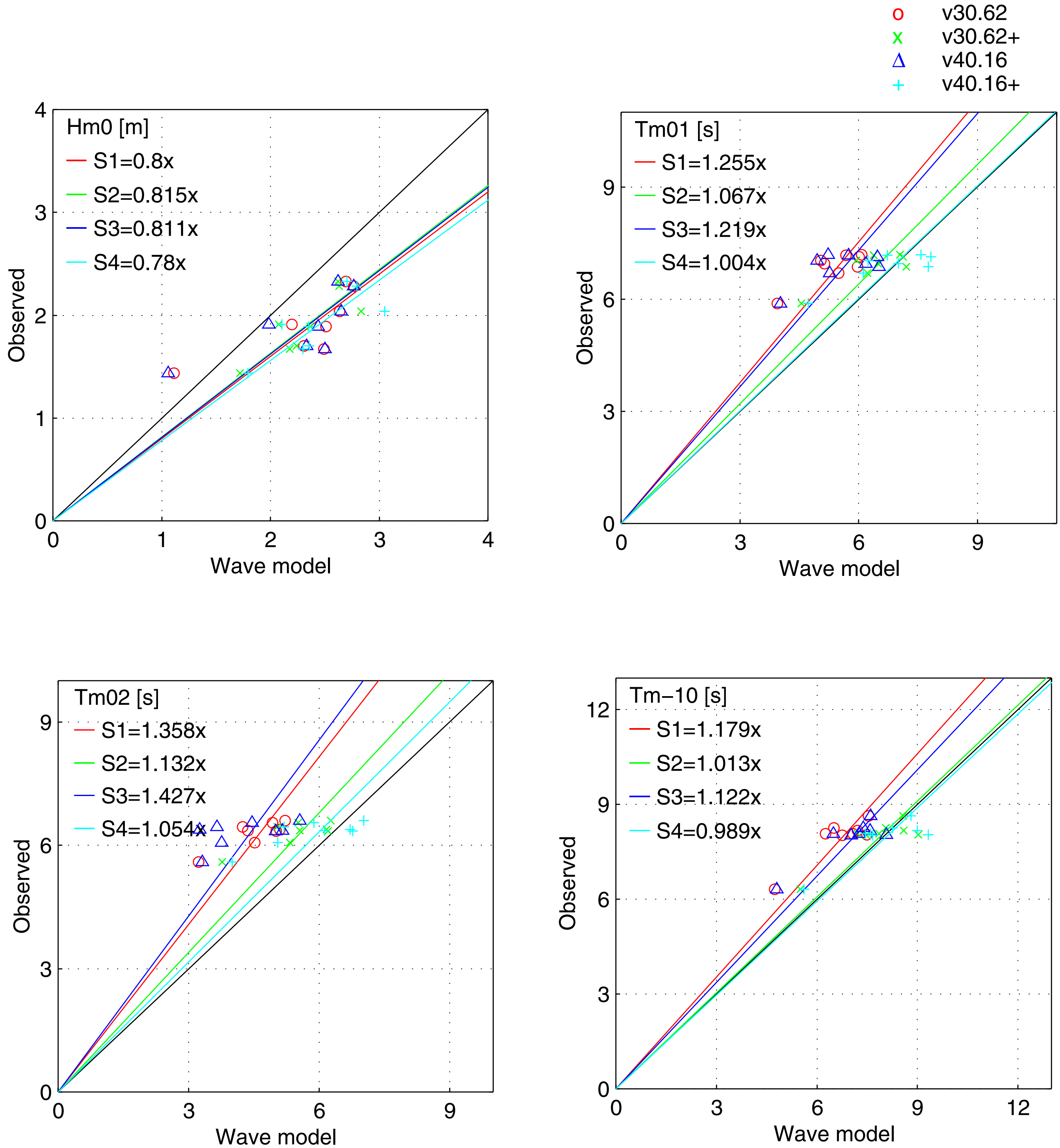

WL | Delft Hydraulics Alkyon Hydraulic Consultancy & Research	H4197/A1044
	all cases
Wave model: SWAN 30.62/40.16 Reliability of SWAN at the Petten Sea Defence	Loc. : **171/175** Fig. : **s10loc01a.a**

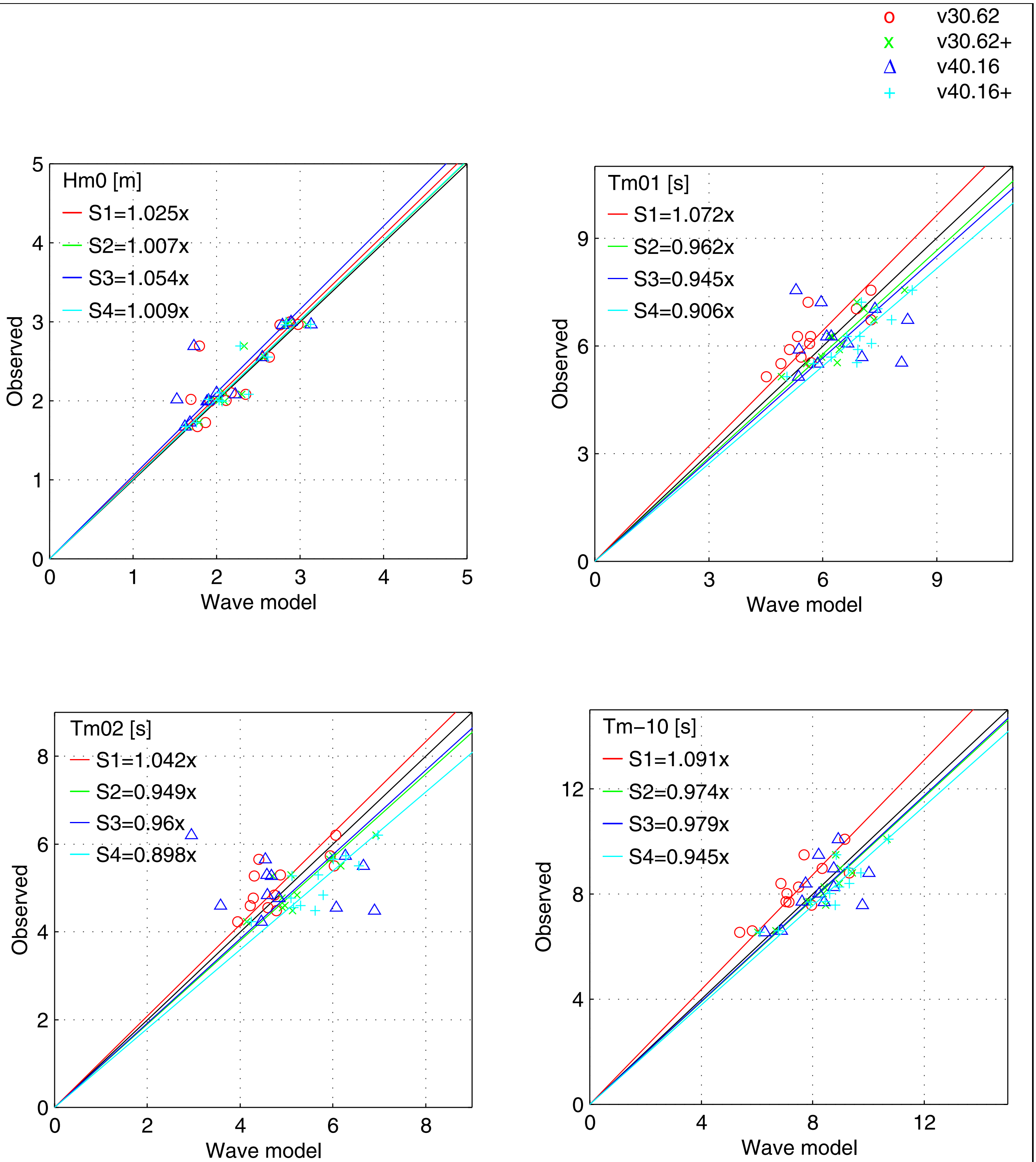

WL | Delft Hydraulics Alkyon Hydraulic Consultancy & Research	H4197/A1044
	all cases
Wave model: SWAN 30.62/40.16 Reliability of SWAN at the Petten Sea Defence	Loc. : **mp5** Fig. : **s11loc01a.a**

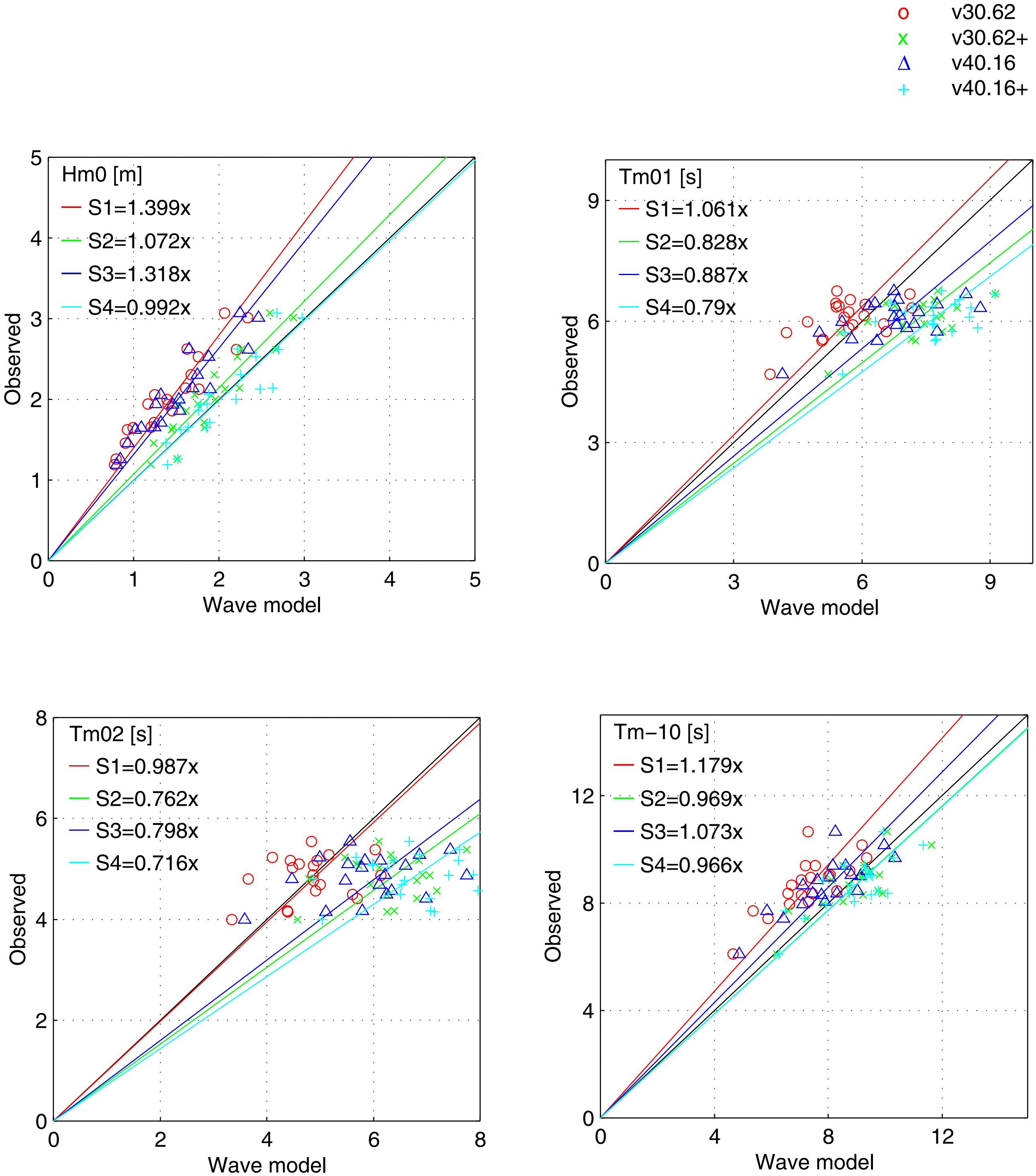

WL | Delft Hydraulics Alkyon Hydraulic Consultancy & Research	H4197/A1044
	all cases
Wave model: SWAN 30.62/40.16 Reliability of SWAN at the Petten Sea Defence	Loc. : **mp6/062** Fig. : **s12loc01a.a**

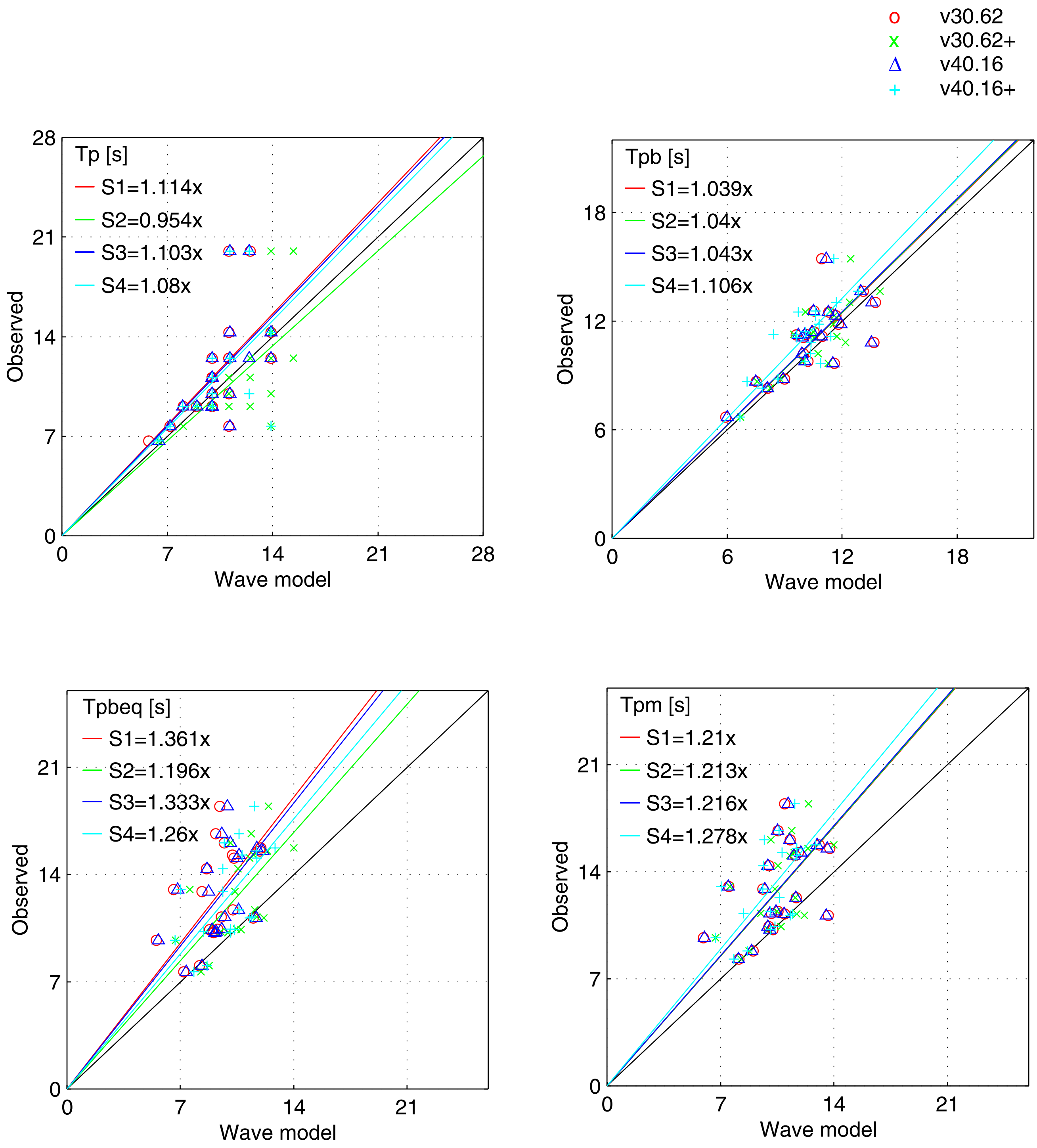

WL | Delft Hydraulics Alkyon Hydraulic Consultancy & Research	H4197/A1044
	all cases
Wave model: SWAN 30.62/40.16 Reliability of SWAN at the Petten Sea Defence	Loc. : **mp6/062** Fig. : **s12loc01b.a**

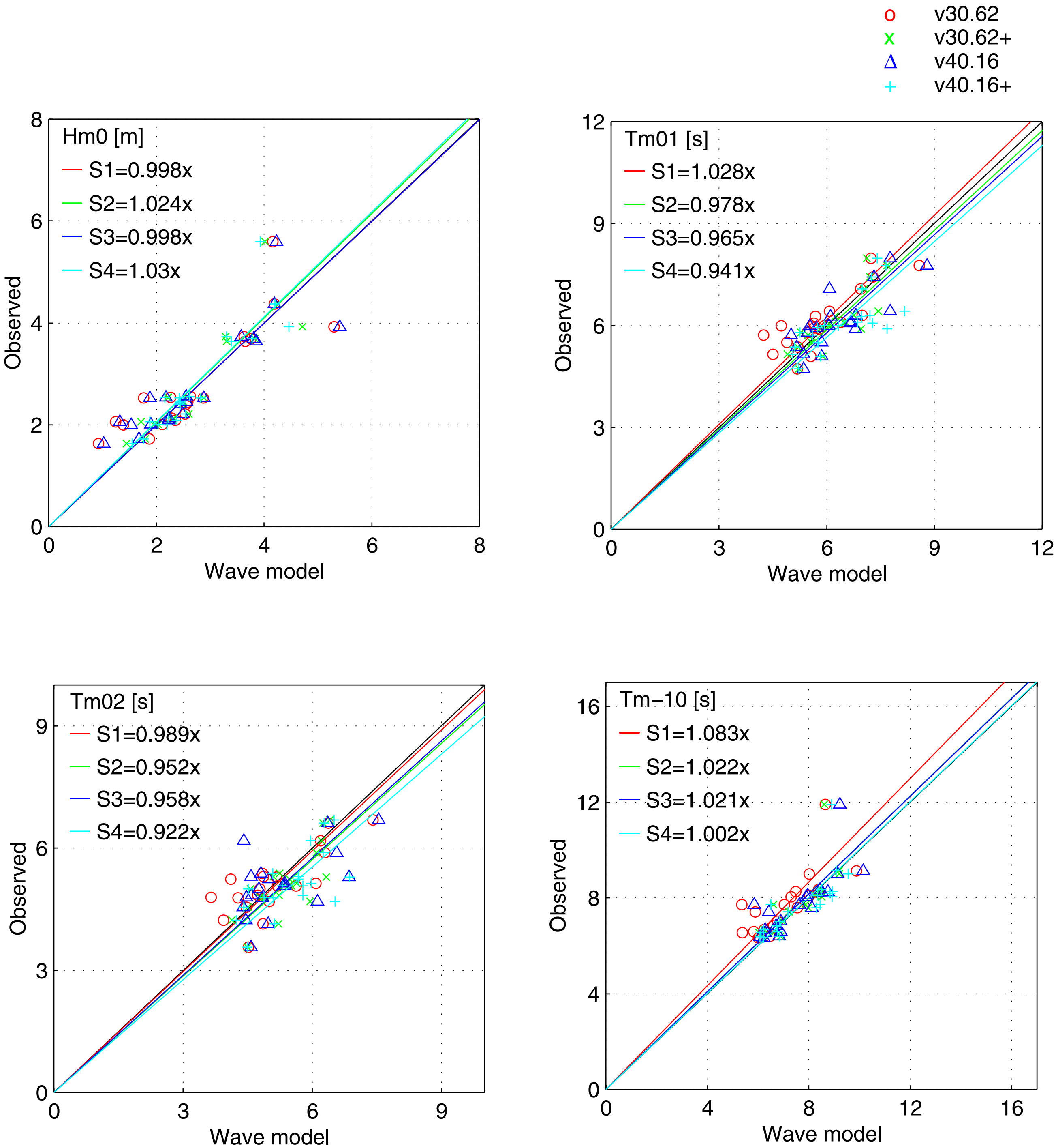

WL | Delft Hydraulics Alkyon Hydraulic Consultancy & Research	H4197/A1044
	all cases
Wave model: SWAN 30.62/40.16 Reliability of SWAN at the Petten Sea Defence	Loc. : **storm 1** Fig. : **s13str01a.a**

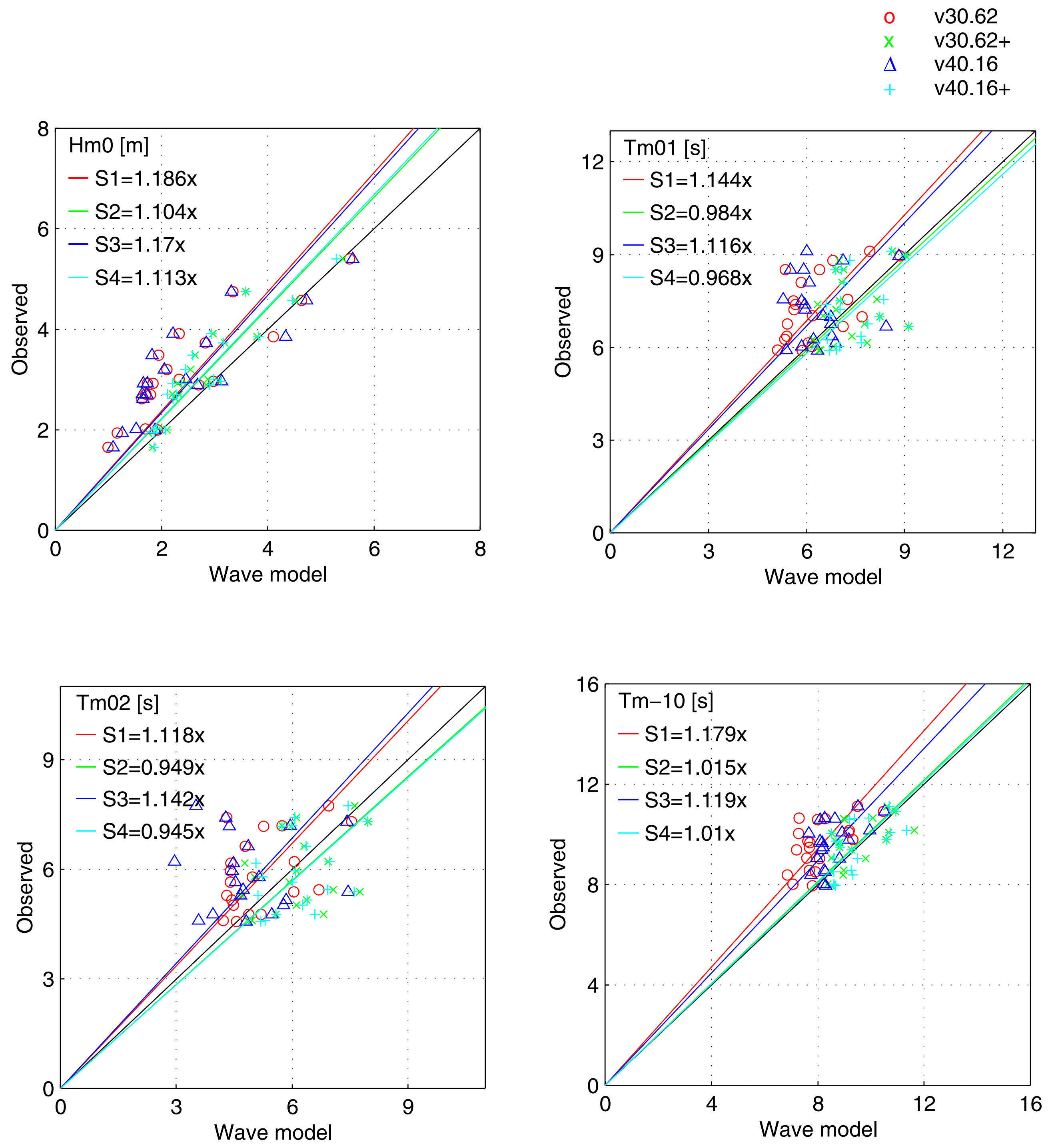

WL | Delft Hydraulics Alkyon Hydraulic Consultancy & Research	H4197/A1044
	all cases
Wave model: SWAN 30.62/40.16 Reliability of SWAN at the Petten Sea Defence	Loc. : **storm 2** Fig. : **s14str01a.a**

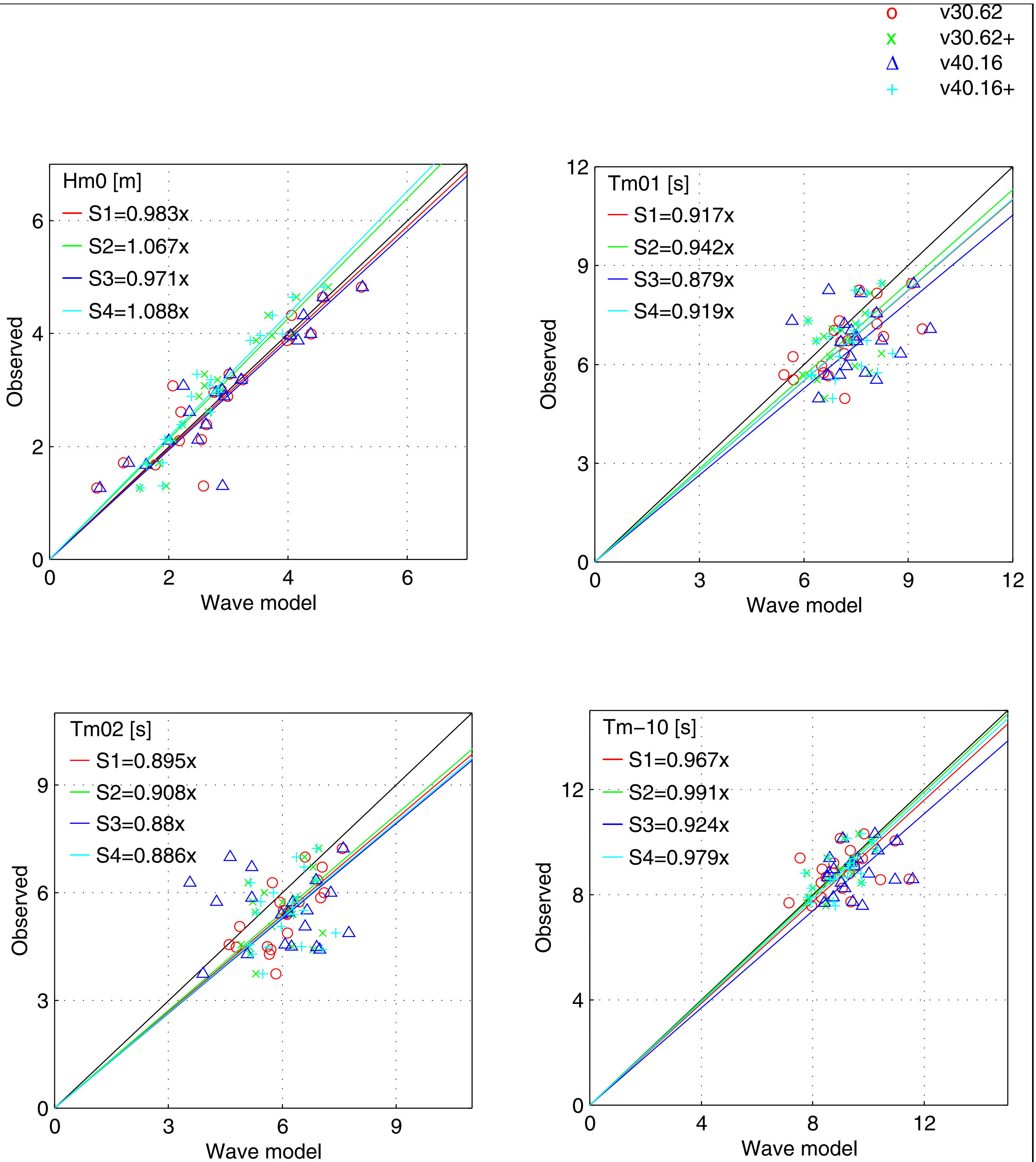

WL | Delft Hydraulics Alkyon Hydraulic Consultancy & Research	H4197/A1044
	all cases
Wave model: SWAN 30.62/40.16 Reliability of SWAN at the Petten Sea Defence	Loc. : **storm 3** Fig. : **s15str01a.a**

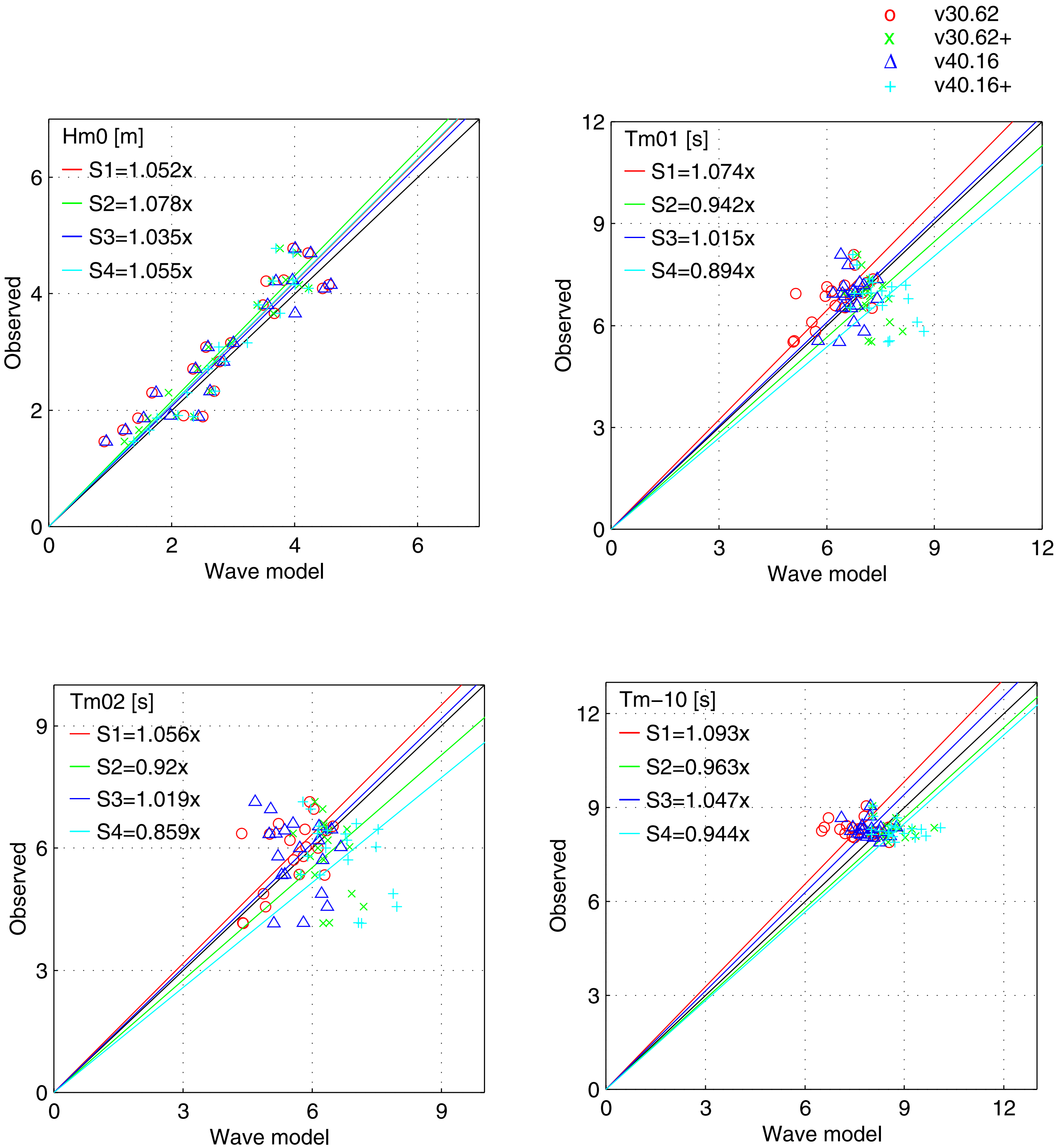

WL | Delft Hydraulics Alkyon Hydraulic Consultancy & Research	H4197/A1044
	all cases
Wave model: SWAN 30.62/40.16 Reliability of SWAN at the Petten Sea Defence	Loc. : **storm 4** Fig. : **s16str01a.a**

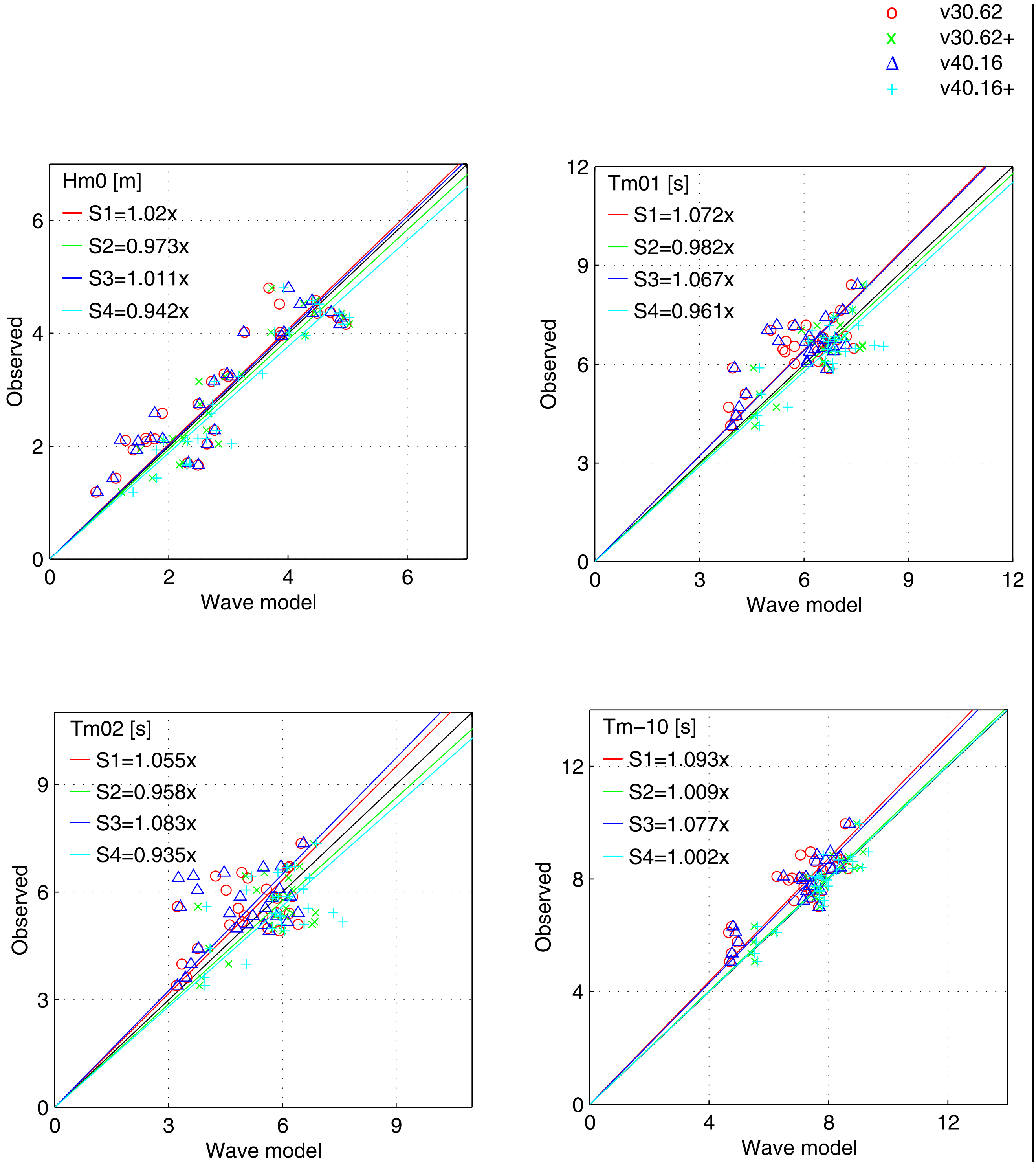

WL | Delft Hydraulics Alkyon Hydraulic Consultancy & Research	H4197/A1044
	all cases
Wave model: SWAN 30.62/40.16 Reliability of SWAN at the Petten Sea Defence	Loc. : **storm 5** Fig. : **s17str01a.a**

A Definition of spectral period measures

A number of additional spectral parameters are computed, such as extra mean period measures, peak period measures and equivalent period measures. To increase the robustness of the computation of some of these parameters for measured spectra a smoothing technique is used. This appendix contains the definitions of these parameters and the smoothing algorithm that is applied. Background information about these parameters and the smoothing algorithm are given in Alkyon (1999), Battjes and Van Vledder (1984).

Mean period measures

Firstly the mean period measures $T_{m0,1}$ and $T_{m0,2}$ are computed. These measures are based on the frequency moments m_i of a wave spectrum:

$$m_i = \int f^i E(f) df \tag{A.1}$$

and read

$$T_{m0,1} = \frac{m_0}{m_1} \tag{A.2}$$

$$T_{m0,2} = \sqrt{\frac{m_0}{m_2}} \tag{A.3}$$

Also the following mean period measure is used:

$$T_{m-1,0} = \frac{m_{-1}}{m_0} \tag{A.4}$$

Since the SWAN computations are carried on a finite frequency domain, both measured and computed mean wave periods are determined by integrating the moments in (A.1) over a finite integration domain with $f_{low} = 0.03\text{Hz}$ and $f_{high} = 0.50\text{Hz}$.

The block peak period T_{pb}

The block peak period T_{pb} is defined as the mean period $T_{m-1,0}$ in an interval around the peak period T_p. The limits of the frequency interval are determined as the frequencies where on the lower and higher frequency (f_1 and f_2) flank around the spectral peak the energy density has a downward crossing with the level of 40% of the energy density level at the spectral peak. The equation for the computation of the block peak period is:

$$T_{pb} = \frac{\int_{f_1}^{f_2} f^{-1} E(f)\,df}{\int_{f_1}^{f_2} E(f)\,df} \qquad \text{(A.5)}$$

Equivalent period measures for double peaked spectra

In the case of a double peaked spectrum the peak periods T_{p1} and T_{p2} and the block peak periods T_{pb1} and T_{pb2} are computed for each sub-spectrum. Based on these peak period measures an equivalent peak period T_{peq} and an equivalent block peak period T_{pbeq} are computed by a weighting with the total amount of energy per sub spectrum and the fourth power of the (block) peak in each sub-spectrum:

$$T_{peq} = \sqrt[4]{T_{p1}^4 \frac{m_0^{(1)}}{m_0} + T_{p2}^4 \frac{m_0^{(2)}}{m_0}} \qquad \text{(A.6)}$$

and

$$T_{pbeq} = \sqrt[4]{T_{pb1}^4 \frac{m_0^{(1)}}{m_0} + T_{pb2}^4 \frac{m_0^{(2)}}{m_0}} \qquad \text{(A.7)}$$

in which m_0 is the total variances of the double peaked spectrum, and $m_0^{(1)}$ and $m_0^{(2)}$ are total wave variance in each sub-spectrum.

Peak period T_{pm}

For double peaked spectra, both the block peak period T_{pb} (based on the highest peak) and the equivalent block peak period T_{pbeq} are computed. Based on these two estimates the characteristic peak period T_{pm} is computed as:

$$T_{pm} = \max\left(T_{pb}, T_{pbeq}\right) \qquad \text{(A.8)}$$

B Definition of statistical parameters

The statistical analysis determines the model performance of the different SWAN versions with a number of statistical parameters. In this appendix these parameters will be discussed briefly. The statistical parameters are subdivided into three types of error measures. These are prediction errors, average errors and the relative error. For detailed information regarding these statistical parameters reference is made to for instance Ris *et al.* (1999).

Prediction error

The prediction error can be characterised with the first and second moment, similar to the moments of a time series. These moments are known as *BIAS* and the standard deviation *STD*, in formula:

$$BIAS = \frac{1}{N}\sum_{i=1}^{N}\left(y_i - x_i\right) = \overline{y} - \overline{x} \tag{B.1}$$

$$STD^2 = \frac{1}{N-1}\sum_{i=1}^{N}\left(y_i - x_i - BIAS\right)^2 \tag{B.2}$$

in which N is the number of the observed (and computed) values (not including the imposed values at the up-wave boundaries), x_i is the observed value at location i and y_i is the value computed by the SWAN model at location i.

$\overline{x}$ and $\overline{y}$ are the mean values of the observations and predictions, respectively:

$$\overline{x} = \frac{1}{N}\sum_{i=1}^{N} x_i \quad \text{and} \quad \overline{y} = \frac{1}{N}\sum_{i=1}^{N} y_i \tag{B.3}$$

Average error

Two measures for the average error are considered important. These are the mean absolute error (*MAE*) and the root mean square error (*RMSE*). The mean absolute error is given by:

$$MAE = \frac{1}{N}\sum_{i=1}^{N}\left|y_i - x_i\right| \tag{B.4}$$

and the root mean square error is defined as:

$$RMSE = \left\{ \frac{1}{N} \sum_{i=1}^{N} \left(x_i - y_i \right)^2 \right\}^{1/2} \tag{B.5}$$

Relative error

For many applications absolute measures of errors are less relevant than relative measures. In the statistical post processing program one straightforward relative measure of errors is used, i.e. the Scatter Index. The Scatter Index *SCI* is defined as the root mean square error normalised with the mean of the observed wave parameters and is given by:

$$SCI = \frac{RMSE}{\left| \bar{x} \right|} \tag{B.6}$$

C Statistical parameters

Computed statistical parameters for case : f1apet01
Number of stations at which computed data is available : 5

	Hm0 [m]				Tm01 [s]				Tm02 [s]				Tm-10 [s]				Tpm [s]			
SWAN	30.62	30.62+	40.16	40.16+	30.62	30.62+	40.16	40.16+	30.62	30.62+	40.16	40.16+	30.62	30.62+	40.16	40.16+	30.62	30.62+	40.16	40.16+
mean	2.093	2.093	2.093	2.093	5.348	5.348	5.348	5.348	4.427	4.427	4.427	4.427	6.729	6.729	6.729	6.729	8.712	8.712	8.712	8.712
bias	-0.108	-0.035	-0.155	-0.064	-0.433	-0.126	-0.078	-0.098	-0.154	0.071	0.106	0.081	-0.921	-0.486	-0.590	-0.507	-1.428	-1.690	-1.398	-1.803
mae	0.282	0.164	0.248	0.119	0.618	0.332	0.415	0.304	0.535	0.299	0.392	0.327	0.921	0.486	0.590	0.507	1.428	1.690	1.398	1.803
rmse	0.355	0.190	0.323	0.181	0.769	0.365	0.468	0.359	0.685	0.460	0.505	0.472	1.207	0.596	0.877	0.630	2.503	2.545	2.505	2.771
sci	0.170	0.091	0.155	0.086	0.144	0.068	0.088	0.067	0.155	0.104	0.114	0.107	0.179	0.089	0.130	0.094	0.287	0.292	0.287	0.318
std	0.378	0.209	0.317	0.189	0.710	0.383	0.517	0.386	0.747	0.508	0.552	0.520	0.872	0.386	0.725	0.418	2.298	2.127	2.323	2.353

Computed statistical parameters for case : f1apet02
Number of stations at which computed data is available : 5

	Hm0 [m]				Tm01 [s]				Tm02 [s]				Tm-10 [s]				Tpm [s]			
SWAN	30.62	30.62+	40.16	40.16+	30.62	30.62+	40.16	40.16+	30.62	30.62+	40.16	40.16+	30.62	30.62+	40.16	40.16+	30.62	30.62+	40.16	40.16+
mean	2.242	2.242	2.242	2.242	5.703	5.703	5.703	5.703	4.918	4.918	4.918	4.918	6.853	6.853	6.853	6.853	7.769	7.769	7.769	7.769
bias	0.024	0.101	-0.035	0.099	-0.349	0.201	0.106	0.216	-0.263	0.338	0.069	0.337	-0.539	0.058	-0.106	0.022	0.172	0.070	0.171	-0.038
mae	0.348	0.238	0.302	0.170	0.538	0.228	0.374	0.313	0.597	0.389	0.391	0.454	0.573	0.172	0.399	0.231	0.278	0.135	0.280	0.233
rmse	0.428	0.283	0.388	0.212	0.673	0.366	0.443	0.390	0.681	0.529	0.476	0.529	0.780	0.243	0.512	0.261	0.322	0.160	0.317	0.278
sci	0.191	0.126	0.173	0.095	0.118	0.064	0.078	0.068	0.138	0.108	0.097	0.107	0.114	0.035	0.075	0.038	0.041	0.021	0.041	0.036
std	0.478	0.295	0.432	0.209	0.644	0.343	0.481	0.363	0.702	0.454	0.527	0.455	0.630	0.264	0.559	0.291	0.304	0.160	0.298	0.307

Computed statistical parameters for case : f1apet03
Number of stations at which computed data is available : 5

	Hm0 [m]				Tm01 [s]				Tm02 [s]				Tm-10 [s]				Tpm [s]			
SWAN	30.62	30.62+	40.16	40.16+	30.62	30.62+	40.16	40.16+	30.62	30.62+	40.16	40.16+	30.62	30.62+	40.16	40.16+	30.62	30.62+	40.16	40.16+
mean	3.374	3.374	3.374	3.374	6.556	6.556	6.556	6.556	5.567	5.567	5.567	5.567	7.965	7.965	7.965	7.965	9.333	9.333	9.333	9.333
bias	-0.180	-0.142	-0.173	-0.107	-0.135	0.236	0.043	0.597	0.043	0.239	-0.201	0.482	-0.299	0.251	0.040	0.536	0.503	0.264	0.568	0.591
mae	0.236	0.201	0.217	0.167	0.254	0.355	0.550	0.702	0.313	0.465	0.892	0.697	0.313	0.251	0.209	0.536	0.503	0.378	0.627	0.641
rmse	0.357	0.252	0.312	0.213	0.310	0.517	0.662	0.925	0.363	0.630	1.082	0.920	0.451	0.293	0.268	0.612	0.617	0.444	0.676	0.695
sci	0.106	0.075	0.092	0.063	0.047	0.079	0.101	0.141	0.065	0.113	0.194	0.165	0.057	0.037	0.034	0.077	0.066	0.048	0.072	0.075
std	0.344	0.232	0.290	0.206	0.311	0.515	0.739	0.790	0.403	0.651	1.188	0.876	0.378	0.169	0.296	0.331	0.400	0.398	0.409	0.411

Computed statistical parameters for case : f1apet04
Number of stations at which computed data is available : 5

	Hm0 [m]				Tm01 [s]				Tm02 [s]				Tm-10 [s]				Tpm [s]			
SWAN	30.62	30.62+	40.16	40.16+	30.62	30.62+	40.16	40.16+	30.62	30.62+	40.16	40.16+	30.62	30.62+	40.16	40.16+	30.62	30.62+	40.16	40.16+
mean	3.448	3.448	3.448	3.448	6.909	6.909	6.909	6.909	5.568	5.568	5.568	5.568	9.300	9.300	9.300	9.300	13.666	13.666	13.666	13.666
bias	-0.078	-0.188	0.001	-0.174	-0.002	0.189	0.650	0.632	0.369	0.369	0.615	0.709	-0.809	-0.523	-0.133	-0.236	-2.420	-3.128	-1.904	-3.121
mae	0.741	0.591	0.735	0.590	0.605	0.570	0.737	0.910	0.458	0.483	0.718	0.785	1.190	0.791	0.935	0.979	3.100	3.302	3.214	3.213
rmse	0.940	0.808	0.933	0.809	0.633	0.659	0.837	1.066	0.566	0.567	0.869	0.924	1.595	1.477	1.310	1.424	4.672	5.318	4.574	5.197
sci	0.273	0.234	0.270	0.235	0.092	0.095	0.121	0.154	0.102	0.102	0.156	0.166	0.171	0.159	0.141	0.153	0.342	0.389	0.335	0.380
std	1.048	0.879	1.043	0.883	0.707	0.706	0.590	0.959	0.480	0.482	0.687	0.663	1.536	1.544	1.458	1.570	4.468	4.808	4.649	4.646

Computed statistical parameters for case : f1bpet01
Number of stations at which computed data is available : 5

	Hm0 [m]				Tm01 [s]				Tm02 [s]				Tm-10 [s]				Tpm [s]			
SWAN	30.62	30.62+	40.16	40.16+	30.62	30.62+	40.16	40.16+	30.62	30.62+	40.16	40.16+	30.62	30.62+	40.16	40.16+	30.62	30.62+	40.16	40.16+
mean	3.961	3.961	3.961	3.961	7.859	7.859	7.859	7.859	6.412	6.412	6.412	6.412	10.417	10.417	10.417	10.417	13.523	13.523	13.523	13.523

bias	-0.043	-0.023	0.092	-0.024	-0.086	0.774	-0.799	0.803	0.242	1.052	-1.201	0.967	-0.887	0.462	-0.801	0.437	-0.695	-0.710	-0.758	-1.274
mae	0.226	0.074	0.312	0.088	0.544	0.965	1.501	1.010	0.617	1.098	2.073	1.081	0.887	0.668	0.801	0.610	0.726	0.782	0.759	1.274
rmse	0.329	0.086	0.355	0.102	0.659	1.273	1.890	1.296	0.733	1.357	2.576	1.282	0.986	0.818	0.953	0.719	1.226	0.951	1.282	1.530
sci	0.083	0.022	0.090	0.026	0.084	0.162	0.241	0.165	0.114	0.212	0.402	0.200	0.095	0.079	0.092	0.069	0.091	0.070	0.095	0.113
std	0.365	0.093	0.384	0.110	0.730	1.130	1.915	1.137	0.774	0.957	2.548	0.941	0.482	0.755	0.578	0.638	1.129	0.707	1.157	0.948

Computed statistical parameters for case : f1bpet02
Number of stations at which computed data is available : 5

	Hm0 [m]				Tm01 [s]				Tm02 [s]				Tm-10 [s]				Tpm [s]			
SWAN	30.62	30.62+	40.16	40.16+	30.62	30.62+	40.16	40.16+	30.62	30.62+	40.16	40.16+	30.62	30.62+	40.16	40.16+	30.62	30.62+	40.16	40.16+
mean	3.003	3.003	3.003	3.003	7.202	7.202	7.202	7.202	5.778	5.778	5.778	5.778	9.769	9.769	9.769	9.769	13.434	13.434	13.434	13.434
bias	-0.645	-0.294	-0.640	-0.288	-1.222	-0.173	-1.002	0.038	-0.808	-0.051	-1.039	0.020	-2.144	-0.574	-1.575	-0.354	-2.782	-2.567	-2.487	-2.451
mae	0.645	0.408	0.640	0.405	1.276	1.104	1.002	1.208	0.977	1.005	1.312	1.072	2.144	0.956	1.575	0.999	2.782	2.645	2.591	2.533
rmse	0.807	0.583	0.802	0.589	1.478	1.193	1.411	1.226	1.149	1.074	1.521	1.107	2.309	1.099	1.816	1.038	3.900	3.436	3.713	3.570
sci	0.269	0.194	0.267	0.196	0.205	0.166	0.196	0.170	0.199	0.186	0.263	0.192	0.236	0.113	0.186	0.106	0.290	0.256	0.276	0.266
std	0.542	0.563	0.539	0.574	0.929	1.320	1.110	1.370	0.914	1.200	1.243	1.237	0.957	1.048	1.009	1.091	3.055	2.554	3.083	2.901

Computed statistical parameters for case : f1bpet03
Number of stations at which computed data is available : 5

	Hm0 [m]				Tm01 [s]				Tm02 [s]				Tm-10 [s]				Tpm [s]			
SWAN	30.62	30.62+	40.16	40.16+	30.62	30.62+	40.16	40.16+	30.62	30.62+	40.16	40.16+	30.62	30.62+	40.16	40.16+	30.62	30.62+	40.16	40.16+
mean	3.130	3.130	3.130	3.130	7.492	7.492	7.492	7.492	6.086	6.086	6.086	6.086	9.599	9.599	9.599	9.599	11.621	11.621	11.621	11.621
bias	-1.221	-0.596	-1.299	-0.650	-1.802	-0.342	-1.434	-0.338	-1.533	0.167	-1.364	0.136	-1.926	-0.670	-1.415	-0.734	-0.050	-0.616	-0.051	-1.100
mae	1.221	0.596	1.299	0.650	1.802	1.028	1.730	0.953	1.577	0.823	1.645	0.782	1.926	0.970	1.415	0.911	0.207	0.616	0.217	1.100
rmse	1.254	0.647	1.339	0.695	2.062	1.174	1.889	1.109	1.851	1.106	1.841	1.033	2.009	1.016	1.576	0.986	0.325	0.638	0.337	1.191
sci	0.401	0.207	0.428	0.222	0.275	0.157	0.252	0.148	0.304	0.182	0.303	0.170	0.209	0.106	0.164	0.103	0.028	0.055	0.029	0.102
std	0.318	0.282	0.362	0.274	1.120	1.256	1.375	1.181	1.159	1.222	1.383	1.145	0.639	0.854	0.777	0.737	0.359	0.187	0.372	0.509

Computed statistical parameters for case : f1bpet04
Number of stations at which computed data is available : 5

	Hm0 [m]				Tm01 [s]				Tm02 [s]				Tm-10 [s]				Tpm [s]			
SWAN	30.62	30.62+	40.16	40.16+	30.62	30.62+	40.16	40.16+	30.62	30.62+	40.16	40.16+	30.62	30.62+	40.16	40.16+	30.62	30.62+	40.16	40.16+
mean	2.559	2.559	2.559	2.559	6.584	6.584	6.584	6.584	5.364	5.364	5.364	5.364	8.590	8.590	8.590	8.590	11.263	11.263	11.263	11.263
bias	-0.877	-0.412	-0.932	-0.453	-0.896	-0.026	-0.225	0.276	-0.820	-0.270	-0.386	0.008	-1.073	0.042	-0.403	0.162	-0.863	-0.612	-0.893	-0.959
mae	0.877	0.412	0.932	0.453	0.896	0.629	0.570	0.713	0.820	0.825	0.787	0.735	1.073	0.322	0.621	0.391	1.670	1.552	1.668	1.615
rmse	0.931	0.474	0.978	0.541	1.047	0.731	0.736	0.797	0.999	0.909	0.921	0.834	1.286	0.390	0.766	0.465	2.803	2.457	2.812	2.759
sci	0.364	0.185	0.382	0.211	0.159	0.111	0.112	0.121	0.186	0.170	0.172	0.155	0.150	0.045	0.089	0.054	0.249	0.218	0.250	0.245
std	0.348	0.262	0.331	0.330	0.606	0.817	0.783	0.836	0.637	0.971	0.935	0.932	0.792	0.433	0.729	0.487	2.982	2.660	2.981	2.892

Computed statistical parameters for case : f2apet01
Number of stations at which computed data is available : 5

	Hm0 [m]				Tm01 [s]				Tm02 [s]				Tm-10 [s]				Tpm [s]			
SWAN	30.62	30.62+	40.16	40.16+	30.62	30.62+	40.16	40.16+	30.62	30.62+	40.16	40.16+	30.62	30.62+	40.16	40.16+	30.62	30.62+	40.16	40.16+
mean	3.964	3.964	3.964	3.964	7.379	7.379	7.379	7.379	6.034	6.034	6.034	6.034	9.647	9.647	9.647	9.647	12.662	12.662	12.662	12.662
bias	-0.225	-0.385	-0.139	-0.382	0.567	0.461	0.813	0.613	0.727	0.638	0.444	0.738	0.201	0.113	0.597	0.227	0.833	-1.081	0.781	-1.261
mae	0.388	0.385	0.307	0.382	0.591	0.653	1.051	0.855	0.727	0.748	1.315	0.922	0.528	0.378	0.629	0.464	1.546	1.262	1.564	1.503
rmse	0.508	0.438	0.423	0.423	0.659	0.916	1.346	1.137	0.832	1.056	1.581	1.265	0.565	0.472	0.764	0.565	1.630	1.616	1.658	1.943
sci	0.128	0.110	0.107	0.107	0.089	0.124	0.182	0.154	0.138	0.175	0.262	0.210	0.059	0.049	0.079	0.059	0.129	0.128	0.131	0.153
std	0.509	0.233	0.447	0.202	0.377	0.885	1.199	1.070	0.452	0.941	1.696	1.148	0.591	0.513	0.534	0.579	1.566	1.343	1.635	1.653

Computed statistical parameters for case : f2apet02
Number of stations at which computed data is available : 5

	Hm0 [m]				Tm01 [s]				Tm02 [s]				Tm-10 [s]				Tpm [s]			

SWAN	30.62	30.62+	40.16	40.16+	30.62	30.62+	40.16	40.16+	30.62	30.62+	40.16	40.16+	30.62	30.62+	40.16	40.16+	30.62	30.62+	40.16	40.16+
mean	3.492	3.492	3.492	3.492	7.053	7.053	7.053	7.053	5.774	5.774	5.774	5.774	9.066	9.066	9.066	9.066	11.644	11.644	11.644	11.644
bias	0.006	-0.126	0.070	-0.223	0.187	0.457	0.350	0.606	0.485	0.734	0.374	0.804	-0.342	0.173	-0.079	0.335	-0.240	-0.740	-0.275	-0.280
mae	0.221	0.187	0.224	0.258	0.511	0.744	0.965	0.922	0.641	0.893	1.319	1.047	0.506	0.575	0.479	0.695	1.416	1.195	1.409	1.374
rmse	0.267	0.228	0.252	0.315	0.562	1.049	1.183	1.186	0.740	1.186	1.619	1.323	0.623	0.757	0.579	0.788	1.764	1.790	1.782	1.704
sci	0.076	0.065	0.072	0.090	0.080	0.149	0.168	0.168	0.128	0.205	0.280	0.229	0.069	0.083	0.064	0.087	0.152	0.154	0.153	0.146
std	0.298	0.213	0.271	0.248	0.592	1.056	1.264	1.139	0.624	1.042	1.761	1.175	0.582	0.824	0.642	0.798	1.954	1.823	1.968	1.880

Computed statistical parameters for case : f2apet03
Number of stations at which computed data is available : 5

	Hm0 [m]				Tm01 [s]				Tm02 [s]				Tm-10 [s]				Tpm [s]			
SWAN	30.62	30.62+	40.16	40.16+	30.62	30.62+	40.16	40.16+	30.62	30.62+	40.16	40.16+	30.62	30.62+	40.16	40.16+	30.62	30.62+	40.16	40.16+
mean	2.635	2.635	2.635	2.635	6.324	6.324	6.324	6.324	5.128	5.128	5.128	5.128	8.411	8.411	8.411	8.411	11.560	11.560	11.560	11.560
bias	-0.103	-0.267	-0.136	-0.337	0.133	-0.050	0.526	0.064	0.275	0.107	0.368	0.233	-0.251	-0.433	0.283	-0.411	-0.398	-2.183	-0.413	-2.477
mae	0.195	0.311	0.164	0.409	0.577	0.570	1.191	0.682	0.568	0.647	1.455	0.739	0.740	0.466	0.698	0.503	1.531	2.183	1.527	2.477
rmse	0.252	0.390	0.216	0.486	0.645	0.657	1.226	0.742	0.737	0.739	1.624	0.816	0.956	0.623	0.736	0.638	2.261	2.961	2.270	3.177
sci	0.095	0.148	0.082	0.184	0.102	0.104	0.194	0.117	0.144	0.144	0.317	0.159	0.114	0.074	0.087	0.076	0.196	0.256	0.196	0.275
std	0.257	0.318	0.187	0.391	0.706	0.733	1.238	0.827	0.764	0.818	1.769	0.874	1.031	0.500	0.759	0.545	2.489	2.236	2.495	2.224

Computed statistical parameters for case : f2apet04
Number of stations at which computed data is available : 5

	Hm0 [m]				Tm01 [s]				Tm02 [s]				Tm-10 [s]				Tpm [s]			
SWAN	30.62	30.62+	40.16	40.16+	30.62	30.62+	40.16	40.16+	30.62	30.62+	40.16	40.16+	30.62	30.62+	40.16	40.16+	30.62	30.62+	40.16	40.16+
mean	1.750	1.750	1.750	1.750	6.076	6.076	6.076	6.076	4.894	4.894	4.894	4.894	8.331	8.331	8.331	8.331	11.039	11.039	11.039	11.039
bias	0.314	0.123	0.347	0.087	1.342	0.689	1.699	0.948	1.063	0.594	0.824	0.867	1.264	0.391	1.892	0.522	2.337	0.015	2.301	-0.266
mae	0.502	0.240	0.536	0.253	1.342	0.905	1.699	1.021	1.063	0.991	1.418	1.088	1.439	0.408	1.892	0.522	2.337	0.845	2.301	0.790
rmse	0.649	0.328	0.766	0.313	1.596	1.077	1.854	1.282	1.219	1.134	1.597	1.305	1.718	0.549	2.118	0.721	2.520	1.083	2.490	0.999
sci	0.371	0.188	0.438	0.179	0.263	0.177	0.305	0.211	0.249	0.232	0.326	0.267	0.206	0.066	0.254	0.087	0.228	0.098	0.226	0.091
std	0.635	0.340	0.764	0.336	0.965	0.925	0.831	0.965	0.668	1.079	1.530	1.092	1.301	0.432	1.065	0.556	1.052	1.211	1.064	1.077

Computed statistical parameters for case : f2bpet01
Number of stations at which computed data is available : 5

	Hm0 [m]				Tm01 [s]				Tm02 [s]				Tm-10 [s]				Tpm [s]			
SWAN	30.62	30.62+	40.16	40.16+	30.62	30.62+	40.16	40.16+	30.62	30.62+	40.16	40.16+	30.62	30.62+	40.16	40.16+	30.62	30.62+	40.16	40.16+
mean	3.414	3.414	3.414	3.414	6.814	6.814	6.814	6.814	5.777	5.777	5.777	5.777	8.455	8.455	8.455	8.455	10.403	10.403	10.403	10.403
bias	-0.535	-0.481	-0.468	-0.409	-0.655	0.219	-0.280	0.403	-0.351	0.457	-0.235	0.660	-1.121	-0.133	-0.745	-0.099	-1.100	-0.921	-0.920	-1.083
mae	0.535	0.481	0.468	0.409	0.655	0.712	0.698	0.954	0.464	0.815	1.047	1.152	1.121	0.363	0.745	0.378	1.100	0.921	0.920	1.083
rmse	0.542	0.513	0.471	0.490	0.716	0.963	0.780	1.223	0.590	1.175	1.291	1.565	1.201	0.424	0.754	0.419	1.670	1.324	1.584	1.667
sci	0.159	0.150	0.138	0.143	0.105	0.141	0.115	0.180	0.102	0.203	0.224	0.271	0.142	0.050	0.089	0.050	0.160	0.127	0.152	0.160
std	0.103	0.206	0.052	0.311	0.335	1.083	0.841	1.334	0.548	1.250	1.466	1.639	0.499	0.465	0.133	0.470	1.450	1.100	1.489	1.463

Computed statistical parameters for case : f2bpet02
Number of stations at which computed data is available : 5

	Hm0 [m]				Tm01 [s]				Tm02 [s]				Tm-10 [s]				Tpm [s]			
SWAN	30.62	30.62+	40.16	40.16+	30.62	30.62+	40.16	40.16+	30.62	30.62+	40.16	40.16+	30.62	30.62+	40.16	40.16+	30.62	30.62+	40.16	40.16+
mean	2.881	2.881	2.881	2.881	6.671	6.671	6.671	6.671	5.761	5.761	5.761	5.761	8.155	8.155	8.155	8.155	9.599	9.599	9.599	9.599
bias	0.111	0.002	0.202	0.068	-0.094	0.777	0.344	1.153	-0.048	0.756	0.132	1.148	-0.139	0.930	0.237	1.149	1.023	0.631	1.174	0.799
mae	0.300	0.188	0.331	0.169	0.396	0.842	0.485	1.219	0.569	0.922	0.838	1.299	0.454	0.930	0.263	1.149	1.133	0.631	1.301	0.799
rmse	0.379	0.249	0.377	0.227	0.534	1.137	0.638	1.536	0.753	1.285	1.053	1.714	0.566	1.036	0.321	1.256	1.315	0.816	1.443	1.026
sci	0.132	0.086	0.131	0.079	0.080	0.170	0.096	0.230	0.131	0.223	0.183	0.298	0.069	0.127	0.039	0.154	0.137	0.085	0.150	0.107
std	0.406	0.278	0.356	0.242	0.587	0.928	0.601	1.135	0.840	1.161	1.168	1.423	0.613	0.511	0.242	0.566	0.924	0.579	0.937	0.720

Computed statistical parameters for case : f2bpet03
Number of stations at which computed data is available : 5

	Hm0 [m]				Tm01 [s]				Tm02 [s]				Tm-10 [s]				Tpm [s]			
SWAN	30.62	30.62+	40.16	40.16+	30.62	30.62+	40.16	40.16+	30.62	30.62+	40.16	40.16+	30.62	30.62+	40.16	40.16+	30.62	30.62+	40.16	40.16+

mean	3.225	3.225	3.225	3.225	6.927	6.927	6.927	6.927	6.076	6.076	6.076	6.076	8.232	8.232	8.232	8.232	9.568	9.568	9.568	9.568
bias	-0.103	-0.100	-0.061	0.052	-0.486	0.406	-0.129	0.884	-0.397	0.427	-0.220	0.942	-0.609	0.442	-0.310	0.724	0.183	0.225	0.226	0.426
mae	0.393	0.271	0.335	0.180	0.498	0.427	0.393	0.884	0.453	0.584	0.753	0.978	0.609	0.442	0.323	0.724	0.357	0.346	0.426	0.452
rmse	0.417	0.288	0.361	0.218	0.635	0.760	0.455	1.221	0.684	0.939	0.908	1.440	0.771	0.521	0.388	0.799	0.444	0.399	0.480	0.513
sci	0.129	0.089	0.112	0.068	0.092	0.110	0.066	0.176	0.113	0.155	0.150	0.237	0.094	0.063	0.047	0.097	0.046	0.042	0.050	0.054
std	0.452	0.302	0.398	0.236	0.457	0.718	0.488	0.941	0.623	0.935	0.985	1.218	0.528	0.308	0.262	0.379	0.453	0.369	0.473	0.321

Computed statistical parameters for case : f2bpet04
Number of stations at which computed data is available : 5

	Hm0 [m]				Tm01 [s]				Tm02 [s]				Tm-10 [s]				Tpm [s]			
SWAN	30.62	30.62+	40.16	40.16+	30.62	30.62+	40.16	40.16+	30.62	30.62+	40.16	40.16+	30.62	30.62+	40.16	40.16+	30.62	30.62+	40.16	40.16+
mean	2.934	2.934	2.934	2.934	6.740	6.740	6.740	6.740	5.741	5.741	5.741	5.741	8.437	8.437	8.437	8.437	10.605	10.605	10.605	10.605
bias	-0.354	-0.357	-0.359	-0.298	-0.794	0.096	-0.419	0.398	-0.549	0.228	-0.434	0.583	-1.209	-0.192	-0.832	-0.090	-0.955	-1.107	-0.862	-1.222
mae	0.468	0.424	0.390	0.376	0.794	0.772	0.607	0.944	0.786	0.977	1.030	1.216	1.209	0.381	0.832	0.367	1.303	1.234	1.211	1.456
rmse	0.506	0.523	0.457	0.529	1.036	0.957	0.845	1.238	1.058	1.153	1.318	1.564	1.340	0.509	0.959	0.528	2.058	1.833	2.043	2.211
sci	0.173	0.178	0.156	0.180	0.154	0.142	0.125	0.184	0.184	0.201	0.230	0.272	0.159	0.060	0.114	0.063	0.194	0.173	0.193	0.208
std	0.405	0.428	0.317	0.488	0.743	1.064	0.821	1.310	1.011	1.264	1.392	1.622	0.647	0.527	0.534	0.582	2.038	1.633	2.071	2.060

Computed statistical parameters for case : f3apet01
Number of stations at which computed data is available : 6

	Hm0 [m]				Tm01 [s]				Tm02 [s]				Tm-10 [s]				Tpm [s]			
SWAN	30.62	30.62+	40.16	40.16+	30.62	30.62+	40.16	40.16+	30.62	30.62+	40.16	40.16+	30.62	30.62+	40.16	40.16+	30.62	30.62+	40.16	40.16+
mean	3.402	3.402	3.402	3.402	6.719	6.719	6.719	6.719	5.944	5.944	5.944	5.944	7.747	7.747	7.747	7.747	8.721	8.721	8.721	8.721
bias	0.071	0.123	0.082	0.230	-0.406	0.041	-0.268	0.229	-0.327	0.083	-0.391	0.292	-0.452	-0.031	-0.287	0.062	0.067	0.005	0.183	-0.007
mae	0.360	0.282	0.314	0.313	0.766	0.491	0.591	0.565	0.794	0.609	0.755	0.706	0.731	0.323	0.558	0.313	0.284	0.114	0.183	0.115
rmse	0.430	0.403	0.379	0.409	0.864	0.573	0.755	0.630	0.896	0.698	1.037	0.776	0.843	0.395	0.636	0.392	0.345	0.139	0.219	0.126
sci	0.126	0.119	0.111	0.120	0.129	0.085	0.112	0.094	0.151	0.117	0.174	0.131	0.109	0.051	0.082	0.051	0.040	0.016	0.025	0.014
std	0.465	0.421	0.405	0.371	0.836	0.626	0.773	0.643	0.914	0.759	1.052	0.788	0.779	0.432	0.622	0.424	0.370	0.152	0.133	0.138

Computed statistical parameters for case : f3apet02
Number of stations at which computed data is available : 6

	Hm0 [m]				Tm01 [s]				Tm02 [s]				Tm-10 [s]				Tpm [s]			
SWAN	30.62	30.62+	40.16	40.16+	30.62	30.62+	40.16	40.16+	30.62	30.62+	40.16	40.16+	30.62	30.62+	40.16	40.16+	30.62	30.62+	40.16	40.16+
mean	1.881	1.881	1.881	1.881	4.847	4.847	4.847	4.847	4.205	4.205	4.205	4.205	5.723	5.723	5.723	5.723	6.955	6.955	6.955	6.955
bias	-0.545	0.080	-0.623	0.143	-0.833	-0.120	-0.745	0.040	-0.799	-0.183	-0.731	0.003	-0.973	-0.102	-0.889	-0.009	-1.353	-0.622	-1.268	-0.559
mae	0.545	0.156	0.623	0.222	0.833	0.568	0.745	0.632	0.799	0.692	0.731	0.778	0.973	0.341	0.889	0.357	1.353	0.788	1.268	0.780
rmse	0.576	0.183	0.662	0.234	1.026	0.700	0.951	0.718	1.142	0.900	1.081	0.917	1.078	0.441	0.987	0.422	1.817	1.355	1.755	1.364
sci	0.306	0.097	0.352	0.125	0.212	0.144	0.196	0.148	0.272	0.214	0.257	0.218	0.188	0.077	0.172	0.074	0.261	0.195	0.252	0.196
std	0.210	0.184	0.250	0.207	0.670	0.771	0.660	0.802	0.911	0.985	0.891	1.025	0.519	0.480	0.479	0.471	1.356	1.346	1.356	1.392

Computed statistical parameters for case : f3apet03
Number of stations at which computed data is available : 6

	Hm0 [m]				Tm01 [s]				Tm02 [s]				Tm-10 [s]				Tpm [s]			
SWAN	30.62	30.62+	40.16	40.16+	30.62	30.62+	40.16	40.16+	30.62	30.62+	40.16	40.16+	30.62	30.62+	40.16	40.16+	30.62	30.62+	40.16	40.16+
mean	3.358	3.358	3.358	3.358	6.523	6.523	6.523	6.523	5.690	5.690	5.690	5.690	7.594	7.594	7.594	7.594	8.637	8.637	8.637	8.637
bias	-0.074	0.173	-0.077	0.245	-0.467	-0.056	-0.589	0.067	-0.386	-0.030	-0.832	0.010	-0.534	-0.075	-0.464	0.050	-0.229	-0.041	-0.020	0.155
mae	0.364	0.387	0.348	0.349	0.599	0.484	0.626	0.485	0.654	0.548	0.832	0.546	0.550	0.367	0.474	0.391	0.319	0.277	0.340	0.326
rmse	0.450	0.407	0.455	0.412	0.917	0.605	0.983	0.574	1.034	0.748	1.325	0.709	0.849	0.465	0.745	0.444	0.333	0.291	0.358	0.412
sci	0.134	0.121	0.136	0.123	0.141	0.093	0.151	0.088	0.182	0.132	0.233	0.125	0.112	0.061	0.098	0.058	0.039	0.034	0.041	0.048
std	0.497	0.412	0.501	0.370	0.882	0.674	0.880	0.638	1.073	0.836	1.152	0.793	0.738	0.513	0.651	0.493	0.271	0.322	0.400	0.426

Computed statistical parameters for case : f3apet04
Number of stations at which computed data is available : 6

Hm0 [m] Tm01 [s] Tm02 [s] Tm-10 [s] Tpm [s]

SWAN	30.62	30.62+	40.16	40.16+	30.62	30.62+	40.16	40.16+	30.62	30.62+	40.16	40.16+	30.62	30.62+	40.16	40.16+	30.62	30.62+	40.16	40.16+
mean	3.186	3.186	3.186	3.186	6.807	6.807	6.807	6.807	5.720	5.720	5.720	5.720	8.541	8.541	8.541	8.541	10.436	10.436	10.436	10.436
bias	-0.190	-0.311	-0.098	-0.124	-0.495	0.059	-0.470	-0.012	-0.320	0.237	-0.579	0.107	-0.821	-0.230	-0.689	-0.389	-0.718	-0.945	-0.409	-1.233
mae	0.650	0.539	0.568	0.441	0.641	0.348	0.654	0.321	0.698	0.636	0.957	0.668	0.821	0.294	0.689	0.389	0.729	0.945	0.831	1.277
rmse	0.712	0.631	0.604	0.523	0.779	0.388	0.783	0.380	0.839	0.669	1.176	0.712	0.985	0.370	0.778	0.532	0.893	1.204	0.918	1.611
sci	0.223	0.198	0.189	0.164	0.114	0.057	0.115	0.056	0.147	0.117	0.206	0.125	0.115	0.043	0.091	0.062	0.086	0.115	0.088	0.154
std	0.767	0.614	0.666	0.568	0.672	0.428	0.699	0.425	0.866	0.699	1.144	0.787	0.609	0.324	0.404	0.407	0.593	0.834	0.919	1.159

Computed statistical parameters for case : f3apet05
Number of stations at which computed data is available : 6

	Hm0 [m]				Tm01 [s]				Tm02 [s]				Tm-10 [s]				Tpm [s]			
SWAN	30.62	30.62+	40.16	40.16+	30.62	30.62+	40.16	40.16+	30.62	30.62+	40.16	40.16+	30.62	30.62+	40.16	40.16+	30.62	30.62+	40.16	40.16+
mean	3.253	3.253	3.253	3.253	7.038	7.038	7.038	7.038	5.887	5.887	5.887	5.887	8.867	8.867	8.867	8.867	11.156	11.156	11.156	11.156
bias	-0.079	0.241	0.028	0.506	-0.383	0.503	-0.367	0.798	-0.126	0.814	-0.400	1.140	-0.832	0.053	-0.693	0.158	-1.071	-1.132	-0.785	-1.157
mae	0.543	0.375	0.460	0.509	0.801	0.845	0.760	1.034	0.828	1.117	1.179	1.317	0.942	0.479	0.693	0.529	1.071	1.132	0.785	1.157
rmse	0.553	0.477	0.478	0.618	0.881	0.930	1.006	1.153	0.938	1.276	1.569	1.551	1.083	0.587	0.847	0.592	1.179	1.187	0.883	1.220
sci	0.170	0.147	0.147	0.190	0.125	0.132	0.143	0.164	0.159	0.217	0.266	0.263	0.122	0.066	0.096	0.067	0.106	0.106	0.079	0.109
std	0.612	0.460	0.534	0.397	0.887	0.875	1.047	0.930	1.039	1.099	1.696	1.176	0.775	0.654	0.545	0.638	0.551	0.398	0.452	0.433

Computed statistical parameters for case : s01opp01
Number of stations at which computed data is available : 20

	Hm0 [m]				Tm01 [s]				Tm02 [s]				Tm-10 [s]				Tpm [s]			
SWAN	30.62	30.62+	40.16	40.16+	30.62	30.62+	40.16	40.16+	30.62	30.62+	40.16	40.16+	30.62	30.62+	40.16	40.16+	30.62	30.62+	40.16	40.16+
mean	2.856	2.856	2.856	2.856	6.601	6.601	6.601	6.601	5.461	5.461	5.461	5.461	8.399	8.399	8.399	8.399	10.406	10.406	10.406	10.406
bias	-0.337	-0.138	-0.349	-0.160	-0.667	0.127	-0.551	0.146	-0.427	0.407	-0.597	0.380	-1.068	-0.159	-0.728	-0.195	-0.500	-0.736	-0.509	-1.054
mae	0.520	0.268	0.540	0.257	0.876	0.639	1.005	0.645	0.831	0.652	1.126	0.661	1.077	0.574	0.801	0.565	0.660	0.806	0.663	1.103
rmse	0.705	0.368	0.737	0.378	1.197	0.904	1.375	0.893	1.106	0.943	1.621	0.896	1.330	0.727	1.052	0.699	1.412	1.397	1.426	1.697
sci	0.247	0.129	0.258	0.132	0.181	0.137	0.208	0.135	0.203	0.173	0.297	0.164	0.158	0.087	0.125	0.083	0.136	0.134	0.137	0.163
std	0.636	0.350	0.666	0.351	1.019	0.918	1.292	0.904	1.047	0.872	1.546	0.833	0.813	0.728	0.779	0.689	1.355	1.219	1.366	1.364

Computed statistical parameters for case : s02par01
Number of stations at which computed data is available : 25

	Hm0 [m]				Tm01 [s]				Tm02 [s]				Tm-10 [s]				Tpm [s]			
SWAN	30.62	30.62+	40.16	40.16+	30.62	30.62+	40.16	40.16+	30.62	30.62+	40.16	40.16+	30.62	30.62+	40.16	40.16+	30.62	30.62+	40.16	40.16+
mean	2.924	2.924	2.924	2.924	6.284	6.284	6.284	6.284	5.279	5.279	5.279	5.279	7.834	7.834	7.834	7.834	9.971	9.971	9.971	9.971
bias	-0.351	-0.098	-0.361	-0.069	-0.467	0.045	-0.173	0.323	-0.319	0.025	-0.307	0.242	-0.737	-0.081	-0.370	0.101	-0.873	-0.828	-0.703	-0.779
mae	0.553	0.349	0.571	0.356	0.637	0.521	0.646	0.688	0.609	0.603	0.792	0.708	0.820	0.414	0.626	0.531	1.389	1.259	1.424	1.315
rmse	0.695	0.478	0.717	0.493	0.835	0.647	0.843	0.833	0.874	0.764	1.068	0.865	1.121	0.752	0.884	0.774	2.588	2.699	2.549	2.725
sci	0.238	0.163	0.245	0.169	0.133	0.103	0.134	0.133	0.166	0.145	0.202	0.164	0.143	0.096	0.113	0.099	0.260	0.271	0.256	0.273
std	0.612	0.477	0.632	0.498	0.707	0.659	0.842	0.784	0.831	0.779	1.044	0.847	0.862	0.763	0.819	0.783	2.486	2.622	2.501	2.665

Computed statistical parameters for case : s03dep01
Number of stations at which computed data is available : 46

	Hm0 [m]				Tm01 [s]				Tm02 [s]				Tm-10 [s]				Tpm [s]			
SWAN	30.62	30.62+	40.16	40.16+	30.62	30.62+	40.16	40.16+	30.62	30.62+	40.16	40.16+	30.62	30.62+	40.16	40.16+	30.62	30.62+	40.16	40.16+
mean	3.097	3.097	3.097	3.097	6.615	6.615	6.615	6.615	5.453	5.453	5.453	5.453	8.692	8.692	8.692	8.692	11.643	11.643	11.643	11.643
bias	-0.432	-0.296	-0.333	-0.177	-0.252	0.629	0.160	0.860	0.070	0.852	0.258	1.068	-0.886	0.094	-0.493	0.172	-1.225	-1.448	-1.121	-1.627
mae	0.482	0.329	0.432	0.292	0.593	0.823	0.667	1.054	0.587	0.958	0.939	1.221	0.958	0.564	0.660	0.639	1.703	1.621	1.702	1.836
rmse	0.569	0.446	0.500	0.428	0.712	1.041	0.938	1.289	0.706	1.215	1.286	1.499	1.242	0.794	0.891	0.836	2.745	2.738	2.715	2.947
sci	0.184	0.144	0.162	0.138	0.108	0.157	0.142	0.195	0.130	0.223	0.236	0.275	0.143	0.091	0.102	0.096	0.236	0.235	0.233	0.253
std	0.374	0.338	0.377	0.394	0.673	0.839	0.934	0.971	0.711	0.876	1.274	1.064	0.879	0.797	0.750	0.828	2.484	2.350	2.500	2.485

Computed statistical parameters for case : s04nde01
Number of stations at which computed data is available : 38

	Hm0 [m]				Tm01 [s]				Tm02 [s]				Tm-10 [s]				Tpm [s]			
SWAN	30.62	30.62+	40.16	40.16+	30.62	30.62+	40.16	40.16+	30.62	30.62+	40.16	40.16+	30.62	30.62+	40.16	40.16+	30.62	30.62+	40.16	40.16+
mean	2.709	2.709	2.709	2.709	6.598	6.598	6.598	6.598	5.620	5.620	5.620	5.620	8.042	8.042	8.042	8.042	9.546	9.546	9.546	9.546
bias	0.072	0.096	0.024	0.080	-0.428	-0.137	-0.221	0.079	-0.434	-0.158	-0.567	0.028	-0.470	-0.050	-0.086	0.084	0.328	-0.142	0.466	-0.131
mae	0.486	0.325	0.502	0.352	0.906	0.438	0.906	0.522	0.823	0.524	1.033	0.537	0.991	0.371	0.855	0.456	0.847	0.590	0.826	0.690
rmse	0.639	0.439	0.683	0.459	1.132	0.613	1.174	0.684	1.062	0.670	1.361	0.671	1.187	0.525	1.110	0.587	1.165	0.817	1.132	0.873
sci	0.236	0.162	0.252	0.169	0.172	0.093	0.178	0.104	0.189	0.119	0.242	0.119	0.148	0.065	0.138	0.073	0.122	0.086	0.119	0.091
std	0.644	0.434	0.692	0.458	1.062	0.606	1.169	0.688	0.983	0.660	1.254	0.679	1.105	0.530	1.121	0.589	1.133	0.815	1.046	0.875

Computed statistical parameters for case : s05dbl01
Number of stations at which computed data is available : 35

	Hm0 [m]				Tm01 [s]				Tm02 [s]				Tm-10 [s]				Tpm [s]			
SWAN	30.62	30.62+	40.16	40.16+	30.62	30.62+	40.16	40.16+	30.62	30.62+	40.16	40.16+	30.62	30.62+	40.16	40.16+	30.62	30.62+	40.16	40.16+
mean	2.426	2.426	2.426	2.426	6.315	6.315	6.315	6.315	5.058	5.058	5.058	5.058	8.730	8.730	8.730	8.730	12.063	12.063	12.063	12.063
bias	-0.401	-0.151	-0.365	-0.074	-0.353	0.783	0.455	1.103	0.008	0.978	0.571	1.275	-1.065	0.173	-0.360	0.284	-0.946	-1.438	-0.953	-1.741
mae	0.459	0.214	0.417	0.203	0.665	0.877	0.810	1.173	0.594	1.029	1.113	1.291	1.139	0.543	0.737	0.669	1.786	1.697	1.783	2.002
rmse	0.546	0.269	0.509	0.269	0.803	1.118	1.056	1.409	0.737	1.302	1.309	1.606	1.346	0.674	0.960	0.779	2.621	2.462	2.606	2.826
sci	0.225	0.111	0.210	0.111	0.127	0.177	0.167	0.223	0.146	0.257	0.259	0.318	0.154	0.077	0.110	0.089	0.217	0.204	0.216	0.234
std	0.375	0.226	0.359	0.263	0.732	0.808	0.967	0.890	0.748	0.873	1.195	0.992	0.834	0.661	0.904	0.736	2.480	2.027	2.461	2.258

Computed statistical parameters for case : s06loc01
Number of stations at which computed data is available : 15

	Hm0 [m]				Tm01 [s]				Tm02 [s]				Tm-10 [s]				Tpm [s]			
SWAN	30.62	30.62+	40.16	40.16+	30.62	30.62+	40.16	40.16+	30.62	30.62+	40.16	40.16+	30.62	30.62+	40.16	40.16+	30.62	30.62+	40.16	40.16+
mean	3.735	3.735	3.735	3.735	7.221	7.221	7.221	7.221	6.096	6.096	6.096	6.096	8.538	8.538	8.538	8.538	9.798	9.798	9.798	9.798
bias	-0.062	-0.050	-0.087	-0.127	-0.101	-0.345	0.002	-0.290	-0.065	-0.206	-0.028	-0.164	-0.090	-0.232	0.041	-0.178	0.387	-0.069	0.435	-0.096
mae	0.599	0.424	0.617	0.424	0.804	0.403	0.780	0.354	0.634	0.452	0.623	0.390	0.893	0.307	0.838	0.314	0.873	0.501	0.869	0.534
rmse	0.787	0.559	0.826	0.545	1.096	0.600	1.064	0.514	0.803	0.552	0.779	0.472	1.216	0.539	1.150	0.471	1.153	0.638	1.149	0.629
sci	0.211	0.150	0.221	0.146	0.152	0.083	0.147	0.071	0.132	0.091	0.128	0.077	0.142	0.063	0.135	0.055	0.118	0.065	0.117	0.064
std	0.813	0.577	0.850	0.549	1.130	0.507	1.102	0.439	0.829	0.530	0.806	0.459	1.255	0.503	1.190	0.451	1.125	0.657	1.101	0.643

Computed statistical parameters for case : s07loc01
Number of stations at which computed data is available : 20

	Hm0 [m]				Tm01 [s]				Tm02 [s]				Tm-10 [s]				Tpm [s]			
SWAN	30.62	30.62+	40.16	40.16+	30.62	30.62+	40.16	40.16+	30.62	30.62+	40.16	40.16+	30.62	30.62+	40.16	40.16+	30.62	30.62+	40.16	40.16+
mean	3.689	3.689	3.689	3.689	7.378	7.378	7.378	7.378	6.381	6.381	6.381	6.381	8.708	8.708	8.708	8.708	10.064	10.064	10.064	10.064
bias	-0.158	-0.170	-0.166	-0.217	-0.680	-0.546	-1.051	-0.549	-0.623	-0.466	-1.606	-0.542	-0.706	-0.482	-0.580	-0.431	-0.009	-0.489	0.032	-0.508
mae	0.434	0.380	0.453	0.429	0.824	0.558	1.121	0.576	0.727	0.509	1.606	0.578	0.906	0.552	0.860	0.554	0.823	0.758	0.799	0.842
rmse	0.585	0.474	0.613	0.526	1.145	0.745	1.431	0.758	1.049	0.686	1.923	0.735	1.215	0.733	1.162	0.708	1.291	1.198	1.237	1.183
sci	0.159	0.128	0.166	0.143	0.155	0.101	0.194	0.103	0.164	0.108	0.301	0.115	0.139	0.084	0.133	0.081	0.128	0.119	0.123	0.118
std	0.578	0.454	0.606	0.492	0.946	0.520	0.998	0.537	0.866	0.517	1.085	0.509	1.014	0.566	1.032	0.576	1.324	1.122	1.268	1.096

Computed statistical parameters for case : s08loc01
Number of stations at which computed data is available : 21

	Hm0 [m]				Tm01 [s]				Tm02 [s]				Tm-10 [s]				Tpm [s]			
SWAN	30.62	30.62+	40.16	40.16+	30.62	30.62+	40.16	40.16+	30.62	30.62+	40.16	40.16+	30.62	30.62+	40.16	40.16+	30.62	30.62+	40.16	40.16+
mean	3.452	3.452	3.452	3.452	6.166	6.166	6.166	6.166	4.962	4.962	4.962	4.962	7.959	7.959	7.959	7.959	9.909	9.909	9.909	9.909
bias	-0.284	-0.292	-0.190	-0.270	0.385	0.522	0.148	0.622	0.649	0.754	-0.041	0.789	-0.073	0.229	0.011	0.340	0.040	-0.427	0.294	-0.296
mae	0.465	0.362	0.477	0.340	0.620	0.584	0.508	0.681	0.817	0.754	0.508	0.789	0.484	0.403	0.509	0.513	0.616	0.616	0.596	0.608
rmse	0.612	0.442	0.633	0.421	0.834	0.696	0.672	0.791	0.971	0.880	0.635	0.892	0.684	0.469	0.658	0.579	0.800	0.782	0.793	0.738
sci	0.177	0.128	0.183	0.122	0.135	0.113	0.109	0.128	0.196	0.177	0.128	0.180	0.086	0.059	0.083	0.073	0.081	0.079	0.080	0.075
std	0.556	0.340	0.619	0.331	0.758	0.472	0.671	0.501	0.741	0.465	0.649	0.426	0.697	0.419	0.674	0.481	0.818	0.672	0.755	0.693

Computed statistical parameters for case : s09loc01
Number of stations at which computed data is available : 8

	Hm0 [m]				Tm01 [s]				Tm02 [s]				Tm-10 [s]				Tpm [s]			
SWAN	30.62	30.62+	40.16	40.16+	30.62	30.62+	40.16	40.16+	30.62	30.62+	40.16	40.16+	30.62	30.62+	40.16	40.16+	30.62	30.62+	40.16	40.16+
mean	3.024	3.024	3.024	3.024	6.661	6.661	6.661	6.661	5.820	5.820	5.820	5.820	8.077	8.077	8.077	8.077	9.831	9.831	9.831	9.831
bias	-0.304	-0.289	-0.260	-0.062	-0.343	0.553	0.187	0.903	-0.237	0.597	0.290	0.985	-0.537	0.451	-0.161	0.597	-0.040	-0.179	-0.037	-0.217
mae	0.304	0.289	0.262	0.160	0.370	0.553	0.325	0.903	0.387	0.597	0.377	0.985	0.538	0.451	0.280	0.608	0.449	0.467	0.448	0.629
rmse	0.333	0.339	0.297	0.209	0.468	0.635	0.384	0.980	0.439	0.718	0.496	1.092	0.620	0.579	0.346	0.759	0.624	0.667	0.624	0.863
sci	0.110	0.112	0.098	0.069	0.070	0.095	0.058	0.147	0.075	0.123	0.085	0.188	0.077	0.072	0.043	0.094	0.064	0.068	0.063	0.088
std	0.147	0.189	0.154	0.214	0.340	0.334	0.359	0.405	0.395	0.426	0.430	0.504	0.331	0.388	0.328	0.502	0.666	0.686	0.665	0.893

Computed statistical parameters for case : s10loc01
Number of stations at which computed data is available : 8

	Hm0 [m]				Tm01 [s]				Tm02 [s]				Tm-10 [s]				Tpm [s]			
SWAN	30.62	30.62+	40.16	40.16+	30.62	30.62+	40.16	40.16+	30.62	30.62+	40.16	40.16+	30.62	30.62+	40.16	40.16+	30.62	30.62+	40.16	40.16+
mean	1.908	1.908	1.908	1.908	6.865	6.865	6.865	6.865	6.291	6.291	6.291	6.291	7.951	7.951	7.951	7.951	8.846	8.846	8.846	8.846
bias	0.432	0.426	0.387	0.524	-1.445	-0.497	-1.317	-0.121	-1.715	-0.810	-2.021	-0.447	-1.252	-0.164	-0.924	0.014	-0.107	-0.040	0.392	0.200
mae	0.513	0.426	0.480	0.524	1.445	0.582	1.317	0.624	1.715	0.810	2.021	0.741	1.252	0.512	0.930	0.558	0.901	0.561	0.805	0.734
rmse	0.540	0.464	0.527	0.573	1.497	0.723	1.451	0.699	1.758	0.980	2.142	0.873	1.316	0.607	1.042	0.671	1.158	0.801	1.031	0.919
sci	0.283	0.243	0.276	0.301	0.218	0.105	0.211	0.102	0.279	0.156	0.341	0.139	0.166	0.076	0.131	0.084	0.131	0.091	0.117	0.104
std	0.347	0.196	0.383	0.248	0.418	0.562	0.651	0.736	0.415	0.589	0.759	0.801	0.435	0.625	0.513	0.717	1.232	0.855	1.019	0.959

Computed statistical parameters for case : s11loc01
Number of stations at which computed data is available : 12

	Hm0 [m]				Tm01 [s]				Tm02 [s]				Tm-10 [s]				Tpm [s]			
SWAN	30.62	30.62+	40.16	40.16+	30.62	30.62+	40.16	40.16+	30.62	30.62+	40.16	40.16+	30.62	30.62+	40.16	40.16+	30.62	30.62+	40.16	40.16+
mean	2.315	2.315	2.315	2.315	6.243	6.243	6.243	6.243	5.096	5.096	5.096	5.096	8.179	8.179	8.179	8.179	10.427	10.427	10.427	10.427
bias	-0.071	-0.015	-0.155	-0.025	-0.465	0.229	0.218	0.621	-0.249	0.244	-0.088	0.555	-0.739	0.193	0.122	0.447	0.601	-0.358	0.617	-0.385
mae	0.200	0.105	0.206	0.133	0.581	0.339	0.929	0.670	0.427	0.391	1.072	0.581	0.887	0.389	0.734	0.627	0.754	0.742	0.766	0.994
rmse	0.303	0.144	0.329	0.174	0.697	0.425	1.231	0.783	0.548	0.443	1.402	0.673	0.977	0.477	0.950	0.696	1.034	0.980	1.014	1.140
sci	0.131	0.062	0.142	0.075	0.112	0.068	0.197	0.125	0.108	0.087	0.275	0.132	0.119	0.058	0.116	0.085	0.099	0.094	0.097	0.109
std	0.308	0.149	0.304	0.180	0.542	0.374	1.266	0.499	0.510	0.386	1.462	0.398	0.667	0.456	0.984	0.557	0.879	0.953	0.840	1.120

Computed statistical parameters for case : s12loc01
Number of stations at which computed data is available : 20

	Hm0 [m]				Tm01 [s]				Tm02 [s]				Tm-10 [s]				Tpm [s]			
SWAN	30.62	30.62+	40.16	40.16+	30.62	30.62+	40.16	40.16+	30.62	30.62+	40.16	40.16+	30.62	30.62+	40.16	40.16+	30.62	30.62+	40.16	40.16+
mean	2.039	2.039	2.039	2.039	6.065	6.065	6.065	6.065	4.837	4.837	4.837	4.837	8.689	8.689	8.689	8.689	12.892	12.892	12.892	12.892
bias	-0.611	-0.141	-0.525	0.016	-0.431	1.185	0.657	1.528	-0.018	1.434	1.104	1.819	-1.399	0.221	-0.685	0.242	-2.375	-2.320	-2.410	-2.862
mae	0.611	0.212	0.525	0.182	0.701	1.207	0.866	1.539	0.574	1.435	1.201	1.819	1.399	0.600	0.837	0.661	2.647	2.504	2.657	2.894
rmse	0.638	0.247	0.555	0.224	0.802	1.401	1.076	1.733	0.704	1.637	1.424	2.034	1.584	0.757	1.037	0.817	3.423	3.215	3.405	3.674
sci	0.313	0.121	0.272	0.110	0.132	0.231	0.177	0.286	0.145	0.338	0.294	0.420	0.182	0.087	0.119	0.094	0.266	0.249	0.264	0.285
std	0.187	0.208	0.184	0.229	0.694	0.767	0.875	0.838	0.722	0.810	0.923	0.934	0.762	0.742	0.799	0.800	2.529	2.284	2.469	2.364

Computed statistical parameters for case : s13str01
Number of stations at which computed data is available : 20

	Hm0 [m]				Tm01 [s]				Tm02 [s]				Tm-10 [s]				Tpm [s]			
SWAN	30.62	30.62+	40.16	40.16+	30.62	30.62+	40.16	40.16+	30.62	30.62+	40.16	40.16+	30.62	30.62+	40.16	40.16+	30.62	30.62+	40.16	40.16+
mean	2.789	2.789	2.789	2.789	6.129	6.129	6.129	6.129	5.120	5.120	5.120	5.120	7.712	7.712	7.712	7.712	9.870	9.870	9.870	9.870
bias	-0.085	-0.066	-0.090	-0.061	-0.230	0.125	0.180	0.337	-0.001	0.254	0.147	0.402	-0.642	-0.175	-0.197	-0.046	-0.793	-1.121	-0.641	-1.093
mae	0.402	0.299	0.376	0.262	0.504	0.371	0.519	0.557	0.476	0.409	0.598	0.566	0.749	0.425	0.533	0.563	1.328	1.376	1.380	1.473
rmse	0.575	0.456	0.553	0.441	0.621	0.492	0.624	0.754	0.588	0.550	0.776	0.742	1.097	0.819	0.840	0.847	2.673	2.957	2.634	2.969
sci	0.206	0.164	0.198	0.158	0.101	0.080	0.102	0.123	0.115	0.107	0.152	0.145	0.142	0.106	0.109	0.110	0.271	0.300	0.267	0.301
std	0.583	0.463	0.559	0.448	0.591	0.489	0.612	0.692	0.604	0.500	0.782	0.640	0.912	0.821	0.837	0.867	2.619	2.808	2.621	2.832

Computed statistical parameters for case : s14str01
Number of stations at which computed data is available : 20

	Hm0 [m]				Tm01 [s]				Tm02 [s]				Tm-10 [s]				Tpm [s]			
SWAN	30.62	30.62+	40.16	40.16+	30.62	30.62+	40.16	40.16+	30.62	30.62+	40.16	40.16+	30.62	30.62+	40.16	40.16+	30.62	30.62+	40.16	40.16+
mean	3.163	3.163	3.163	3.163	7.284	7.284	7.284	7.284	5.910	5.910	5.910	5.910	9.594	9.594	9.594	9.594	12.460	12.460	12.460	12.460
bias	-0.697	-0.331	-0.695	-0.354	-1.001	0.058	-0.865	0.195	-0.730	0.225	-0.998	0.283	-1.507	-0.185	-1.049	-0.122	-1.098	-1.126	-1.047	-1.446
mae	0.743	0.372	0.796	0.399	1.130	0.932	1.201	0.971	0.998	0.938	1.454	0.918	1.507	0.729	1.103	0.728	1.346	1.399	1.309	1.631
rmse	0.894	0.498	0.938	0.532	1.411	1.113	1.555	1.123	1.253	1.123	1.816	1.076	1.731	0.875	1.349	0.834	2.484	2.188	2.421	2.455
sci	0.283	0.157	0.297	0.168	0.194	0.153	0.213	0.154	0.212	0.190	0.307	0.182	0.180	0.091	0.141	0.087	0.199	0.176	0.194	0.197
std	0.575	0.381	0.646	0.408	1.020	1.141	1.326	1.135	1.045	1.129	1.557	1.065	0.874	0.877	0.870	0.847	2.286	1.925	2.240	2.036

Computed statistical parameters for case : s15str01
Number of stations at which computed data is available : 20

	Hm0 [m]				Tm01 [s]				Tm02 [s]				Tm-10 [s]				Tpm [s]			
SWAN	30.62	30.62+	40.16	40.16+	30.62	30.62+	40.16	40.16+	30.62	30.62+	40.16	40.16+	30.62	30.62+	40.16	40.16+	30.62	30.62+	40.16	40.16+
mean	2.960	2.960	2.960	2.960	6.708	6.708	6.708	6.708	5.458	5.458	5.458	5.458	8.864	8.864	8.864	8.864	11.726	11.726	11.726	11.726
bias	-0.002	-0.164	0.036	-0.214	0.557	0.389	0.847	0.558	0.638	0.518	0.502	0.660	0.218	0.061	0.673	0.168	0.633	-0.997	0.598	-1.071
mae	0.326	0.281	0.308	0.325	0.755	0.718	1.226	0.870	0.750	0.820	1.377	0.949	0.803	0.457	0.924	0.546	1.707	1.371	1.700	1.536
rmse	0.451	0.355	0.468	0.391	0.963	0.939	1.428	1.106	0.904	1.043	1.605	1.196	1.069	0.609	1.219	0.683	2.075	1.985	2.078	2.108
sci	0.152	0.120	0.158	0.132	0.144	0.140	0.213	0.165	0.166	0.191	0.294	0.219	0.121	0.069	0.138	0.077	0.177	0.169	0.177	0.180
std	0.463	0.323	0.479	0.336	0.806	0.877	1.179	0.980	0.657	0.929	1.564	1.023	1.074	0.622	1.043	0.679	2.028	1.761	2.042	1.863

Computed statistical parameters for case : s16str01
Number of stations at which computed data is available : 19

	Hm0 [m]				Tm01 [s]				Tm02 [s]				Tm-10 [s]				Tpm [s]			
SWAN	30.62	30.62+	40.16	40.16+	30.62	30.62+	40.16	40.16+	30.62	30.62+	40.16	40.16+	30.62	30.62+	40.16	40.16+	30.62	30.62+	40.16	40.16+
mean	3.097	3.097	3.097	3.097	6.787	6.787	6.787	6.787	5.842	5.842	5.842	5.842	8.313	8.313	8.313	8.313	10.025	10.025	10.025	10.025
bias	-0.203	-0.221	-0.156	-0.133	-0.500	0.383	-0.113	0.726	-0.335	0.468	-0.187	0.842	-0.751	0.283	-0.395	0.448	-0.166	-0.260	-0.052	-0.227
mae	0.418	0.334	0.376	0.277	0.582	0.687	0.538	1.003	0.573	0.825	0.910	1.161	0.834	0.538	0.530	0.669	0.966	0.776	0.967	0.940
rmse	0.461	0.407	0.416	0.387	0.756	0.963	0.691	1.316	0.800	1.143	1.148	1.574	1.009	0.678	0.655	0.833	1.486	1.213	1.495	1.489
sci	0.149	0.131	0.134	0.125	0.111	0.142	0.102	0.194	0.137	0.196	0.196	0.269	0.121	0.082	0.079	0.100	0.148	0.121	0.149	0.149
std	0.426	0.351	0.397	0.374	0.583	0.908	0.701	1.128	0.746	1.072	1.164	1.366	0.692	0.634	0.536	0.721	1.517	1.217	1.535	1.512

Computed statistical parameters for case : s17str01
Number of stations at which computed data is available : 26

	Hm0 [m]				Tm01 [s]				Tm02 [s]				Tm-10 [s]				Tpm [s]			
SWAN	30.62	30.62+	40.16	40.16+	30.62	30.62+	40.16	40.16+	30.62	30.62+	40.16	40.16+	30.62	30.62+	40.16	40.16+	30.62	30.62+	40.16	40.16+
mean	3.031	3.031	3.031	3.031	6.399	6.399	6.399	6.399	5.507	5.507	5.507	5.507	7.696	7.696	7.696	7.696	9.163	9.163	9.163	9.163
bias	-0.154	0.063	-0.129	0.201	-0.512	0.084	-0.479	0.225	-0.389	0.180	-0.579	0.310	-0.712	-0.075	-0.592	-0.022	-0.633	-0.526	-0.435	-0.539
mae	0.487	0.345	0.457	0.365	0.729	0.545	0.672	0.606	0.756	0.716	0.886	0.799	0.801	0.360	0.657	0.392	0.733	0.631	0.662	0.707
rmse	0.549	0.443	0.521	0.456	0.896	0.660	0.896	0.733	0.973	0.880	1.245	0.979	0.969	0.456	0.801	0.479	1.051	0.961	0.970	1.086
sci	0.181	0.146	0.172	0.150	0.140	0.103	0.140	0.115	0.177	0.160	0.226	0.178	0.126	0.059	0.104	0.062	0.115	0.105	0.106	0.119
std	0.538	0.447	0.515	0.417	0.749	0.668	0.772	0.712	0.909	0.879	1.124	0.947	0.670	0.458	0.550	0.488	0.855	0.820	0.884	0.962

D Contents of CD-ROM

The accompanying CD-ROM contains the following information:

Tb_ssc : Software and output from testbed, that has been used and generated during the analysis of the SWAN results

Programs: Software to transform spectra in data-format to SWAN format and to determine spectral parameters

Make_table	Create tables with results of statistical analysis
SPC2INT	Compute integral wave parameters based on SWAN 1d spectra
mea2sp1	Convert measured spectra to SWAN format
sp30_40v1	Convert spectra in SWAN 30+ format to SWAN 4-+ format
gen_boun	Convert measured spectra to SWAN input spectra

Data_analysis: Matlab scripts to analyse the data provided by RIKZ, as well as the data itself

Report

report:	PDF and DOC file of the final report, including figures
figures:	Figures in report, including scatter plots of mean wave measures based on peak period

SWAN_RUNS: Run script, executables and input files for SWAN computations

inputs:	SWAN input files
block:	for storing SWAN block files
bnests:	for storing nest files
bottom:	bottom files
bspec:	boundary spectra
current:	current fields
errors:	for storing error messages
inputs:	SWAN input files
level:	water level fields
points:	output points
spectra:	for storing SWAN output spectra
table:	for storing SWAN output tables
wind:	wind fields

PS_PLOTS : PostScript plots

block:	spatial variation of integral wave parameters
bottom:	modified bottoms
bspec:	boundary spectra
currents:	current fields
levels:	water levels
winds:	wind fields

SWAN_results:

block:	Zipped SWAN block files
spectra:	Zipped SWAN spectrum files
tables:	Zipped SWAN tables